MAGNETIC SPOROPOLLENIN BASED CYCLODEXTRIN AND CALIXARENE: MOLECULAR MODELLING, CHARACTERIZATION AND APPLICATION FOR DETERMINATION OF NON-STEROIDAL ANTI-INFLAMMATORY DRUGS

SYED FARIQ FATHULLAH BIN SYED YAACOB

FACULTY OF SCIENCE
UNIVERSITY OF MALAYA
KUALA LUMPUR

2019

MAGNETIC SPOROPOLLENIN BASED CYCLODEXTRIN AND CALIXARENE: MOLECULAR MODELLING, CHARACTERIZATION AND APPLICATION FOR DETERMINATION OF NON-STEROIDAL ANTI-INFLAMMATORY DRUGS

SYED FARIQ FATHULLAH BIN SYED YAACOB

THESIS SUBMITTED IN FULFILMENT OF THE REQUIREMENTS FOR THE DEGREE OF DOCTOR OF PHILOSOPHY

DEPARTMENT OF CHEMISTRY
FACULTY OF SCIENCE
UNIVERSITY OF MALAYA
KUALA LUMPUR

2019

UNIVERSITY OF MALAYA

ORIGINAL LITERARY WORK DECLARATION

Name of Candidate: **SYED FARIQ FATHULLAH BIN SYED YAACOB**

Matric No: **SHC 140079**

Name of Degree: **DOCTOR OF PHILOSOPHY**

Title of Thesis ("this Work"):

MAGNETIC SPOROPOLLENIN BASED CYCLODEXTRIN AND CALIXARENE: MOLECULAR MODELLING, CHARACTERIZATION AND APPLICATION FOR DETERMINATION OF NON-STEROIDAL ANTI-INFLAMMATORY DRUGS

Field of Study: **ENVIRONMENTAL CHEMISTRY**

I do solemnly and sincerely declare that:

(1) I am the sole author/writer of this Work;
(2) This Work is original;
(3) Any use of any work in which copyright exists was done by way of fair dealing and for permitted purposes and any excerpt or extract from, or reference to or reproduction of any copyright work has been disclosed expressly and sufficiently and the title of the Work and its authorship have been acknowledged in this Work;
(4) I do not have any actual knowledge nor do I ought reasonably to know that the making of this work constitutes an infringement of any copyright work;
(5) I hereby assign all and every rights in the copyright to this Work to the University of Malaya ("UM"), who henceforth shall be owner of the copyright in this Work and that any reproduction or use in any form or by any means whatsoever is prohibited without the written consent of UM having been first had and obtained;
(6) I am fully aware that if in the course of making this Work I have infringed any copyright whether intentionally or otherwise, I may be subject to legal action or any other action as may be determined by UM.

Candidate's Signature Date:

Subscribed and solemnly declared before,

Witness's Signature Date:

Name:

Designation:

MAGNETIC SPOROPOLLENIN BASED CYCLODEXTRIN AND CALIXARENE: MOLECULAR MODELLING, CHARACTERIZATION AND APPLICATION FOR DETERMINATION OF NON-STEROIDAL ANTI-INFLAMMATORY DRUGS

ABSTRACT

The interaction between β-CD and calixarene with selected non-steroidal anti-inflammatory drugs (NSAIDs), namely, indoprofen (INP), ketoprofen (KTP), ibuprofen (IBP) and fenoprofen (FNP) was investigated using modelling approach. In molecular modelling study, molecular dynamics and AM1 semi-empirical method was used to perform the geometry optimization calculation 1:1 ratio stoichiometry of host and guest molecule complexes. Complexation of host with each selected NSAIDs was investigated at all possible orientation, coordinates and different system. For β-CD host complexation, the most optimum position of each NSAIDs was located at center of β-CD cavity with range energy of -0.02 to -0.37 Hatrees (-13.15 to -230.22 kcal/mol). Most optimum position of selected NSAIDs for calixarene host complexation was situated at outside cavity of calixarene with energy between -0.01 to -0.13 Hatrees (-5.57 to -82.30 kcal/mol). Several hydrogen bonds were measured indicating there are intermolecular forces existed between host and guest molecules. From molecular modelling study, the result showed that there is interaction between NSAIDs with β-CD and calixarene. Therefore, β-CD and calixarene have been chosen as receptor for application of trace analysis of NSAIDs. In experimental approach, β-CD and calixarene framework functionalized bio-polymeric spores of sporopollenin hybrid magnetic materials (**MSp-TDI-βCD** and **MSp-TDI-calix**) were synthesized and applied as sorbents of magnetic solid phase extraction (MSPE) for determination of NSAIDs. The structure of **MSp-TDI-βCD** and **MSp-TDI-calix** were characterized by Fourier-transform infrared spectroscopy (FTIR), X-Ray diffraction (XRD), field emission scanning electron microscopy

(FESEM), energy dispersive X-Ray spectroscopy (EDX), Brunauer-Emmett-Teller (BET) analysis and vibrating sample magnetometer (VSM) measurement. In order to develop the extraction performance of synthesized adsorbents, decisive MSPE affective parameters were optimized such as sorbent amount, sample volume, extraction and desorption time, type and amount of organic eluent as well as pH solution prior high performance liquid chromatography (HPLC) determination. The best working conditions for both adsorbents as follow; 10 mg of **MSp-TDI-βCD** and 30 mg of **MSp-TDI-calix**, 30 min extraction time, 30 min desorption time for **MSp-TDI-βCD** and 10 min desorption time for **MSp-TDI-calix**, 200 mL sample volume, 1.5 mL of acetonitrile and sample solution at pH 4. Under the optimized conditions, the analytical validity of MSPE procedure for both adsorbents was evaluated and the following merits were obtained: linearity over concentration range of 0.5 - 500 µg/L, limits of detection (LOD) from 0.16 - 0.37 µg/L for **MSp-TDI-βCD** and 0.06 - 0.27 µg/L for **MSp-TDI-calix**, limits of quantification (LOQ) for **MSp-TDI-βCD** and **MSp-TDI-calix** between 0.53 - 1.22 µg/L and 0.20 - 0.89 µg/L, respectively. Excellent precision in terms of reproducibility and repeatability with inter-day (n = 15) and intra-day (n = 5) relative standard deviation were acquired for **MSp-TDI-βCD** in range of 2.5 - 4.0 and 2.1 - 5.5 respectively and for **MSp-TDI-calix** between 2.5 - 3.2 and 2.4 - 3.9, respectively. The application of prepared adsorbent **MSp-TDI-βCD** and **MSp-TDI-calix** towards environmental real samples on tap water, drinking water and river water was successfully studied. Good percentage recovery was achieved for both adsorbents (92.5 - 123.6% for **MSp-TDI-βCD**) and (88.1 - 115.8% for **MSp-TDI-calix**) with acceptable %RSD of 1.9 - 12.4% and 1.6 - 4.6% respectively.

Keywords: Sporopollenin; β-cyclodextrin; *p*-tertbutylcalixarene; NSAIDs; Magnetic Solid Phase Extraction; Molecular Modelling

MAGNETIK SPOROPOLLENIN BERDASARKAN SIKLODEKSTRIN DAN KALIKSARENA: PERMODELAN MOLEKUL, PENCIRIAN DAN APLIKASI PENENTUAN UBAT ANTI-RADANG BUKAN STEROID

ABSTRAK

Interaksi antara β-CD dan kaliksarena dengan ubat anti-radang bukan steroid (NSAIDs) yang terpilih dinamakan indoprofen (INP), ketoprofen (KTP), ibuprofen (IBP) dan fenoprofen (FNP) telah dijalankan dengan menggunakan pendekatan permodelan molekul. Melalui kajian permodelan molekul, molekul dinamik dan kaedah AM1 semiemperikal telah digunakan untuk menjalankan pengoptiman geometri dengan nisbah stokiometri 1:1 terhadap molekul kompleks perumah dan tetamu. Pengkompleksan perumah dengan setiap NSAIDs terpilih telah dikaji pada semua kemungkinan orientasi, koordinat dan sistem yang berbeza. Untuk pengkompleksan perumah β-CD, posisi paling optimum bagi setiap NSAIDs adalah terletak pada kedudukan tengah-tengah rongga β-CD dengan julat tenaga -0.02 hingga -0.37 Hatrees (-13.15 hingga -230.22 kcal/mol). Posisi optimum bagi NSAIDs terpilih untuk pengkompleksan perumah kaliksarena adalah terletak di luar rongga kaliksarena dengan julat tenaga antra -0.01 hingga -0.13 Hatrees (-5.57 hingga -82.30 kcal/mol). Beberapa ikatan hidrogen telah dikenalpasti menunjukkan kewujudan daya antara molekul di antara molekul perumah dan tetamu. Daripada kajian permodelan molekul, keputusan menunjukkan bahawa terdapat interaksi antara NSAIDs dengan β-CD dan kaliksarena. Maka, β-CD dan kaliksarena telah dipilih sebagai reseptor untuk aplikasi analisis surih NSAIDs. Dalam pendekatan eksperimen, β-CD dan kaliksarena pemfungsian spora bio-polimerik *sporopollenin* bahan hibrid bermagnet (**MSp-TDI-βCD** dan **MSp-TDI-calix**) telah dihasilkan dan diaplikasikan sebagai penjerap pengekstrakan fasa pepejal bermagnetic (MSPE) untuk penentuan NSAIDs. Struktur **MSp-TDI-βCD** dan **MSp-TDI-calix** dikenalpasti oleh Fourier-spektroskopi inframerah (FTIR), pembelauan sinar-X (XRD), mikroskopi pengimbas

pelepasan elektron (FESEM), spektroskopi tenaga penyebaran X-Ray (EDX), analisis Brunauer-Emmett-Teller (BET), dan pengiraan magnetometer sampel bergetar (VSM). Dalam rangka untuk membangunkan prestasi pengekstrakan oleh penjerap yang dihasilkan, efektif MSPE parameter telah dioptimumkan seperti jumlah penjerap, isipadu sampel, masa pengekstrakan dan nyahserap, jenis dan jumlah pelarut organik, dan juga pH larutan sebelum penentuan oleh kromatografi cecair berprestasi tinggi (HPLC). Keadaan hasil yang terbaik untuk kedua-dua penjerap adalah seperti berikut; 10 mg untuk **MSp-TDI-βCD** dan 30 mg untuk **MSp-TDI-calix**, 30 min masa pengekstrakan, 30 min masa nyahserap untuk **MSp-TDI-βCD** dan 10 min masa nyahserap untuk **MSp-TDI-calix**, 200 mL isipadu sampel, 1.5 mL asetonitril dan larutan sampel pada pH 4. Di bawah keadaan yang dioptimumkan, kesahan analitikal untuk prosedur MSPE bagi kedua-dua penjerap telah dinilai dan berikut adalah merit yang diperolehi: kelinearan dengan julat kepekatan 0.5 - 500 µg/L, had pengesan (LOD) daripada 0.16 - 0.37 µg/L untuk **MSp-TDI-βCD** dan 0.06 - 0.27 µg/L untuk **MSp-TDI-calix**, had kuantifikasi (LOQ) untuk **MSp-TDI-βCD** dan **MSp-TDI-calix** di antara 0.53 - 1.22 µg/L dan 0.20 - 0.89 µg/L, masing-masing. Ketepatan yang sangat baik dalam terma kebolehulangan dengan sisihan piawai relatif antara hari (n = 15) dan hari yang sama (n = 5) diperolehi untuk **MSp-TDI-βCD** dalam julat 2.5 - 4.0 dan 2.1 - 5.5, masing-masing dan untuk **MSp-TDI-calix** di antara 2.5 - 3.2 dan 2.4 - 3.9, masing-masing. Aplikasi untuk penjerap **MSp-TDI-βCD** dan **MSp-TDI-calix** terhadap sampel alam sekitar iaitu air paip, air minuman dan air sungai telah berjaya dikaji. Peratusan kebolehdapatan semula yang baik telah dicapai untuk kedua-dua penjerap (92.5 - 123.6% untuk **MSp-TDI-βCD**) dan (88.1 - 115.8% untuk **MSp-TDI-calix**) dengan %RSD yang boleh diterima iaitu 1.9 - 12.4% dan 1.6 - 4.6% masing-masing.

Kata Kunci: Sporopollenin; β-siklodekstrin; *p*-tertbutilkalix; NSAIDs; Pengekstrakan fasa pepejal bermagnetik; Permodelan Molekul

ACKNOWLEDGEMENTS

In the name of Allah, Most Gracious, Most Merciful

I would like to express my deepest appreciation to my supervisor, Associate Professor Dr. Sharifah Binti Mohamad for your tremendous guidance, encouragement, and supervision throughout my research works and giving me the opportunity to embark my doctorate degree. I also would like to express my gratitude to visiting lecture, Dr. Muhammad Afzal Kamboh for advices, ideas and valuable discussion. My gratitude also goes to Professor Wan Aini Wan Ibrahim and Associate Professor Dr. Vannajan Sanghiran Lee as my mentor for valuable advices, criticism and ideas. Special appreciation to my beloved family especially my parent, Mr Syed Yaacob Syed Agil and Mrs Raja Fauziah Raja Shahrin, my parent in law, Mr. Mohd Daud Hamdan and Mrs. Maimon Mohamad, my wife and my son, Siti Nur Haslinda Mohd Daud and Syed Mujahid Fathullah for their prayers, blessings, and sacrifices from beginning of my study. Special thanks to my sisters, Sharifah Fairuz, Sharifah Shazila and Sharifah Shahira for your moral support. Special gratitute to all my friends from Ikatan Muslimin Malaysia especially Dr Osman Rasip, Fauzi Ahmad, Nukman Halim, my smart circle-mate and all members in Kelab Remaja ISMA. To all my labmates especially Siti Khalijah, Nurul Yani, Ahmad Razali, Naqhiyah Farhan, Faris Zikri, Nur Faizah, Husam Kafena, and Ali Mansor for their for moral support for me through my successful and disappointments. Special thanks to all the staff from Department of Chemistry, Faculty of Science, University of Malaya especially Ms. Norzalida Zakaria, Mrs. Rohaida, Mrs. Norlela, and Mr. Shukri for their help and technical support throughout my studies. Finally, I would like to thanks to Ministery of Higher Education for the financial support through MyBrain15/MyPhD scheme and University of Malaya for funding my research under intensive postgraduate grant PG046-2015A for financial support.

TABLE OF CONTENTS

LIST OF FIGURES

LIST OF TABLES

LIST OF SYMBOLS AND ABBREVIATIONS

%RSD	:	Percentage relative standard deviation
BET	:	Brunauer-Emmett-Teller
FESEM	:	Field emission scanning electron microscopy
FNP	:	Fenoprofen
FTIR	:	Fourier-transform infrared spectroscopy
HPLC	:	High performance liquid chromatography
IBP	:	Ibuprofen
INP	:	Indoprofen
KOH	:	Potassium hydroxide
KTP	:	Ketoprofen
LOD	:	Limit of detection
LOQ	:	Limit of quantification
MNP	:	Magnetic nanoparticle
MSPE	:	Magnetic solid phase extraction
MSp-TDI-calix	:	Magnetic sporopollenin functionalized *p*-tertbutylcalix[4]arene
MSp-TDI-βCD	:	Magnetic sporopollenin functionalized beta-cyclodextrin
NaOH	:	Sodium hydroxide
NP	:	Nanoparticle
NSAIDs	:	Non-steroidal anti-inflammatory drugs
Sp	:	Sporopollenin
TDI	:	Toluene diisocyanate

CHAPTER 1: INTRODUCTION

1.1 Background of study

For many years, the fate and occurrence of pharmaceutical residue in environment especially in water bodies have raised an environmental concern. These compounds pass into the water system through many possible ways such as human or animal excretion which are directly discharge into river stream, the disposal of expired or unused medicines, and improper disposal during the pharmaceutical product manufacturing (Fick et al., 2009; Leung et al., 2012; Liu & Wong, 2013). Due to incomplete wastewater discharge removal, the pharmaceutical residue continuously enters the aquatic environmental and have been identified as contaminates (Peng et al., 2008). During the lifetime in aquatic environment, these contaminates can either transformed to other active/inactive compound or it can be maintained their original structure and concentration, thus harmful to surrounding creatures (Tsang et al., 2017). Therefore, it is crucial to handle these contaminates safely and arise the analytical method to assess the profiles and occurrences pattern of pharmaceutical residue in environmental samples.

Over the years, many researches have been conducting the detection of pharmaceutical residue in many type of water samples (Ashton et al., 2004; De Andrade, Oliveira, Da Silva, & Vieira, 2018; Kosjek et al., 2005; Koutsouba et al., 2003; Ollers et al., 2001; Peng, Gautam, & Hall, 2019; Phonsiri et al., 2019; Rodrıguez et al., 2003; Sacher et al., 2001; Heberer & Stan, 1997). The main factor for this compound occurrence in the environment is due to their overall consumption by animal or human and the fate of individual compound (Kosjek et al., 2007). Among pharmaceutical compounds, non-steroidal anti-inflammatory drugs (NSAIDs) have been subjected as outmost subscribed drugs globally and has been used as anti-inflammatory and as analgesic therapy in lower dosages. Due to its high consumption, it must be monitored regularly because of high water solubility and poor degradation properties which leads to contamination of

groundwater, drinking and surface water and thus, possessed high potential risk for affecting consumer health (Reddersen et al., 2002; Ternes et al., 2002). Usually, the concentration of NSAIDs detected in water samples are practically in the trace level in range of ppt to ppm level and it can persist longer time in sediments and soils about g/kg (Hernando et al., 2006). Hence, highly selective and sensitive technique for reaching these level remains challenging; nevertheless, simple, inexpensive and suitable sample preparation steps need to be selected to reach the trace level limit of detection required.

Many technique and suitable instruments have been proposed in modern analytical chemistry for determination of interest analytes in different kind of samples matrix. Mostly, targeted analytes present at trace or ultra-trace level in sample and analytical instrument are not sensitive for direct measurement of trace analytes. Thus, preliminary steps are required to isolate the analytes from original sample matrix and enrichment the analytes above limit of detection. Sample preparation is most important steps as it can eradicate sample matrix interference as well as to pre-concentrate the targeted analytes. Example of sample preparation have been reported such as stir rod sportive extraction (SRSE) (Luo et al., 2011), solid phase microextraction (SPME) (Peng et al., 2008), liquid-liquid extraction (LLE) (Wen., 2004), solid phase extraction (SPE) (Rodil et al., 2009; Santos et al., 2005), magnetic solid phase extraction (MSPE) (Alinezhad et al., 2018), cloud point extraction (CPE) (Noorashikin et al., 2013, 2014; Zain et al., 2016) and dispersive liquid-liquid microextraction (DLLME) (Yao et al., 2011). Initiative from SPE method, MSPE was developed as an alternative technique due to its magnificent characteristics which applicable to overcome the limitations of SPE. Since SPE involving tedious procedure and organic solvent consumption, MSPE only required a simple and economical step and less consumption of organic solvent, promising a greener and safety to environment. Moreover, MSPE offers rapid separation since its adsorbent consists of

magnetic property which can be isolated easily by using simple external magnet (Ibarra et al., 2015; Wan Ibrahim et al., 2015).

Along with growth of MSPE in sample preparation technique, however, there is increasing concern over the preparation of appropriate sorbent since it contributes to achieve the adequate recovery of target analytes. One of suitable sorbent selection is involving magnetic nanoparticles (MNPs) that is iron oxide such as magnetite (Fe_3O_4). MNP has been attracting considerable interest due to their economic value, high surface area, simple preparation, low toxicity and superparamagnetic properties which is to easy the isolation of interest analytes from sample (Du et al., 2012; Gill et al., 2007). Moreover, its capability to functionalize with wide range of material at surface to become more selective sample extraction and treatment towards certain analytes is another considerable and advantage of MNP. With this type of surface modification, it will enhance adsorption capacity and efficiency of MNP, possessed high number of active sites at surface and sensitivity and selectivity improvement for removal and extraction of analytes from sample matrices (Huang et al., 2014).

Despite its advantages and benefits, MNP suffers from several major drawbacks including easily oxidize in open air, agglomerate in aqueous solution, instable in acidic medium and poor selectivity because of its highly hydrophilic properties (Liu et al., 2008). This deficiency limits its potential as adsorbent towards organic pollutants extraction from environment. Hence, various approaches can be implementing to modify the MNP surfaces via grafting, functionalizing or immobilizing with organic molecule such as polymers, surfactants and biomolecules. In this thesis, the study presented focusing on the modification of MNP surface by simple, economical and ready accessible modifying agent. In this circumstance, application of bio-polymer sporopollenin biomolecule is the suitable candidate modifying agent as solid support for MNP.

Due to its intractability regarding to chemical analysis, the sporopollenin information is limited discussed. However, based on spectroscopic analyses, it provides some data regarding sporopollenin composition. Sporopollenin is originated from plant which is possessed a stable chemical structure and highly resistance to chemical reaction such as mineral acids and bases (Ayar et al., 2007; Hemsley et al., 1993). It is categorized as natural polymer and exhibits a component of spore walls with 2 μm thick perforated walls hollowed exine. This structure makes the sporopollenin a porous molecule and allowed the guest molecule bind at inner and outer surface of sporopollenin (Kamboh et al., 2016). MNP also can easily embedded on the surface thus possess magnetic properties. Beside this, the sporopollenin surface can be functionalized with suitable functional group for removal or extraction of interest analytes.

Concept of host-guest chemistry involves two or more molecules complement each other and bind between them with either by electrostatics force, hydrogen bonding, inductive and dispersion forces, hydrophobic force and π-π interaction (Albrecht, 2007; Ariga & Kunitake, 2006; Shen et al., 2011; Steed et al., 2007). This concept allows guest molecules with certain size, shape and polarity bind with host molecules and have been used in many kinds of application such as pharmaceutical (Kristmundóttir et al., 1996), cosmetics (Scalia et al., 1999), foods (Mar Sojo et al., 1999), analytical applications (Rahim et al., 2016, 2018) and biotechnology industry (Hedges, 1998). This increasing interest in host guest supramolecular chemistry applications makes the urges the development of new materials based supramolecular compounds to trap the pollutants since it is economical and safe to environment. Cyclodextrins (CDs), the synthetic supramolecular host has attracted attention in host-guest field in last past decades due to its capability to bind with variety of guest molecules. It is composed by 6-12 glucose pyranose unit joined together by α-1,4-glycosidic linkage to form hydrophobic inner cavity and hydrophilic properties at outer surface. With this superior feature, CDs capable

to form noncovalent inclusion complex through host-guest interaction with other guest molecules by encapsulation entirely or partially trap and holds in the cavity (Chalasani & Vasudevan, 2012). As a consequence, various application of CDs has been expanding widely in many kinds of field such as pharmaceutical in drug release applications (Tudisco et al., 2012), catalysis (Chalasani & Vasudevan, 2013), environmental (Badruddoza et al., 2010; 2011; Kang et al., 2011), and synthesis of adsorbents in analytical chemistry (Badruddoza et al., 2012; Ghosh et al., 2011).

Another type of supramolecular host has been continuously expanding in last past decade is calixarenes. Calixarenes are classified as third generation supramolecular after crown ether and cyclodextrins. Alike CDs, calixarene acts as encapsulating agent to entrap targeted analytes through host-guest interaction. However, calixarenes structure can be tuned by functionalized at both lower and upper rim as well as methylene bridge to achieve desired properties makes it more flexible compared to cyclodextrin (Mokhtari et al., 2011; Sayin et al., 2013).

By combining supramolecular host modified magnetic nanoparticles and sporopollenin as solid support, in this thesis we have reported the synthesis of novel nanocomposites for MSPE adsorbents (**MSp-TDI-βCD** and **MSp-TDI-calix**) for extraction of NSAIDs from water samples. To the extent of our knowledge, no previous study demonstrates the preparation of supramolecular host functionalized toluene diisocyanate (TDI) modified bio-polymer sporopollenin for the extraction of NSAIDs. Implementation of magnetic properties by embedded MNPs at adsorbent surface also makes the adsorbent easily separated from solution by using external magnetic field. The main interest of these new adsorbent is the application of host-guest interactions between host and analytes by formation of hydrogen bonding, hydrophobic interaction and π-π interaction between them and indirectly selectively capture and bind NSAIDs at lipophilic cavity. The combination of these two concepts will increase the affinity and strength

towards the extraction of NSAIDs. Moreover, a simple and shorter preparation steps for synthesized of adsorbent by using smallest amount organic solvents promising towards greener research in order to preserve the environmental concern.

Molecular modelling can be interpreted as a study involving molecule and molecular system (Kollman, 1996). It also about discovery the solution for mathematical model using a computer. It is a multidisciplinary fields created on theories and law stemming from biology, mathematics and chemistry. In chemistry, molecular modelling known as "computational chemistry" as it is always related to computer simulation in order to understanding the chemical process and nature of reaction at molecular level (Nadendla, 2004). It usually required the combination of chemical theory and simulation software helps to justify and rationalize the experiment results and predicts the outcome of future experiment. Not only that, the information of molecule and reaction which are impossible to determine through experiment and lab work can be provided by computer simulation (Jorgensen, 1997). Therefore, computer modelling is important and independent research areas and it could be an alternative research pathways that can be explored beside experimental lab work.

One type of molecular modelling is molecular dynamics (MD) which has been widely applied for understanding the properties of molecule assemblies and the interaction between the molecules. The application of MD on host-guest simulations has been extensively used in order to investigate the structural features of hosts and its complexes (Alvira, 2017; Suwandecha et al., 2017; Varady et al., 2002). MD allows us to discover the global and local conformational minima distinct from a certain starting geometry and the energy hypersurfaces of molecules. Hence, the investigation on the molecules geometry of the host-guest inclusion complexes are beneficial to get some idea to understanding the detailed about interaction, geometries structural and driving forces of the inclusion complexes.

1.2 Objective of the research

The objectives of this study are as follow:

(i) To model and develop complexes via computational method:

a. To investigate the possible binding sites of NSAIDs onto cavity of β-CD and *p*-tertbutylcalix at which forming the most stable complexes conformation using molecular docking calculation.

b. To determine the structural change and stability of complexes by molecular dynamics simulation and quantum mechanics simulation.

c. To identify the type of interactions exists between NSAIDs and host molecule (β-CD and *p*-tertbutylcalix) in their complexes respectively.

(ii) To synthesis and characterize the new adsorbents:

a. β-cyclodextrin functionalized bio-polymeric spores of sporopollenin hybrid magnetic materials (**MSp-TDI-βCD**).

b. *p*-tertbutylcalix functionalized bio-polymeric spores of sporopollenin hybrid magnetic materials (**MSp-TDI-calix**).

(iii) To develop and apply the prepared adsorbents (**MSp-TDI-βCD** and **MSp-TDI-calix**) as magnetic solid phase extraction (MSPE) adsorbent for determination of selected non-steroidal anti-inflammatory drugs (NSAIDs) from tap, drinking and river water samples.

1.3 Outline of thesis

The present thesis is consisting of five constituent chapters. Chapter 1 discussed the brief introduction on the background and objective of the research. In Chapter 2, a compilation of related literature review about bio-polymer functionalization, supramolecular chemistry, application of magnetic nanoparticles and computational chemistry is presented. Chapter 3 discusses the overview of procedure for molecular

modelling which consists of three different approach that is molecular docking simulation, molecular dynamics simulation and quantum mechanics simulation. Moreover, for experimental procedure of synthesis and characterization of cyclodextrin and calixarene framework functionalized bio-polymeric spores of sporopollenin hybrid magnetic materials (**MSp-TDI-βCD** and **MSp-TDI-calix**) is also discussed. The optimization procedure for magnetic solid phase extraction of selected NSAIDs using synthesizing adsorbents prior HPLC determination and the method validation steps of developed method on different type of water samples is discussed. For result and discussion in Chapter 4, this chapter is divided into two part which is Part A reporting and discussing the molecular modelling simulation. This is including the geometry optimization of single and complexes molecules, molecular docking, molecular dynamics, quantum mechanics and interaction within host and guest molecules. As for Part B, the results about the characterization of synthesizing adsorbents, optimization and its application as magnetic solid phase extraction adsorbents toward various water samples prior HPLC measurement is presented. For final chapter, the conclusion and recommendation for future works is mentioned in Chapter 5.

CHAPTER 2: LITERATURE REVIEW

2.1 Sporopollenin

2.1.1 Origin and its properties

"*Spores*", the term derived from Greek word means for seed is refer to cells that formed by multiple of organism such as fungi, algae, bacteria and plants (Parker, 2001). Spores is the mobile reproductive cells of plant and it generally consists of one or two cells which are contains various types of vitamins, fats, carbohydrates and some proteins (Barrier, 2008). The production of spores is originated from loculus, the internal cavity of sporangia- the sexual organs of plants. Spores usually have a size between 1 - 250 µm and it was protected by a wall which are highly complex and robust double layer wall. This double layer wall consists of inner and outer layer called intine and exine respectively. Intine is build up from cellulose and few types of polysaccharides and exine highly contains of sporopollenin, a resistant biopolymer organic material known (Barrier, 2008; Huang, 2013). The study of spores is known as palynology and has been applied in broad of areas including allergy studies, fossil and pollen analysis and also forensic sciences (Bell, 2018; Huang, 2013). Figure 2.1 shows the composition of spores.

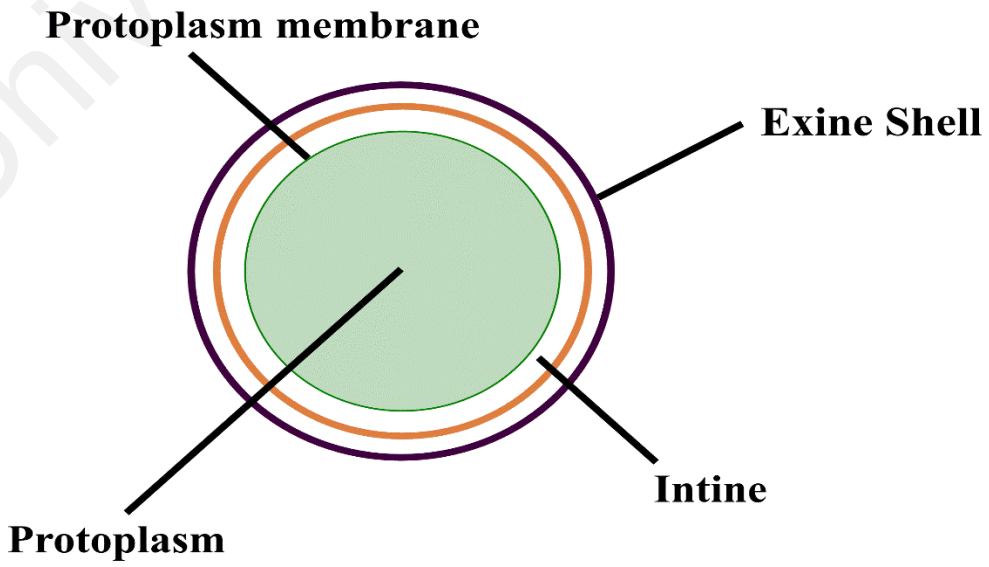

Figure 2.1: The composition of spore (Blackwell, 2007)

In 1814, the term "*pollenin*" was introduced by John and studied about the inertness of the tulip exine compared to other pollen wall towards chemical reagent (Brooks & Shaw, 1978). This study was the earliest documented study on spore/pollen exine. In year 1829, Braconnot supporting John experiment by using pollen from bulrush (Mhlana, 2017). A year after, Berzelius (1830) has successfully characterized the sporopollenin. After a century, Zetzsche (1931) developed the inertness of spore exine from lycopodium clavatum and come out with term "*sporonin*". Finally, few years after, Zetzsche proposing the compound "*sporopollenin*" as resistant compound exine material which forms both pollen and spore grain walls due to sharing same chemical character (Brooks & Shaw, 1978; Huang, 2013).

The definition of sporopollenin based International Symposium on Sporopollenin proposal is well-defined as natural biopolymer material possess chemically inert properties and it can be found in plant species such as vegetables, algae and fungal species (Brooks et al., 1971). However, sporopollenin exine found in spore and pollen grains is classified as most resistant natural biopolymer compared in other plants (Barrier et al., 2010; Bernard et al., 2015). Although some researcher reported ratio stoichiometry of sporopollenin is $C_{90}H_{144}O_{27}$, but the different study reported the chemical structure of sporopollenin is in forms of an oxidative polymer of carotenoids and carotenoids esters (Brooks et al., 1971; Brooks & Shaw, 1978). Another study also reported that the inner sporopollenin genetic material showed an antioxidant properties due to presence of conjugated phenol group (Diego-Taboada et al., 2014; Mackenzie et al., 2015; Thomasson et al., 2010). Hence, the chemical properties were poorly characterized and exact structure still unknown and remained debated.

In the past few years, there is broad interest in the development and application of sporopollenin in chemistry and material sciences. The exclusive properties owing by

sporopollenin makes it superior material include possessing good elasticity, resistance to harsh physical and chemical activity, shielding capability toward UV and high thermal stability (Bernard et al., 2015; Brooks et al., 1971; Mhlana, 2017). These properties enable the genetic material of the plant can be protected from surrounding such as UV sunlight, oxidation and physical attack. Moreover, sporopollenin are easily obtained in large quantities makes it more economical and it can be renewable (Barrier, 2008; Blackwell, 2007; Mackenzie et al., 2015).

2.1.2 Surface modification of sporopollenin

As described above, sporopollenin has been known as "*one of the best materials most resistant in the world*". Sporopollenin potentially acts as a best candidate for immobilization/functionalized with wide range of compound with suitable functional group such as linkers and enzymes because of its unique morphological surface (Dyab, 2016; Tutar, 2009). The exine, outer layer of sporopollenin surface with 2 μm thick perforated wall which makes the material porous is available for binding with other molecules (Kamboh et al., 2016; Yaacob et al., 2018). Based reported literature, sporopollenin has been functionalized for many type of applications such as synthesis of solid phase peptide and ion exchange (Pehlivan & Yildiz, 1988; Shaw et al., 1988). Living cells such as yeast and different organic and inorganic materials has been successfully encapsulated at the surface of sporopollenin from lycopodium clavatum plant as reported in literature (Hamad et al., 2011; Paunov et al., 2007). Sayin and co-workers reported the surface modification of sporopollenin with dihydrazine amide derivative of *p*-tertbutylcalix[4]arene for removal of sodium dichromate (Sayin et al., 2013). Ahmad and co-workers represent the modification of sporopollenin with 1-(2-hydroxethyl) piperazine loaded with magnetic nanoparticles for removal of metal ions Pb(II) and As(III) from aqueous solution. The functionalized sporopollenin showed outstanding removal of metal

ions and provides good separation, stabilization and simple process (Ahmad et al., 2017). Besides that, Barrier and co-workers also reported that chloromethyl group could be immobilized at the surface of sporopollenin by reaction with chlorodimethyl ether and stannic chloride. Then, they also observed that amino acid could be functionalized to the chloromethylated sporopollenin by using hydrobromo acid in trifluoracetic acid without any alteration the morphology of sporopollenin surface observed (Barrier et al., 2010). Therefore, research regarding the uses of functionalized of sporopollenin have been expand for various purposes for example catalyst and solid-phase support, microencapsulation and drug delivery in medicine, food and cosmetic industry as well as environmental purposes (Yusuf et al., 2016).

2.2 Supramolecular chemistry

2.2.1 Some historical and its concepts

During past decades, supramolecular chemistry has been developed and become frontier in chemistry field especially in analytical and physical chemistry. It is the branch of chemistry associated from simple molecular component to formation of complex molecular entities. Nobel Prize winner in 1987, Jean-Marie Lehn as one of the leading proponents in this field has defined supramolecular chemistry as "*chemistry of molecular assemblies and of the intermolecular bond*" (Steed & Atwood, 2009). Another terms that can be used to express the definition of supramolecular chemistry is "*non-molecular chemistry*" and "*the chemistry of the non-covalent bond*" (Steed & Atwood, 2009). Basically, supramolecular chemistry involving non-covalent interaction between "*host*" and "*guest*". The relationship in terms function and structure among host and guest in supramolecular chemistry is illustrated in Figure 2.2.

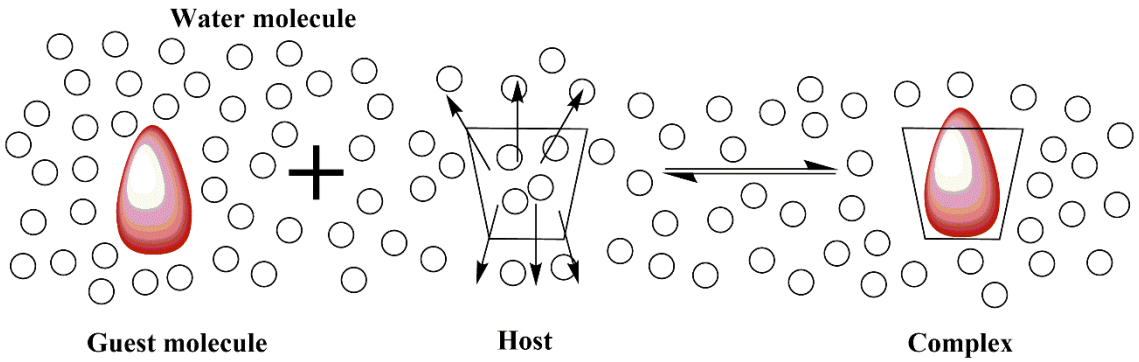

Figure 2.2: The formation of complex between host and guest molecule (Szejtli, 2004)

Besides the terms mention above, further expression is used interchangeably with supramolecular chemistry concept such as "*host-guest chemistry*", "*inclusion phenomena*" and "*molecular recognition*" (Cragg, 2005). This concept has attracted the attention most of the researcher because there is an implicit act of design to prepare molecular assemblies by using existing molecules or by synthesis of new molecules for achieve particular desirable qualities. In simplest way, supramolecular involving a molecule e.g. a host binding with another molecule e.g. a guest via non-covalent binding or complexation event in binding sites (Ariga & Kunitake, 2006; Steed et al., 2007). A host basically a large molecule owns a sizeable and specific cavity or central hole convergent binding sites such as enzyme or synthetic cyclic compound. A guest may in several of size and type such as monoatomic cation and anion, ion pair and also hormone or neurotransmitter which possesses divergent binding sites. The most extensively studied related host molecule including crown ether, cyclodextrins and calixarenes.

2.2.2 Cyclodextrins (CDs)

Cyclodextrins are well known as cyclic oligosaccharides. It is composed of several numbers of D-glucopyranose units as basic monomer. Under degradation by glucosyltransferase (CGT), the starch is naturally undergoing intermolecular reaction and converted into six, seven or eight cyclic glucopyranose namely α-cyclodextrin, β-

cyclodextrin and γ-cyclodextrin. These glucopyranose were linked by α-1,4-glycosidic linkages to form cyclodextrins with different sizes. Figure 2.3 illustrates the molecular structure of D-glucopyranose unit with formula $C_6H_{10}O_5$ linked to each other.

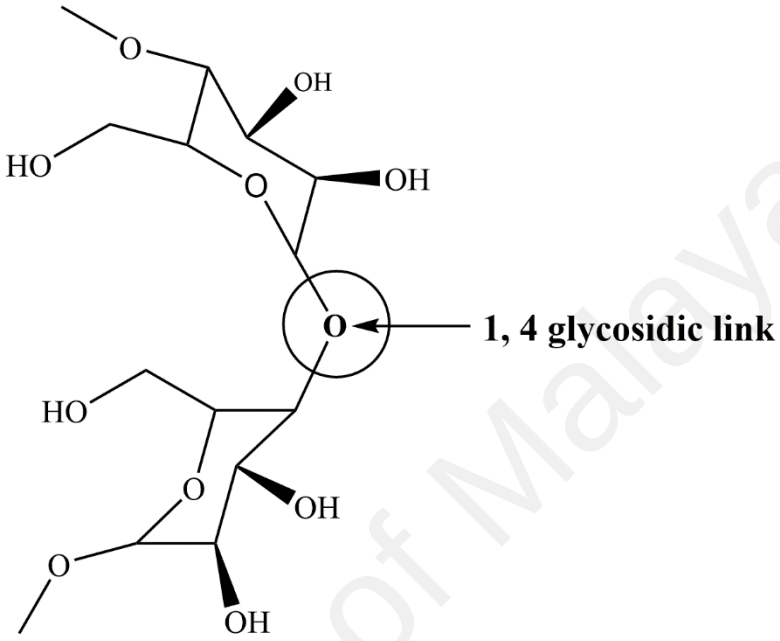

Figure 2.3: Structure of D-glucopyranose

Previously studies suggested that formation of cyclodextrins with higher than ten membered rings can be formed theoretically. However, it encounters quite challenging due to high solubility in water and weak complex forming ability (Frömming & Szejtli, 1993). With larger size of cavity also result of more energy is required to hold the guest tightly from slipping and escape out from cyclodextrin cavity. Apart from that, it also reported that formation less than six-member rings cannot be form due to steric reason (Frömming & Szejtli, 1993). Cyclodextrin ring possesses cylindrical in shape or precisely like a conical cylinder which is usually illustrates as a doughnut or wreath-shaped truncated cone (Frömming & Szejtli, 1993; Szejtli, 2004). Since glucopyranose exist as chair conformation, this condition makes a hydrophilic surface because hydroxyl functional group toward to the cone exterior with the primary hydroxyl situated at narrow

and wider edge. Additionally, this surface also provides the hydrophilic environment which can be dissolved in water. Meanwhile, the ethereal oxygen and skeletal carbon of glucopyranose unit form the central cavity which gives cyclodextrin a hydrophobic inner surface that enables the cyclodextrin function as host to trap a wide variety of guest molecules (Yang, 2008). Figure 2.4 showed the interactive surfaces of β-CD and its hydroxyl group.

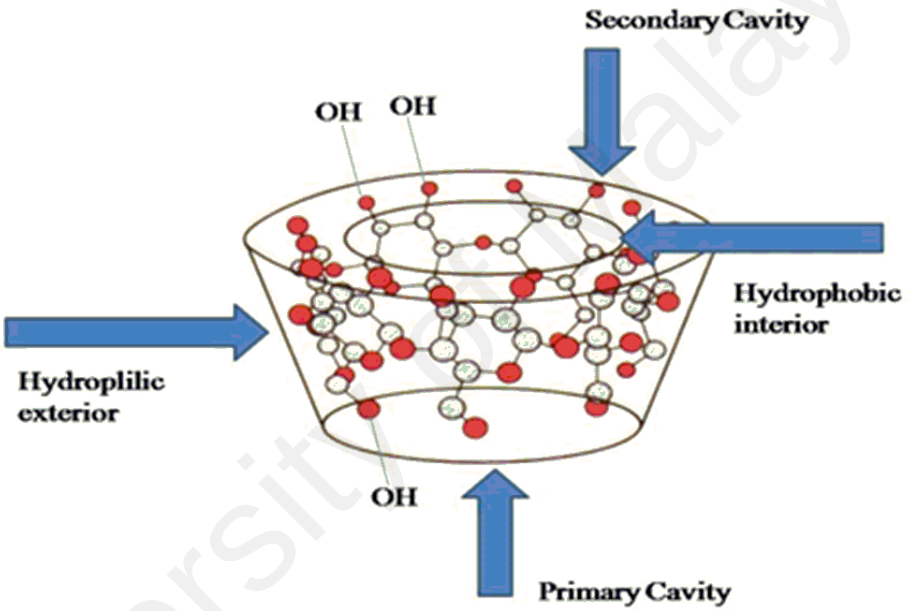

Figure 2.4: Hydrophilic and hydrophobic region of β-cyclodextrin (Li & Purdy, 1992)

In the past decades, cyclodextrin-based materials have been significantly developed owing to cyclodextrin unique character which can form noncovalent inclusion complex with other compounds through host-guest interactions by encapsulating either completely or partially fit into the lipophilic cavity. The cavity of cyclodextrin provides a hydrophobic space in which a guest can be sequestered in an aqueous medium. Cyclodextrin are known to form stable complexes with a wide range of compounds, including dyes (Arslan et al., 2013; L. Fan et al., 2012; Ozmen et al., 2008; A. Yilmaz et

al., 2006; E. Yilmaz et al., 2010), organic compounds (Cho et al., 2015; Raoov et al., 2013; Zain et al., 2016) and metal ions (Badruddoza et al., 2011; Leilei Li et al., 2013; Wang et al., 2014).

2.2.2.1 Functionalization of β-cyclodextrin

As we mention earlier, the hydroxyl group at primary and secondary rims form the hydrophilic exterior and surround the internal hydrophobic cavity of cyclodextrin. These hydroxyl group could be modified and attach covalently with variety of functional group (Breslow, 1995; Breslow et al., 1980). By performing this modification enable the alteration of cyclodextrin complexation behaviour and enhancing the properties of cyclodextrin, e.g. solubility of β-CD could be increased (Tungala et al., 2013; van der Boogard, 2003; Zain et al., 2016). In addition, selective modification also can be achieved by placing several functional groups on the periphery of cyclodextrin (van der Boogard, 2003). Cyclodextrin could create enzyme like activity by modified it with catalytic group. These functionalization of cyclodextrin divided into two parts; fully functionalization and selective functionalization but we cover for selective functionalization only since it is most widely utilized and ready accessible (Popr, 2016).

2.2.2.2 Selective functionalization of cyclodextrin

Selective functionalization of cyclodextrin has been widely explored and studied for primary hydroxyl and not as much for secondary hydroxyl face. Functionalization of specific hydroxyl group is quite challenging since there are 21 hydroxyl group attached on the β cyclodextrin surface and 7 out of 21 is categorized as primary hydroxyl group (Biagi, 2012). What makes the selective functionalization at primary hydroxyl attractive is that primary hydroxyl groups are more nucleophilic compared secondary hydroxyl counterparts makes primary hydroxyl slightly more reactive than secondary hydroxyl

groups in presence of organic solvents (Biagi, 2012). Thus, modification at primary part is easier than the reverse. Moreover, secondary hydroxyl groups are sterically crowded in the presence of more hydroxyl functional groups and intramolecular hydrogen bonding (Khan et al., 1998; Teranishi, 2000). For such consequences, many researcher have put tremendous effort to selectively modify primary rim such as alkylation and esterification. Modification of primary hydroxyl group at position C6 with tosyl chloride in tosylation process is example for further chemical modification with various substituents including amino derivatized (Fetter et al., 1990) and azido groups (Hanessian et al., 1995; Tungala et al., 2013). Figure 2.5 shows the example of scheme for tosylation process of cyclodextrin take place.

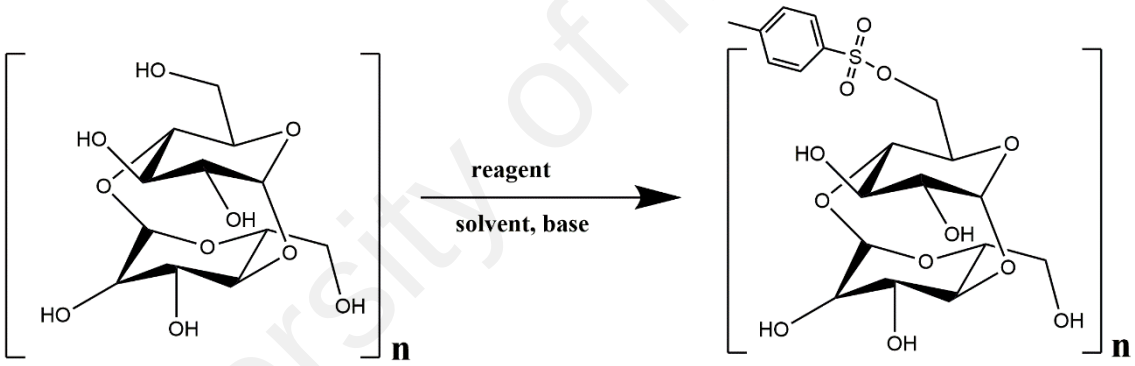

Figure 2.5: Example of tosylation process for β-cyclodextrin (Popr, 2016)

2.2.2.3 Application of functionalization cyclodextrins in separation systems

Modified cyclodextrins have been widely utilized for separation purpose over past years because of its unique structure and properties. Host-guest concept play important role for inclusion complexes with various type of analytes in different fields such as adsorbents, chiral selector, chemical separation and stationery phases as summarized in Table 2.1.

Table 2.1: Summary of cyclodextrin based material studied for complexation with various type of analytes

Cyclodextrin based material	Analytes	References
Ionic liquid cyclodextrin functionalized magnetic core dendrimer nanocomposite	Pyrethroids	(Liu et al., 2018)
Cyclodextrin-metal organic framework (CD-MOF)	Sulfonamides	(Li et al., 2018)
Cyclodextrin functionalized silicon nano-adsorbent	Methylene blue	(Jing Li et al., 2018)
β-cyclodextrin modified Fe_3O_4/Au magnetic composite microsphere	R-S mandelic acid	(Deng et al., 2018)
Silica coated MNP grafted graphene oxide and β-cyclodextrin	Plant growth regulators	(Jiuyan Chen et al., 2018)
Ionic liquid functionalized β-cyclodextrin	Dansyl amino acid and naproxen	(Jingtang Li et al., 2018)
Carbon black-β-cyclodextrin	Flutamide and 4-nitrophenol	(Kubendhiran et al., 2018)
Neutral red functionalized SH-β-cyclodextrin@Au nanoparticles	Nitrite ions	(Xiaoyang Du et al., 2018)
Sulfoether-bridged cationic per(3,5 dimethyl)phenylcarbamoylated β-cyclodextrin	Benzene homolog, aromatic amines, flavonoids and β-blockers	(Tang et al., 2018)
Magnetic β-cyclodextrin polymer	Benzoylurea insecticides	(Liang et al., 2018)
β-cyclodextrin modified 3D graphene oxide wrapped melamine foam	Flavonoids	(Hou et al., 2018)
Cyclodextrin modified miceller	Catechin and theanine	(Fiori et al., 2018)
Beta and gamma cyclodextrin modified microporous silica	Phenolic compounds and polyclyclic aromatic hydrocarbon	(Belenguer-Sapiña et al., 2018)

2.2.3 Calixarenes

Calixarenes, the third generation of supramolecular is the outstanding and remarkable of macrocyclic host which are synthesized from condensation of formaldehyde with phenol under alkaline solutions (Agrawal et al., 2009; Gutsche, 2008; Lei Li et al., 2006). The word "*calix*" origin from Latin and Greek which means for "*vase*" and it was fully interpreted and introduced by Gutsche in 1970 (Mandolini & Ungaro, 2000; Neri et al., 2016). However, calixarenes already introduced in early 1870 for the first time and was disregarded until early 1940 when Zinke and his co-worker Erich Ziegler decided to simplify the preparation of calixarenes through condensation reaction of *p*-subsituted phenol with formaldehyde (Agrawal et al., 2009; Vicens & Böhmer, 1991). After that, in 1975, Gutsche proposed these compound having special characteristic of space filling models of the tetramer a chalice or like a cup which has shape of reminiscent of a Greek crater vase (Neri et al., 2016; Vicens & Böhmer, 1991).

Calixarenes is defined as a class cyclooligomers which have upper and lower rims and central annulus. It is composed of several phenol as basic monomer and categorized according to their monomer unit as minor, major and large calixarenes (Stewart & Gutsche, 1999). Usually minor calixarenes composed by 5 - 7 phenol unit and major calixarenes having 4,6, or 8 phenol unit and finally large calixarenes possessed of 9 - 20 phenol unit as monomer. Upper ring has the R substituent in *p*-position of phenol group and lower ring defined by the phenolic oxygen and the pendant groups attached to them. Between these two rims formed a hydrophobic cavity of aromatic rings (Kane, 1998; Pandya et al., 2013). Figure 2.6 shows the structure of calixarenes.

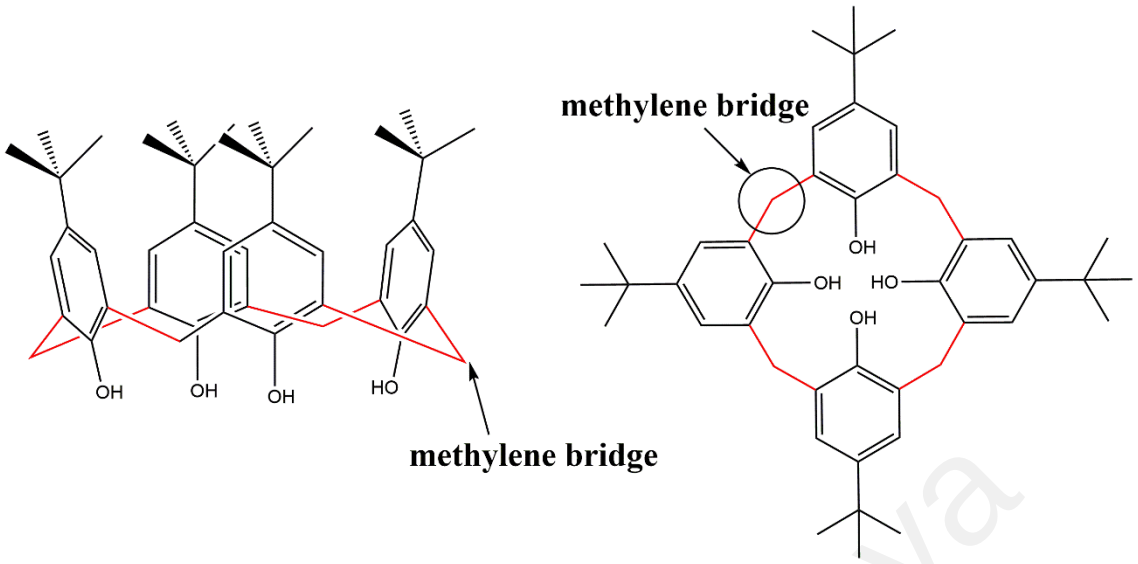

Figure 2.6: Structure of calixarene from side and top view

Alike cyclodextrins, calixarenes are macrocyclic molecules which composed by monomer as repeating unit and both possessed cage-like molecules with hydrophobic inner cavity (Akceylan et al., 2009; Pandya et al., 2013; Yang & de Villiers., 2005). But in terms of structure, calixarenes showed highly flexible molecules, capable to invert ring completely and ability to perform minor flexing compared to cyclodextrin to achieve desired properties (Segneanu et al., 2016; Yang & de Villiers., 2005). Calixarenes also possessed high melting points above 300 °C and low solubility in common organic solvents. These physical behaviours can be enhanced and improved by functionalization at both the lower and upper rims and also the methylene bridge (Gutsche et al., 1986). For example, by modified with strong hydrophilic heads (SO_3^-) at upper rim will provides hydrophilic surrounding cavity to achieve solubility up to 0.3 mol L^{-1} (Schuette et al., 1992). By this modification also, calixarenes can perform host guest inclusion complex with many of guest compound including metal ions (Ling et al., 2010; Sayin et al., 2013), amines group (Akceylan et al., 2009; Erdemir et al., 2009; Gungor et al., 2008) and organic compound (Kalchenko et al., 2009; Kamboh et al., 2016; Shamsipur et al., 2009). Thus, this concept allows calixarenes used as trapping agent to entrap targeted analytes throughout host-guest interactions for several of applications.

2.2.3.1 Functionalization of calixarenes at lower rim and its applications

As mentioned earlier, calixarenes possessed lower and upper rims consist of hydroxyl and phenyl group respectively that are fascinating site for modification and functionalization to achieve desired properties. Usually, different derivatization route is required for attachment of ligand on lower and upper rims. S_N2 substitution reaction mechanism is required for functionalization at lower rim where hydroxyl group was deprotonated by a suitable base such as NaOH or KOH followed by addition of electrophile to produce calixarenes derivatives (Gutsche & Lin, 1986; Sreejit Rajiv Menon, 2016).

Various preparation and characterization of functionalized calixarenes have been established by immobilized with numerous of ligands including phosphates (Harrowfield et al., 1996), amides (Yaftian et al., 1998), and oxides (Yaftian et al., 2003). Such modified calixarenes has been well-studied and utilized in many kinds of applications. For extraction purposes, calixarenes reported as good extraction agents for extraction of lanthanides and actinides by using solvent extractions (Dam et al., 2007). Moreover, modified calixarenes also have been reported as coordinating agent for numerous metal ions including alkaline earth, transition and lanthanide metals (Atanassova & Kurteva, 2016; Hertel et al., 2009; Shinkai, 1993). Furthermore, modified calixarenes have been applied in area of recognition chemistry and separation chemistry by immobilized modified calixarenes at solid support surfaces and used as stationery phases (Gebauer et al., 1998; Gezici & Bayrakci, 2015; Gutsche, 2000; Ludwig, 2000).

2.3 Toluene diisocyanate (TDI) as coupling agent

The development and usage of diisocyanate started since 1940 based on the work introduced by Bayer in late of year 1937 (Allport et al., 1998). In the past decades, diisocyanate became exciting targets due to its extensive usage to make polyurethane products such as coatings, adhesives and sealants products. In 2000, the consumption of common diisocyanates reach almost 4.4 million tons worldwide (Weissermel & Arpe, 2003). These products become more comfort and safer using polyurethanes made from diisocyanates.

The common isocyanates are toluene diisocyanate (TDI), methylene diphenyl diisocyanate (MDI), isophorone diisocyanate (IPDI) and hexamethylene diisocyanate (HMDI) as showed in Figure 2.7. The presence of isocyanate group (N=C=O) makes these isocyanates compounds are highly reactive but their reactivity can be different according to their individual structure (Sonnenschein, 2015; Telli, 2014). The reactivity of isocyanates can be improved by substituents that alter the nature of electropositivity at -NCO carbon atom. This can be explained by attacking of nucleophiles to carbocation and attacking of electrophiles to negative character of oxygen and nitrogen atom (Sharmin & Zafar, 2012). The reactivity of isocyanates will be lower with the presence of electron donating group as substituent, meanwhile the electron withdrawing group will enhances the reactivity of -NCO group (Ionescu, 2005). But, in the case aromatic group as substituent, it will act as electron withdrawing character and the negative charge will be delocalized at aromatic ring. Therefore, isocyanates which are own aromatic ring such as TDI and MDI have higher reactivity than aliphatic isocyanates such as IPDI and HMDI (Ionescu, 2005; Sharmin & Zafar, 2012). More than that, the reactivity also depends on the steric hindrance. For such reason, MDI have higher reactivity than TDI due to less steric hindrance. For aromatic isocyanates, the position of -NCO functional groups at aromatic ring result different reactivity. For example, -NCO at para position is higher

reactivity than ortho position with ratio of 100:12 in 2,4-TDI. In case of MDI, the -NCO group attached in different aromatic rings, thus the reactivities are same for -NCO functional groups.

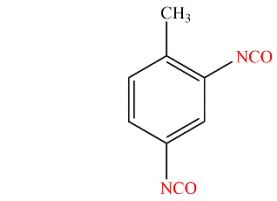

2, 4- toluene diisocyanate (TDI)

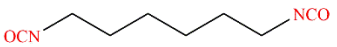

1, 6- hexamethylene diisocyanate (HMDI)

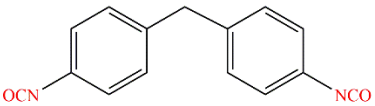

1, 4- methylene diphenyl diisocyanate (MDI)

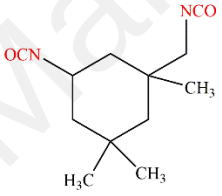

1, 5- isophorone diisocyanate (IPDI)

Figure 2.7: Structure of common isocyanates group

As coupling function, isocyanates have been applied as important agent in wide area of chemistry for incorporated between compounds from polymers and material to biomolecular science because of its high and specific reactivities. The functional group -NCO is highly vulnerable to react with hydroxyl group attached at foreign compounds (Gironès et al., 2007; Joseph et al., 2003; Nair & Thomas, 2003). Wu et. al also successfully grafted isocyanate-terminated elastomers onto the hydroxyl and carboxyl attached at carbon fibers surface (Wu, Pittman, & Gardner, 1996). Isocyanate also have been attached onto hydroxyl group at fiber surface as reported in literature (Joseph et al., 1996; Paul et al., 1997; Sreekala & Thomas, 2003). Based on reported work by Joseph and co-workers (Joseph et al., 1996), TDI applied as coupling agent for incorporation between cellulosic sisal fiber and cardanol. First, urethane cardanol derivative of TDI was

prepared by reaction of cardanol and TDI. In final step, the fiber will be attached at reserved isocyanate functional group and formed sisal fiber-LDPE composites. This showed the isocyanate act as bridge to link cardanol and cellulose fiber. More than that, the use of coupling agent also helps to improves the interfacial bonding strength in fiber-polymer composite and improving mechanical properties of the composite by slowing down the mitigated movement of moisture throughout the composite (Bengtsson & Oksman, 2006; Nachtigall et al., 2007).

2.4 Nanoparticles

Science based nanomaterial and nanotechnologies has been rising and provided a new broad dimension to solving the challenges facing in various scientific fields including biomedical (Akrami et al., 2015), engineering (Dalvand et al., 2016), chemistry (Khoobi et al., 2014), environmental (Khoobi et al., 2015; Sadri et al., 2014) and biotechnology (Tarasi et al., 2016). This extensive development in nanotechnology makes it become important technique to produce many recent advance researches due to its ability working at molecular and cellular levels. Among different nanomaterial types, nanoparticles (NPs) have been intensively used worldwide in many kinds of application such as drug delivery (Liu et al., 2006), analytical separations (Rozi et al., 2017), catalysis (Zhang et al., 2013) and environmental remediation (Xu et al., 2012).

Application NPs as sorbent for sample preparation have been developed and widely used in analytical separation. The high surface area-to-volume ratio properties possessed by NPs assurances the better performance compared to other sorbents (Xie et al., 2014). It can easily be functionalized and modified to improve the selectivity and sensitivity of targeted analytes. Moreover, the functionalization of NPs renders it protected from agglomeration, makes them well-suited in other phases, enhances the chemical, physical and mechanical properties of NPs as well as control the desired properties in a suitable

way to accomplish the specific applications (Neouze & Schubert, 2008; Ruckenstein & Li, 2005; Schulz-Dobrick et al., 2005). Some of reported literature, NPs have been functionalized with various of molecule for example thiol (Woehrle & Hutchison, 2005), nitriles (Fan et al., 2005), carboxylic acid (Roux et al., 2005) and amines (Zayats et al., 2005).

In past years, the magnetism application become exciting trends in various field. By this arise, many scientists started to take advantage with the development of NPs to begin working with magnetic nano-material or magnetic nanoparticles to make better improvement on existing technologies. It offers a great benefit in many applications. For example, in analytical technique, magnetic interaction is not influenced by chemical parameters such as pH, surface charge or concentration and also it can allow to control fluid motion in microsystem which are crucial for chromatographic separation (Faraji, 2016; Xie et al., 2014).

Magnetic nanoparticles (MNPs) is one of NPs that widely used in various kind of applications. There are several types of MNPs including iron oxides (Fe_3O_4 and Fe_2O_3), manganese, nickel, cobalt and magnesium (Beveridge et al., 2011). But the most commonly used and employed in analytical technique is iron oxides which is magnetite (Fe_3O_4), hematite (α-Fe_2O_3) and maghemite (γ-Fe_2O_3) due to easily synthesized with high magnetic moments. Iron oxides also is mostly reported in literature because of their biocompatible and have good susceptibility and saturation magnetization. Thus, it become the only NPs material that have been approved by U.S Food and Drug Administration (US FDA) for use (Beveridge et al., 2011). For separation and pre-concentration purposes, applying MNPs as sorbent promising in development of new technique which is faster, simple and more accurate compared to available methods. The most useful of MNPs in this methodology is the MNPs can easily be separated from solution by a simple and compact process and reduce the producing of secondary wastes.

MNPs also have a high surface area for a given mass, low toxicity, low price, and have ability to immobilise the targeted particles at specific location in a column by applying an external magnetic field (Ibarra et al., 2015).

Various method and technique have been reported for synthesis of MNPs with suitable and proper particle size, structure, shape and poly-disparity (Taeghwan Hyeon, 2003). Co-precipitation (Khalafi-Nezhad et al., 2015), chemical vapour deposition (Park et al., 2006), sol-gel method (Liu et al., 2013), hydrothermal (Takami et al., 2007), microemulsion (Malik et al., 2012) and electrochemical (Starowicz et al., 2011) are the example of MNPs synthesis method. So far, the preparation of MNPs for industrial purposes is applicable by using limited technique because of high cost and safety problem. In lab scale, chemical co-precipitation has been widely used for preparation of MNPs due to its large volume capability, simple steps, economical and produce good yield of product (Vashist, 2013). This method allowing both nucleation and growth of iron hydroxide nuclei to be controlled since it was carried out in aqueous monophasic liquid medium and produced insoluble solid. The technique is based on the reaction of hydrated ferric and ferrous chloride in base aqueous solutions at room temperature (Indira & Lakshmi, 2010). The viscous iron hydroxide precipitates produced are isolated by centrifugation or decantation. In order to electrostatically stabilize the iron hydroxide precipitate, it was treated with concentrated acid or base solutions or by heat the precipitate in the presence of suitable surfactants. Based on reported work, synthesizing MNP by this method results of broad particle size distributions and irregular morphology structure (Tartaj et al., 2003). However, to obtained suitable diameter, surface properties and magnetic responsiveness of MNPs, it is depending on appropriate stoichiometry ratio of ferrous and ferric salt mixture in aqueous solution as well as experimental parameters such as pH, time types of salts, temperature, base concentration, and ionic strength. The

synthesis of MNPs using co-precipitation shown in equation (Vashist, 2013; (Indira & Lakshmi, 2010).

$$Fe^{2+} + 2Fe^{3+} + 8OH^{-} \rightarrow Fe(OH)_2 \quad (2.1)$$

$$Fe(OH)_2 + 2Fe(OH)_3 \rightarrow Fe_3O_4 + 4H_2O \quad (2.2)$$

2.5 Application of magnetic hybrid materials as adsorbent in sample pre-treatment

In analytical method, sample pre-treatment is the important steps for whole analytical process as it can eliminate matrix effects and pre-concentrate the analytes (Wierucka & Biziuk, 2014). For such purpose, suitable and effective adsorbent is necessary capture and extract the analytes from environmental samples. Adsorbent is defined as solid substance upon it surface the adsorption may occur. Adsorbent can exist in various of shape such as pellets, rods, monolith or moldings with diameter of 0.5 to 1.0 mm. Absorbent usually resistance to abrasion, high thermal conductivity and high surface area to ensure surface area is highly exposed and thus high surface capacity for adsorption obtained. For gaseous vapour, it recommended to adsorbent possess distinct pore structure for fast transport. Another important properties of adsorbent are high selectivity, high regeneration, economical and good interaction with adsorbate. Adsorbent also can be categorized according their characteristic such as pore sizes, structure and nature of surfaces. Table 2.2 shows a classification of adsorbent based on their pore sizes (Eduard Musin, 2013; Sayigan, 2013).

Table 2.2: Classification of adsorbents based on pore sizes

Classification	Pore size, d (nm)					
	Macro	**Meso**	**Micro**	**Super micro**	**Ultra-micro**	**Sub micro**
IUPAC	>50	25	2-0.4	0.7	<0.7	<0.4
Dubinin	>200 - 400	200 - 400>d >1.0	<0.8	1.0>d >0.8	-	-
Cheremkoj	>2000	-	2000>d> 200	-	<0.5	<200
Kodikara	0.01	-	0.03	0.025	<0.75	-

It is well-known that adsorption is an important phenomenon which adsorbent surface are interact with any liquid or gaseous substance known as adsorbate as shown in Figure 2.8. It is occurring at solid-liquid interface because of atomic or molecular interaction (Sayigan, 2013). Adsorption also can be physisorption or chemisorption or combination of those depending on type of interaction exist at the boundary of two phases. Adsorption process is frequently studied and well establish method and actively applied by many industrial and institution worldwide for treating wastewater effluent. More than that, this technique found to be interesting and excellent method for many kind of application such as gas separation of N_2 from O_2 and purification of organic from gas phase (Repo, 2011).

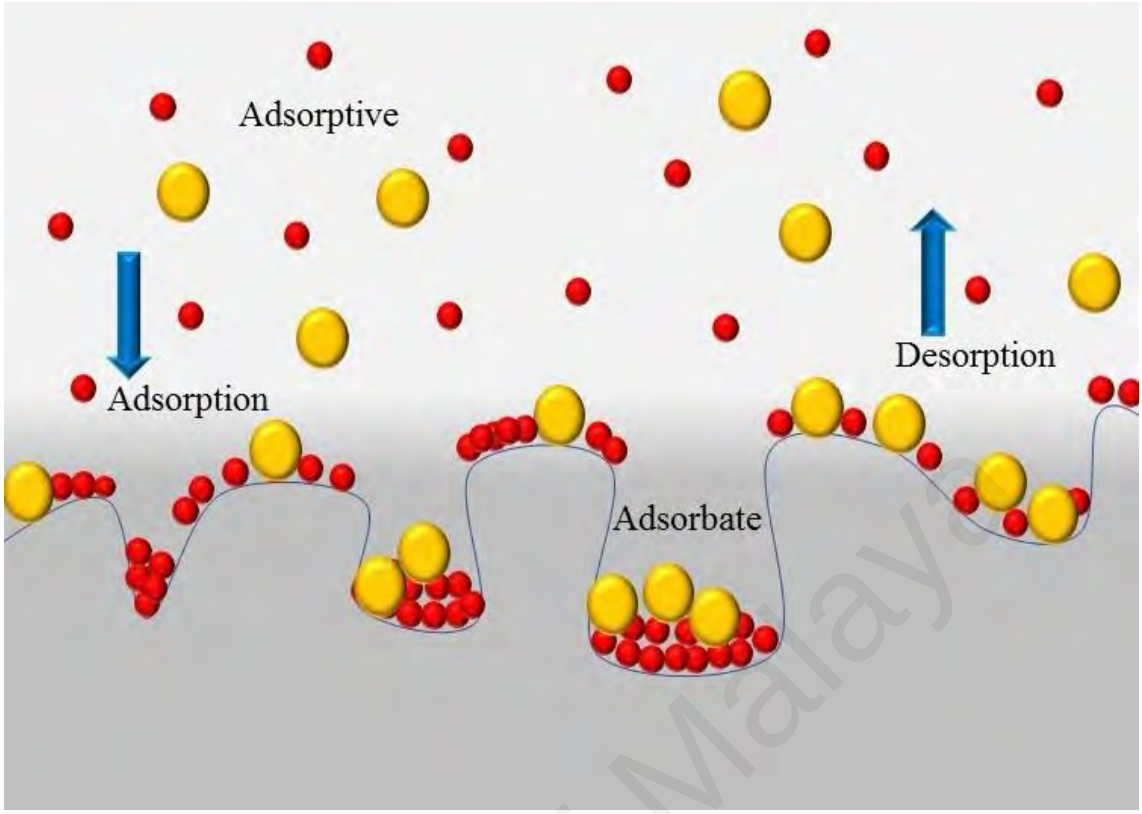

Figure 2.8: Phenomena of adsorption (Sayigan, 2013)

Analysis of trace level residues usually involve a tedious and difficult process. Sampling, sample preservation, storage, sample pre-treatment and analysis are the steps of analytical procedure. During sample pre-treatment, the analytes can be contaminated or loss to surrounding. Thus, a suitable adsorbent selection, complexity of analytical matrix and analytes concentration in sample become an important factor for promising successful extraction (Ibarra et al., 2015).

In recent years, there has been an increasing amount of literature on magnetic hybrid material that can be magnetically separated for many application especially analytical and environmental chemistry. Numerous of reported publication have attempted to explain the useful of magnetic hybrid material for pre-concentration and extract the pollutants. Nodeh and co-workers successfully synthesize the magnetic graphene-based cyanopropyltriethoxysilane material for extraction of organophosphorus pesticides in cow milk (Nodeh et al., 2016). Extraction of organic pollutant such as bisphenol A (BPA)

also have also been proposed by Ji and co-workers using magnetic moleculary imprinted (MIP) modified with methacryloxypropyltrimethoxysilane (MAPS) and mixed with template of BPA, vinylpyridine as functional monomer, cross linking ethylene glycol dimethacrylate and hexadecanol as hydrophobic agent to produce magnetic BPA-MIP (Fe_3O_4-BPA-MIP). This magnetic hybrid MIP showed excellent selectivity of BPA and give higher adsorption of BPA in aqueous solution (Ji et al., 2009). Other type of contaminate such as poly aromatic hydrocarbons (PAHs) have been extracted in environmental samples (Bai et al., 2010). Their research work on preparation of magnetic hybrid material of carbon-ferromagnetic nanocomposite (Fe_3O_4@C). The exclusive properties of prepared sorbent that it was designed with a hydrophilic surface and hydrophobic sublayer to give high extraction efficiency and provide compatibility surroundings with sample matrix. Moreover, the prepared adsorbent is further studied by Heidari and co-worker for the extraction of pesticides from water samples (Heidari & Razmi, 2012). Apart from that, research conducted by Saraji and co-worker (Saraji & Ghani, 2014) synthesized a novel magnetic aluminium-magnesium layered double hydroxide adsorbent and applied as an effective sorbent for extraction of organic compound. It was found that some of phenolic acid compounds such as benzoic acid, syringic acid and ferulic acid can be extracted from fruit juices water sample and achieve a good limit of detection between 0.44 - 1.30 μg/L.

By combination of magnetic hybrids materials and adsorptive process helps to improvise for purification of water and environmental technology. In sample pre-treatment, the rapid, simple and efficient technique are required to ensure a high recoveries of analytes at trace level prior instrumental analysis. The most likely reason behind this circumstances is common chromatographic analysis such as liquid chromatography (LC) and gas chromatographic (GC) is not well-suited and insufficient in terms of selectivity and sensitivity for direct measurement and detection of analytes

which are usually at trace level and having complex sample matrices. Due to this scenario, magnetic solid phase extraction (MSPE) was developed and received a tremendous interest during recent years. MSPE is based by using solid magnetic as adsorbent to extract the targeted compound from the samples (Ibarra et al., 2015).

Historically, Šafařîková and Šafařîk announced and presented the new magnetic SPE technique in 1999 as a new method for pre-concentrating the targeted analytes by using of magnetic adsorbent. The first experiment conducted by employing this new technique is the experiment separation of safranin O and crystal violet by using copper phthalocyanine dye attached silanized magnetite and magnetic charcoal as adsorbent with the results up to 460-fold of enrichment factors (Šafaříková & Šafařík, 1999). This method adapted from classical solid phase extraction (SPE) which is most reliable and virtual methods compared to another classical method such as liquid-liquid extraction due to its high recovery and selectivity. However, this SPE technique have some drawbacks for example tedious procedures, time consuming, large solvents loss, not environmentally friendly due to large waste and high exorbitant for sample equipment (Asgharinezhad et al., 2014). Thus, MSPE as alternative technique was developed to overcome the limitations of SPE. Most literature reported MSPE was a simple, economical, high rapidity and efficiency and most of important is no requirement of filtration and/or centrifugation for sample separation (Wan Ibrahim et al., 2015; Wang et al., 2013).

The procedure of MSPE is illustrated in Figure 2.9. Magnetic adsorbent is applied and dispersed in water samples or suspension to adsorb the interest analytes. This enable the magnetic adsorbent to make direct contact of with water sample, thus enhance the adsorption selectivity of analytes on the magnetic adsorbent surfaces. Then, the magnetic adsorbent was removed from the solution assisted by external magnetic field without include any additional process such as filtration or centrifugation. Finally, the suitable

organic solvent with appropriate amount was used to desorb the analytes from the solution (Šafaříková & Šafařík, 1999).

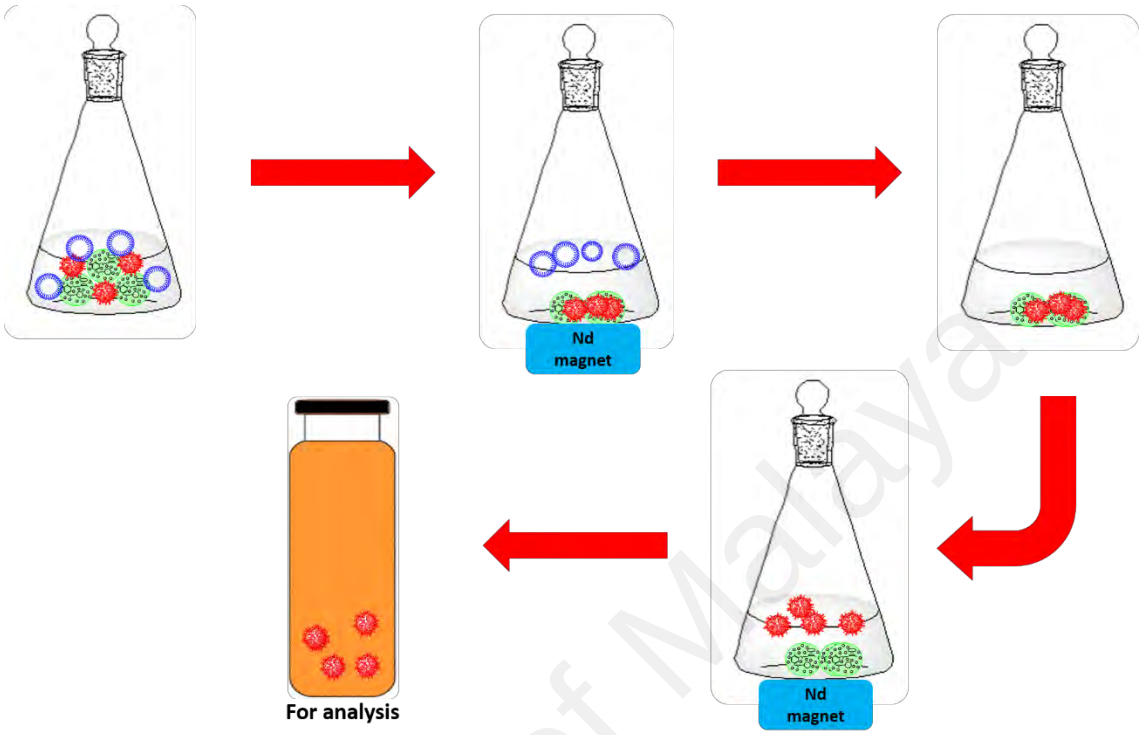

Figure 2.9: Summary of MSPE process

Several literatures have been reporting the application of MSPE in various environmental sample matrices. Mirzajani and co-worker reported the extraction of malachite green dye from food and water sample by using melamine supported magnetic iron oxide nanoparticles (Fe_3O_4@Mel). The sample was analysed by using UV-Vis spectrophotometer. MSPE applied in this experiment showed an excellent recovery 90.1% - 107.8% in water sample and 87.5% - 103.7% in food sample. The limit of detection of dye was measured is 0.05 mg/ml (Mirzajani & Ahmadi, 2015). In tea drink samples, pyrethroids one of pesticides have been identified and quantified by applying the MSPE as sample pre-treatment using polyaniline coated magnetic particle (Fe_3O_4/C/PANI microbowls) as demonstrated by Wang and co-workers (Wang et al., 2014). Low LOD (0.025 - 0.032 ng/ml) with high recovery of 72.1% - 118.4% as well as

reusability up to 15 times indicating MSPE giving rapidity and frequent use without effecting in recovery. Moreover, the combination of microbowls and polyaniline increased the reusability and stability of prepared adsorbent because of its π-electron. Pre-concentration of metal ion lead from tomato paste and parsley vegetables prior AAS analysis was carried out by applied a magnetic adsorbent of 3-aminopropyl-triethoxysilane-phthalic anhydride functionalized calcium ferrite. Good selectivity towards lead ion in sample matrix with recovery of 99.7% in tomato real sample and 91.3% in parsley proved the applied MSPE is suitable technique to determine trace amount of lead with excellent LOD up to 0.78 ng/ml (Pirouz et al., 2015). Another application MSPE in different type of samples is summarized in Table 2.3. Based on pioneering work reported showed MSPE became the important and trending as substitute method for replacing classical technique for extracting and pre-concentrating of trace analytes in various kind of environmental matrices.

Table 2.3: Summary of MSPE application using different magnetic adsorbent material towards various type of analytes in real samples

Adsorbent magnetic material	Analytes	Type of real samples	Limit of detection (LOD)	Recovery	Reference
Magnetic nanoparticles grafted superhydrophobic free fatty acid (FFA@MNP)	Polycyclic aromatics hydrocarbons	Water samples (leachate and sludge)	0.001-0.05 ng/ml	82.8 - 116.6	(Khalijah et al., 2016)
MMIP-Fe_3O_4-oxyetetracycline	Tetracycline	Biological samples (eggs and tissue)	<0.2 ng/g	72.8 - 96.5	(Chen et al., 2009)
Fe_3O_4@SiO_2@ionic liquid	Linuron	Food samples (apple and lettuce)	0.04 - 20 µg/ml	95.0- 98.5	(Jieping Chen & Zhu, 2015)
Aptamer for ochratoxin immobilized magnetic nanosphere	Ochratoxin A	Food sample (cereal)	0.3 µg/kg	67.2 - 87.8	(Mashhadizadeh et al., 2013)
Lead imprinted polymer-vinyl-diphenylcarbazide@ SiO_2@ Fe_3O_4@ ethylene glycol dimethylacrylate and azobisisbutyronitrile	Lead	Biological samples (muscle and liver)	1.3 ng/ml	95.0 - 115.0	(Najafi et al., 2013)

Table 2.3, continued

Adsorbent magnetic material	Analytes	Type of real samples	Limit of detection (LOD)	Recovery	Reference
MMIP (Fe_3O_4@SiO_2)-chloramphenicol-oleic acid0-ehylene glycol dimethacrylate	Chloramphenicol	Food sample (honey)	0.047 ng/g	84.3 - 90.9	(Chen & Li, 2013)
Zinc imprinted polymer-2-vunylpyridine-ethylene gycol dimethacrylate-Fe_3O_4	Zinc	Food samples (parsley and basil)	0.15 mg/L	95.0 - 99.0	(Behbahani et al., 2014)
Fe_3O_4@magnesium-aluminium layered double hydroxide	Phenolic acids	Drinking water samples (fruit juice)	0.44-1.3 ng/ml	81.2 - 100.0	(Saraji & Ghani, 2014)
Cyano-ionic liquid functionalized magnetic nanoparticles (MNP@CN/IL)	Polycyclic aromatics hydrocarbons, chlorophenols	Water samples (leachate and sludge)	0.40-0.59 ng/ml (PAHs) 0.35-0.67 ng/ml (CPs)	89.5 - 110.2 (PAHs) 80.67-112.7 (CPs)	(Bakhshaei et al., 2016)
Tetraethylenepentamine functionalized magnetic polymer	Additives	Drinking waters (soft drinks)	0.06-0.15 mg/L	80.1 - 97.1	(Zhao et al., 2013)

2.6 Pharmaceuticals in the environmental

2.6.1 Overview

Each year, nearly 100,000 different of pharmaceutical based product are manufactured and their consumption can be varying for certain country (Kümmerer, 2009). Over last decade, over 50,000 of pharmaceutical product were registered in Germany and most of products has been sold in the 100 tons per year. These include the diclofenac (85 tons), carbamazepine (87 tons) and acetylsalicyclic acid (836 tons) (Kümmerer, 2008). Meanwhile in England, approximately 390 tons of paracetamol and 345 tons of ibuprofen have been sold within past years (Fent et al., 2006). This extensive and high consumable of pharmaceutical in human as well for veterinary treatment has become great concern among environmentalist due to highly toxic and high biologically activity of pharmaceutical residues that affecting biological systems (Pascoe et al., 2003). Numerous research have been employed on detection various of compounds such as antibiotic, pesticides, synthetic estrogens, polychlorinated biphenyls, and polycyclic aromatic hydrocarbons. Filby and co-workers reported that synthetic estrogens such as 17β-estradiol and 17α-ethinylestradiol are ubiquitous in environment in trace level (ng/L) and affects the health and physiology of wildlife (Filby et al., 2007). Diaz-Cruz and co-workers also reported the highly intake of antibiotics has led to genetic selection of resilient and harmful bacteria which is put the human and environmental at risk (Díaz-Cruz et al., 2003).

Pharmaceuticals were introduced into natural streams through several routes. Pharmaceutical enter the aquatic ecosystem and pose toxic effect which harm not only to aquatic life but also to human health (Jones et al., 2005). This is because pharmaceutical compound exists as complex mixture in aquatic surrounding which produce high toxic effect compared individual toxicity. Quinn and co-workers proves that the toxicity of individual effluent pharmaceuticals and a mixture was found to be 2 to 3-fold of

magnitude greater compared the toxicity of individual drugs (Quinn et al., 2009). Pharmaceutical and their residues enter the wastewater treatment plants (WWTPs) after human application throughout urine and faeces. Some of the pharmaceutical compound which are not degradable are discharged within wastewater effluents caused the water continuously receiving input of pharmaceutical compounds at low concentration. Yu et al. confirmed that wastewater treatment process was not adequate to remove the pharmaceutical products based on analysis of sewage sample from Baltimore Black River, USA (Yu, Bouwer, & Coelhan, 2006). Wastewater discharged from pharmaceutical industries and hospitals also contribute the amounts of pharmaceutical compounds in the environment. In addition, the sludges produced in WWTPs that used as fertiliser in various fields will contaminate the soil (Bound & Voulvoulis, 2005). The manure collected from the animal which are contaminated with pharmaceutical compound in veterinary procedure has been used and applied to landfill are potentially leaching to ground waters or reach surface water via run-offs (Koutsouba et al., 2003). Besides that, the uses of additives such as growth promoters and antibiotics in agriculture field leading to direct contamination in soil and waters (Díaz-Cruz et al., 2003). Figure 2.10 illustrates the route of pharmaceutical enter the environment.

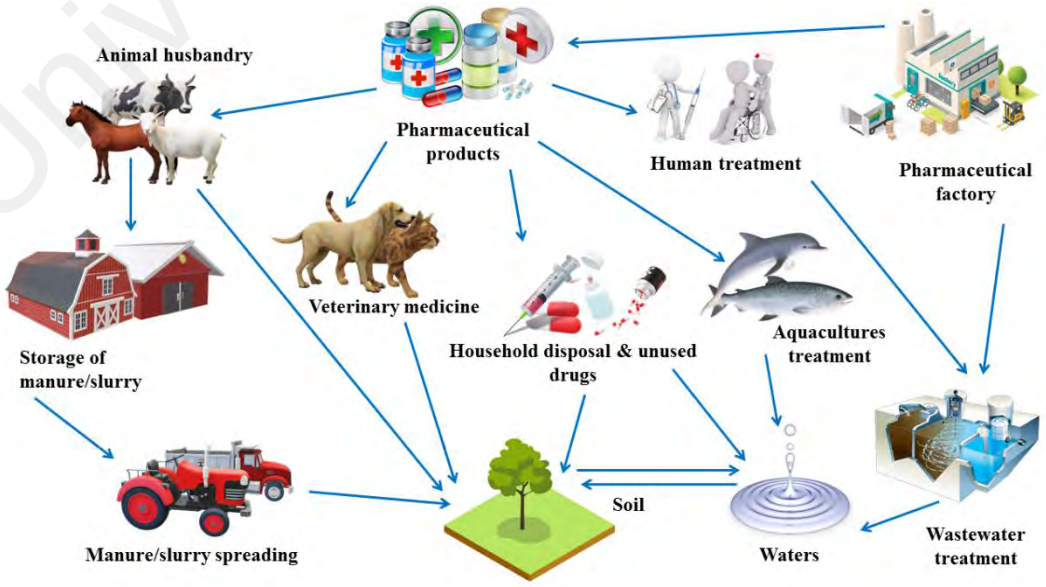

Figure 2.10: Schematic pathway of pharmaceutical enter the environment

2.7 Non-steroidal anti-inflammatory drugs (NSAIDs)

Non-steroidal anti-inflammatory drugs (NSAIDs) are pharmaceutical drugs which are categorized as a group of anti-inflammatory, antipyretic and analgesic to relieve pain and inflammatory, as well as related clinical effects (Gentili, 2007). Back to 1899, acetylsalicylic acid was the first registered NSAIDs synthesized by German Bayer Company (Feng, 2014). Nowadays, there are more than hundred compound covered under NSAIDs group on the market worldwide. NSAIDs is prominent drugs that have been consumed by more than 30 million of people worldwide and by the animal in veterinary practices (Feng, 2014).

In USA, more than 30 billion of doses of NSAIDs were taken and as for children under five-year-old, about 50, 801 of ingestions of NSAIDs have been documented (Gummin et al., 2017). More than that, based on annual report from Italian Agency for Drugs (AIFA), more than 393.7 million of daily doses were distributed in Italy for past few years (Mainero Rocca et al., 2015). In Malaysia, according to Anatomical Therapeutic Chemical (ATC) in year 2007, NSAIDs ranking among top ten most frequently utilized drugs and cause increment of life cost and poor lifestyle (Khairudin et al., 2017). Figure 2.11 illustrates the structure of selected NSAIDs with pK_a value.

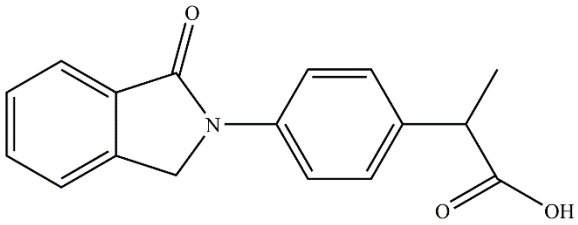

Indoprofen (pK_a = 4.4)[a]

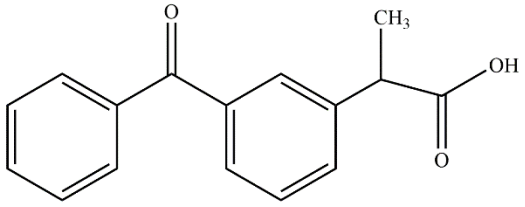

Ketoprofen (pK_a = 4.2)[a]

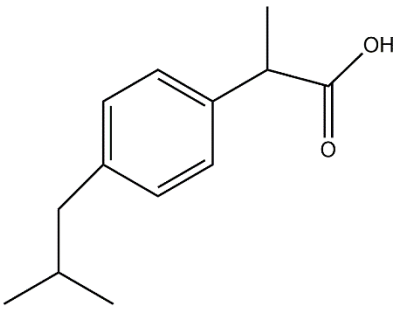

Ibuprofen (pK_a = 4.51)[a]

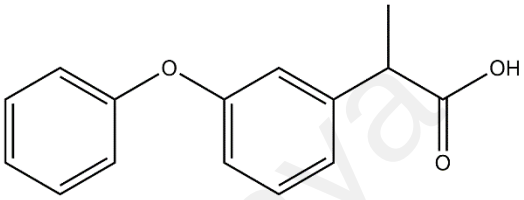

Fenoprofen (pK_a = 4.5)[b]

Figure 2.11: Structure of selected NSAIDs

NSAIDs are composed of heterogeneous group of drugs with several of therapeutic properties that rank intermediately between major opioid analgesics properties in one part and corticoids with anti-inflammatory on other part (Feng, 2014). These drugs have different chemical structure and have three mutual features in term of therapeutic capacity such as have similar pharmacological properties, same adverse effects and identical basic mechanism of action (Meucci et al., 2014). NSAIDs can be grouped based on their chemical structures. This includes salicylic acid derivatives, aryl propionic acids, pyrazolon derivatives, enolic acids, *p*-aminophenol derivatives, indole indene derivatives, heteroaryl acetic acid, anthralinic acids and alkanones (Fan et al., 2014). The classification and properties of selected and other types of NSAIDs are tabulated in Table 2.4.

Table 2.4: Classification and physical properties of NSAIDs

NSAIDs	Formula	Molecular mass (g/mol)	Solublity (mg/L) at 25 °C	pK_a	Classification	IUPAC name
Indoprofen	$C_{17}H_{15}NO_3$	281.3	42.2	4.4	Carboxylic acids	2-[4-(3-oxo-1H-isoindol-2-yl)phenyl]propanoic acid
Ketoprofen	$C_{16}H_{14}O_3$	254.3	51.0	4.2	Carboxylic acids	2-(3-benzoylphenyl)propanoic acid
Ibuprofen	$C_{13}H_{18}O_2$	206.3	21	4.5	Carboxylic acids	2-(4-(2-methylpropyl)phenyl)propanoic acid
Fenoprofen	$C_{15}H_{14}O_3$	242.2	81.1	4.5	Carboxylic acids	2-(3-Phenoxyphenyl)propanoic acid
Naproxen	$C_{14}H_{14}O_3$	230.3	144	4.15	Carboxylic acids	(S)-(+)-2-(6-Methoxy-2-naphthyl)propionic acid
Acetylsalicylic acid	$C_9H_8O_4$	180.2	4600	3.5	Carboxylic acids	2-acetoxybenzoic acid
Paracetamol	$C_8H_9NO_2$	151.2	12900	9.38	*p*-aminophenol	N-(4-hydroxyphenyl)acetamide
Meloxicam	$C_{14}H_{13}N_3O_4S_2$	351.4	7.15	4.2	Enolic acids	4-hydroxy-2-methyl-*N*-(5-methyl-2-thiazolyl)-2*H*-1,2-benzothiazine-3-carboxamide-1,1-dioxide
Phenylbutazone	$C_{19}H_{20}N_2O_2$	308.4	47.5	4.4	Enolic acids	4-butyl-1,2-diphenyl-3,5-pyrazolidinedione

NSAIDs usually consumed by human in tablet form via orally administered but it also may be alternatively administered via intramuscularly and intravenously referred as parenteral administered which has potentially reducing the gastric irritation, rectally or topically (Garth-greeves, 2016). NSAIDs begin to show its effects to reduce the pain within several minutes after intravenous administration, meanwhile for oral administration is expected to be relatively slow until one hour after administration. The solubility of NSAIDs in gastrointestinal tract and absorption in the body also plays an important factor to determine the bioavailability of the compound to reach the specific organs (Garth-greeves, 2016).

All types of NSAIDs have similar mode of action as analgesic, antipyretic and anti-inflammatory properties. Although the exact mode of action is not well defined, however the main role of NSAIDs is inhibits the production of cyclooxygenase enzyme (COX) (Modi et al., 2012). NSAIDs can prevent and blocking the fatty acid such as arachidonic acid from being metabolized by COX enzyme. This arachidonic acid acts as substrate for inflammatory mediators and produce eicosanoid mediators through a series of cascade reactions. With presence of this mediators; thromboxane and prostaglandin level will increase which are responsible for express pain, fever and inflammation within human body. Therefore, by consumption of NSAIDs will supress these chemicals and inhibits the inflammation at the injury site (Chandrasekharan & Simmons, 2004; Fan et al., 2014; Ishikawa & Herschman, 2007; Kovala-Demertzi, 2006; Vane, 1971).

Although NSAIDs brings many advantages to human in terms of medication, their long terms and continuous administration may bring negative side effects such as cardiovascular and gastrointestinal bleeding. Ulcer, nephrosis, aplastic anaemia, live and kidney failure and some minor effects such as nausea, diarrhoea, vomiting, loss appetite and constipation are some of associated negative side effects of NSAIDs if taken in overdose. Even worst, it can cause death during the treatment without any symptom for

people who consumed prolonged NSAID, alcoholic and illness elderly people (Shukri et al., 2015).

Not only harmful to human if overdose, NSAIDs also give negative effects to environment. As discussed earlier, pharmaceutical products can enter the water samples in several of routes and affecting the environment. This also applicable for NSAIDs who has been reported as emerging pollutants to environment due to high environmental distribution and its toxicological effects to ecosystem (Kuo et al., 2010). Besides human and animal excreted wastes, NSAIDs can reach to environment by another factors, for example the improper disposal of wastes such as flushing the expired or unused drugs, commercial food treatment process, and hospitals as well as pharmaceutical industries (Farré et al., 2008; Toledo-Neira & Álvarez-Lueje, 2015). It has been recorded that up to 16 000 tons of pharmaceutical NSAIDs are disposed from human medical care and estimated about 70% of these disposed product was flushed in toilet or disposed with normal household waste procedure each year in Germany (Scheytt et al., 2006; Ziylan & Ince, 2011).

NSAIDs owned high polarity and poor degradation effect in water against biological and conventional chemical treatment and makes NSAIDs are not removed completely during water treatment process. Due to this circumstances, NSAIDs ubiquitous founded in ground water, surface water, drinking water, river water and wastewater treatment plant (Farré et al., 2008). Based on reported literatures, the detection limit of NSAIDs in these water have reached at the ppt - ppb level (Kuo et al., 2010). For example, ketoprofen has been detected in wastewater treatment plant effluents with concentration up to 3.92 ppb (Luo et al., 2014). In river water, ibuprofen has been found at low concentration between 1.4 ppb (Costi et al., 2008). Finally, in surface water, more than 0.37 ppb of diclofenac has been found at Greifensee Lake, Switzerland (Buser et al., 1998).

NSAIDs are designed persistent to overcome biodegradation and maintain their chemical structure consistently. This is reason NSAIDs has a high bioavailability ability working as healing agent. Due to this scenario, and also high consumption and high excretion to environment, they will remain in water samples for a long period and considered as lethal compound. Once NSAIDs being released to aqueous water samples, it would become toxic and harmful to human and animals. Some research shown the development and reproduction of fish has been affected after chronic exposure of ibuprofen (David & Pancharatna, 2009; Flippin et al., 2007). Ketoprofen also has been detected in high toxic level in vulture food supply based on surveys of livestock carcasses in India. Moreover, in outside Asia, the presence of flunixin has been detected in kidney and liver samples of wild Eurasian Griffon Vulture which is responsible for bird's visceral gout and massive die-off (Wang et al., 2017).

The most challenging part for pharmaceutical in environment is to reach down the detection limit in trace level with complex matrix effect in real samples. Different instrumentation has been developed and employed to determine NSAIDs in environmental water samples such as high-performance liquid chromatography (HPLC), gas chromatography (GC), capillary electrophoresis (CE), with various of detector and/or mass spectrometry (MS). However, GC technique are incompatible with most pharmaceutical compound due to lack of volatility and be go through with derivatized process. Although GC is well established and less affected by sample matrix interferences, but it cannot avoid of lengthy process which is time-consuming and also labour-intensive (Koutsouba et al., 2003; Metcalfe et al., 2003). CE offers a high efficiency separation but low sensitivity as a drawbacks (Ahrer et al., 2001). Therefore, numerous study has employed HPLC to analyse and detection of NSAIDs in low concentration (Abbasi, Haeri, & Sajjadifar, 2019; Li, Chen, & Shi, 2019; Wang, Li, & Chen, 2018). High resolution, high reproducibility and great automation in HPLC

promises an excellent result in determination of NSAIDs (Fan et al., 2014). Several of study have been reported including Hirai and co-workers (Hirai et al., 1997) with development method for HPLC for determination of 12 NSAIDs in urine samples and Laqicque et al. reported the quantification of 16 NSAIDs in plasma using HPLC (Lapicque et al., 1989).

2.8 Computational simulation and its application

2.8.1 Molecular docking

Molecular docking can be defined as a method to measure the suitable binding sites with a best evaluation of energy with as many degree of freedom as possible (Goodsell & Olson, 1990). It also can be described as approach to find the best binding sites between receptor and ligand (Fatiha et al., 2015). Molecular docking can be classified into two classes which are molecular docking and reverse molecular docking. Molecular docking is an approach where the molecule of interest is screened toward various receptor from various unrelated database, whereas the reverse molecular docking can be defined as the method of searching a molecule-receptor target over a large database of possible protein target. This reverse molecular docking starts from the ligand molecule and molecular docking usually begin with potential receptors (Park & Cho, 2017).

Several docking methods such as FLEXx, GOLD and DOCK has been used with combination with empirical scoring function to guess ligand orientation and position in binding affinities and binding sites towards receptor. This approaches enable the system explored a large area of the conformational space in calculation but in order to keep limited computational issues, the use of simple scoring function (energetic models) is required (Ewing et al., 2001; Jones et al., 1997; Kramer et al., 1999). Molecular docking can be divided into two stages such as conformational search and conformational energy calculation. For conformational search stage, the implementation of different algorithm

needs to be considered to achieve different objective and algorithm geometry also need to be employed for fast conformational search stages. For large database scanning, program such as TarFisDock and DOCK is very useful for finding the relevant algorithm (Ewing et al., 2001). In case for detailed conformational search, genetic algorithm or combination with other conformational approaches usually has been applied and the most suitable program implemented was AutoDock which it can emphasize on detailed molecular interaction (Morris et al., 1998). As for energy calculation conformational, energy calculation usually based on AMBER force field and more conserved.

Several works have been published to evaluate the possible binding sites of host and guest molecule via molecular docking technique. The study of interaction inclusion complex between β-CD and insulin dimer using molecular docking. The results revealed that four β-CD molecule are able to bind with insulin molecule (Fatiha et al., 2015). In addition, the binding interaction of D-glucose with insulin also has been studied using molecular docking (Zoete, Meuwly, & Karplus, 2004). The application of molecular docking to investigate the activities of novel co-crystal containing 5-fluorouracil against colorectal cancer target protein have been reported. The result found that the co-crystal was interact with protein via formation of hydrogen bonding (Izzati et al., 2016). Hence, the molecular docking was useful to rationalize the interaction between host and guest molecule.

2.8.2 Molecular dynamics (MD)

First exposure of molecular dynamics simulation was developed in 1970 to simulate hundreds of atoms to system with various of chemical and biological relevance such as protein, membrane and large macromolecular. Nowadays, simulation of system of having until approximately one hundred thousands of atoms become a routine and 500 000 of simulation can be done when the computer facilities are available (Hospital et al., 2015).

This remarkable enhancement of technology due to some limitation in experimental research such as the difficulty of controlling and defining the environment of experiment, the non-observability of physical property, the limitation of art apparatus and the inaccessible of materials in experiment. With computer simulation, these limitations can be overcome and provide a wider scope in the explanation of fundamental physics. The uses of high performance computing (HPC) and the simplicity of the basic MD algorithm causes the remarkable improvement in computer simulation. The data from experiment structures and comparative modelling data can setup as the pioneer model of the system. This simulated system can be represented at different levels of detail. One of the best system that leads to the reproduction of the actual systems is atomistic representation. However, when comes to long simulation or large system are required, coarse-grained representation become more convenient (Hospital et al., 2015).

In system definition, the key issues kept discussed is solvent representation. The explicit representation of the solvent molecule is the simplest method compared to another analysed approached methods although this method expands the size increase of simulated systems. The most solvation effects of real solvent such as hydrophobic effect could be recovered by explicit solvent. The forces acting at every atoms are known as force-fields where this potential energy is deduced from molecular structure and these forces obtained by deriving equations once system already built (Hospital et al., 2015). Although this force-fields are easy to calculate, but they are complex equations to ensure the energy and force calculations are fast for a large systems. After the individual atoms obtained the forces, classical Newton's law of motion is applied to calculate the velocities and accelerations of an atoms as well as the position of an atoms. Due to the integration of movement is numerically calculated, a shorter time step than fastest movement in the molecule would be used to avoid the instability. For biological simulation processes, it required repeatedly calculation cycle over 109 times rather just using microsecond-long

simulation, and this is the one of the advantages of coarse-grained methodologies. More simplified representation systems are being used, larger time steps are possible and thus, the effective length of the simulations could be extended. As the consequence, this would expense the simulation accuracy of the system. The application of advance algorithmic such as parallelization, fine-tuning of energy calculation or the use of graphical processing units (GPUs) will significantly improve the performance of MD simulations (Hospital et al., 2015). The Figure 2.12 illustrates the MD basic algorithm of a system.

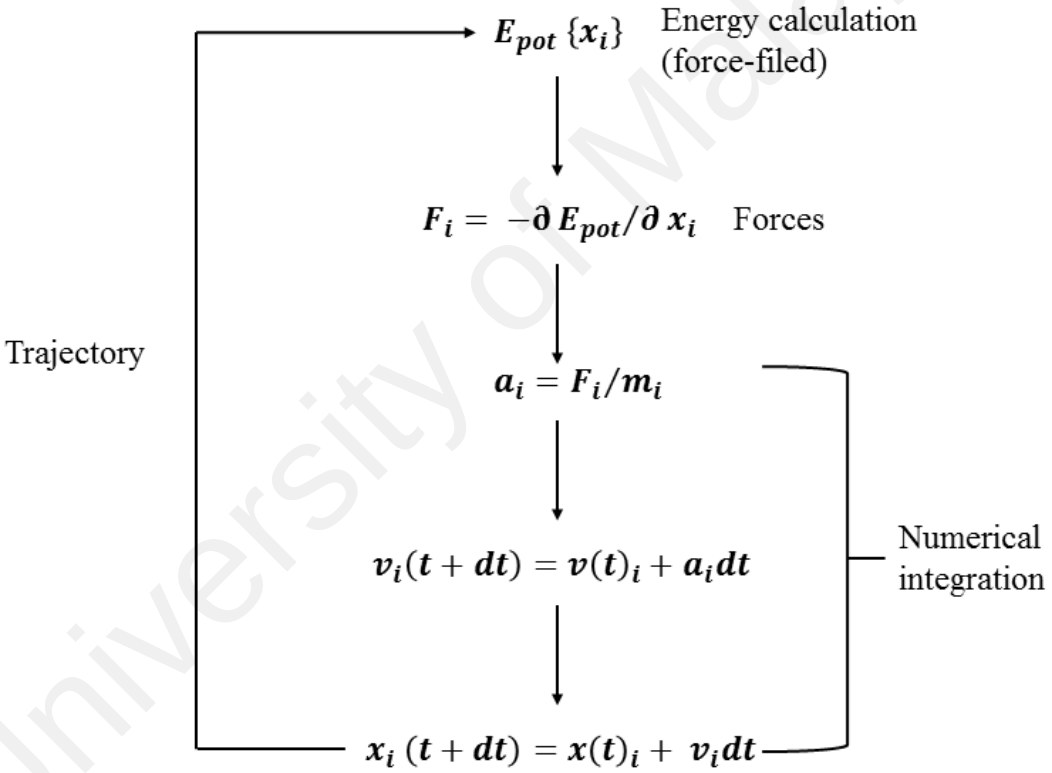

Figure 2.12: MD basic algorithm (Hospital et al., 2015)

Several simulation studies have been conducted to investigate the properties of host-guest complexes molecule by using MD simulation. β-CD complexes with benzene molecule at different temperature has been studied by using molecular dynamics, quantum mechanics and COSMO-RS techniques (Köhler & Grczelschak-Mick, 2013).

Grigera and co-workers reported the computational simulation of native cyclodextrin with phenylalanine in aqueous and vacuo medium (Grigera et al., 1998). MD simulation was carried out to study the formation and stoichiometry of cyclodextrin-fullerene complexes in explicit water as reported in literature (Raffaini & Ganazzoli, 2010). The supramolecular complexes of cyclodextrin and sodium dodecyl sulphate (SDS) have been characterized in aqueous medium by performing MD simulation at several temperatures (Brocos et al., 2010). The combination of molecular mechanics and MD has been conducted as reported by Fermeglia and co-workers to perform a β-CD-guest complexes in solvent model and its forces interaction including dipole moments, hydrogen bonding and Van der Waals interaction between host and guest to stabilizing the inclusion complexes (Fermeglia, Ferrone, Lodi, & Pricl, 2003).

2.8.3 Quantum mechanics

The main objective performing the quantum mechanics is demonstrating as spatial positions of electrons and all nuclei in an atom. Molecular orbital theory (MOT) is usually implemented where the electron reaches the lowest energy state which they allowed the freely move around fixed nuclei to achieve self-consistence field (SCF). In this state, all nuclei and electrons having repulsive and attraction forces in steady state and the nuclei can move iteratively until energy of system cannot go further to ant lower state. This state is known as geometry optimization or energy minimization which allow us to predict the most stable structure and electronic feature of the molecules (Lipkowitz, 1995). Schrodinger equation was used to solve the quantum mechanics to determine the feature and energy of molecule as shown in Equation 2.3 where H is Hamiltonian operator, E is energy and φ is wave function.

$$H\varphi = E\varphi \tag{2.3}$$

Several parameters have been derived in quantum mechanics experimental data to ease the calculation. Semi-empirical method is one of example parameter derived from QM and method that most commonly used in semi-empirical method including Austin Method 1 (AM1) (Rescifina et al., 2019), Parametric Method 3 (PM3) (Yang et al., 2004) and Parametric Method 6 (PM6) (Floresta & Rescifina, 2019). The benefits in terms of cost and accuracy is the advantages using semi-empirical method compared to another semi-empirical parameter such as ab-initio. Moreover, semi-empirical method can solve the Schrodinger equation depends to different experimental parameter with different system studied and give the calculation geometrical results in ground state accurately. Thus, this method gives a strong reasonable qualitative explanation for a molecular simulation that has been studied (Lipkowitz, 1998).

Large number of studies have been carried out in quantum semi-empirical method to investigate the application in host guest chemistry especially in the theoretical study of cyclodextrin. AM1 method have been used to study the β-CD complexes with 1,7-dioxaspiro[5.5]undecane and nonanal by carrying out the calculation with 1:1 stoichiometry as reported by Botsi and co-workers (Botsi et al., 1996). Next, the AM1 also have been carried out for calculation for β-CD complexes with steroid targeted-brain guest molecule (Bodor & Buchwald, 2002). Li and co-workers also reported the application of PM3 and AM1 calculation for comparison of native cyclodextrin complexes respectively (Li et al., 2000). With this molecular simulation, the information from computational results are useful for understanding the molecular interaction between host and guest molecule in order to improve the complex formation and for advance application in future.

CHAPTER 3: METHODOLOGY

3.1 Molecular modelling instrumental

Computer with Intel (R) Core™ i54570 CPU @ 3.20 GHz processor with Random Achieve Memory (RAM) 4.00 GB, using operational Microsoft Windows 7 Professional version 2009 64-bit system was used in the modeling and calculation for all molecules. Software GaussView & Gaussian 09W (Frisch et al., 2009), Discovery Studio (DS) Client v2.5.0.9164 (Studio, 2015), AutoDock Tools version 1.5.6 (Goodsell & Olson, 1990) and ChemBioDraw Ultra 15.0 software were used to determine all molecules structure including optimization, minimization, dynamics equilibration, dynamics production and interaction energy calculation.

3.2 Molecular docking simulation

The x-ray crystal structure for all molecules host and selected NSAIDs was retrieved from PubChem (https://pubchem.ncbi.nlm.nih.gov/) with PubChem CID as follows; β-CD (444041), *p*-tertbutylcalix[4]arene (3081771), indoprofen (3718), ketoprofen (3825), ibuprofen (3672) and fenoprofen (3342). Before performing molecular docking simulation, geometry optimization was completed. All single molecules including structure β-CD, *p*-tertbutylcalix and selected guest molecules; INP, KTP, IBP, and FNP were optimized and the most optimized single structures were determined based on the minimum energy measured in optimization process. To determine the favourable binding sites and prediction of free energy interaction between host (β-CD and calixarene) with selected NSAIDs, AutoDock Tools program and AutoDock Vina was used to perform docking studies. In docking simulation, β-CD and calixarene were used as receptor and selected NSAIDs were used as ligand. All structures were prior minimized using the AM1 method using Gaussian 09W. The files in pdbqt format were generated using AutoDock Tools as required to AutoDock Vina as input files. During docking simulation, all selected

NSAIDs were docked to host molecule individually by using the following Cartesian coordinates which is x = -0.028 Å y = -0.028 Å and z = -0.028 Å as the center of the search space and the grid maps were prepared using a 40 x 40 x 40 Å grid box. Other parameters were set as default values by AutoDock Vina. After docking process, the stable confirmation which has a lowest energy binding free energy was analyzed and selected as initial molecule for next process.

3.3 Molecular dynamics simulation

The molecular dynamics (MD) simulation was performed using several modules including Minimization process, Dynamics (Equilibrium and Production) and Interaction Energy module in the simulation package of DS 2.5. The complexes were minimized using the CHARMm force field with Momany-Rone partial charges (Momany & Rone, 1992). The parameters were set up in minimization module as follows; 500,000 steps, smart minimizer algorithm, RMS gradient of 0.001 and Distance-Dependent Dielectrics of 78.5. After minimization, the receptor-ligand complexes were performed Dynamics Equilibrium and Production Dynamics which were set for NVT ensemble for 1 ns with the target temperature of 300 K and the time step of 0.001 ps using Distance-Dependent Dielectrics of 78.5. In final module, the Interaction Energy protocol were performed on the last 500 ps trajectories of molecular dynamics complexes. Finally, the optimum pose of each ligand with the lowest binding interaction was then selected based on the CHARMm interaction energy (Dai et al., 2010).

3.4 Quantum mechanics simulation

The predicted binding model structure from docking and molecular dynamics was used as the starting material of QM simulation. The series of possible conformation complexes were subjected to optimized and calculated the interaction energy by using semi-

empirical AM1 method. The same method also was applied to calculate the geometry optimization for single molecule of host and selected NSAIDs to obtain the most optimum and stable geometrical structure. Binding energy upon complexation, ΔE for 1:1 of the single selected NSAIDs with host β-CD and calixarene respectively was calculated based on the relative energy of complex ($E_{complex}$) and the isolated host and single selected NSAIDs as the following Equation 3.1:

$$\Delta E_{1:1} = E_{complex} - \left(E_{host} + E_{guest}\right) \tag{3.1}$$

3.5 Chemicals and reagents

"*Lycopodium clavatum*" sporopollenin with a particle size of 25 μm was purchased from Aldrich (Steinheim, Germany). Selected NSAIDs namely indoprofen (INP) and fenoprofen (FNP) were obtained from Sigma-Aldrich (St Louis, MO, USA), ketoprofen (KTP) was obtained from MP Biomedicals Inc. (Fountain Pkwy, Solon, Ohio, USA) and ibuprofen was obtained from EMD Chemicals (San Diego, CA, USA). Toluene diisocyanate (TDI), and *p*-tert-butylphenol ($C_{10}H_{14}O$) were purchased from Sigma Aldrich (St Louis, MO, USA). β-cyclodextrin (β-CD) was obtained from Acros Organic (New Jersey, USA). Iron (II) chloride tetrahydrate ($FeCl_2.4h_2O$), iron (III) chloride hexahydrate ($FeCl_3.6H_2O$), ammonia (NH_3), hydrochloric acid 37% (HCl) and diphenyl ether ($C_{12}H_{10}O$) were purchased from R&M chemicals (Essex, UK). Acetic acid was obtained from J. T. Baker Avantor Performance material Inc. (Center Valley, PA, USA). Sodium hydroxide (NaOH), formaldehyde 37% (CH_2O), ethyl acetate ($C_4H_8O_2$) and other organic solvents including methanol (MeOH), ethanol (EtOH) and acetonitrile (ACN) were obtained from Merck (Darmstadt, Germany). All chemicals used were of analytical grade and used without further purification. All commercial grade solvents stored over molecular sieves (4 Å, 8 - 12 mesh) from (Steinheim, Germany). The pH of the solution

was adjusted by mixing appropriate volume of hydrochloric acid (HCl) and/or sodium hydroxide (NaOH) with concentration of 0.1 M respectively. Deionized water that had been passed through a Milli-Q system (Lane End, UK) was used for the preparation of solutions.

3.6 Instruments

The FTIR spectrum was obtained using ATR mode on a Spectrum 400 Perkin Elmer X1FTIR (UT, USA) in the range of 4000 - 450 cm^{-1} with diamond as a detector. X-ray diffraction (XRD) patterns of the samples were taken using PANalytical Empyrean X-ray diffractometer (EA Almelo, The Netherlands) from $2\Theta = 15°$ to 75° at room temperature utilizing Cu Kα radiation at a wavelength of 1.5418 Å at a scan rate of 0.02 s^{-1}. FESEM-EDX analysis was performed by using a HITACHI SU8220 scanning electronic microscopy from OXFORD Instrument (Oxfordshire, UK). The magnetization of functionalized MNP was measured using vibrating sample magnetometer (VSM LakeShore 7400 series) from Lake Shore Cryotronics, Inc (OH, USA). The surface area and porosity were measured using Brunauer-Emmett-Teller (BET) by nitrogen adsorption-desorption isotherm in Micromeritics Tristar II ASAP 2020, (GA, USA). HPLC system (Kyoto, Japan) consisted of LC-20AT pump, SPD-M20A diode array detector, SIL-20A HT autosampler and CTO-10AS VP column oven was used for NSAIDs determination. The system was equipped with a Hypersil gold C-18 reverse phase column (250 x 4.6 mm), particle size (5μm) from ThermoScience (MA, USA). The ultraviolet-visible spectrophotometry (UV-Vis) analyses were conducted by using UV-Vis spectrophotometer Shimadzu UV1800 (Kyoto, Japan) with quartz cuvette 10 mm light pathway and dimension (12.5 x 12.5 x 45 mm).

3.6.1 HPLC conditions

HPLC-DAD system was used for the chromatographic identification of the selected NSAIDs from the water samples. The chromatographic separation was carried out using acidified (1% with acetic acid) water/acetonitrile (50:50 v/v) as a mobile phase with a flow rate of 1.0 mL min^{-1} for selected NSAIDs. The column temperature of HPLC was set at 40 °C and the sample injection volume was set at 10 µL. The DAD detection for the selected NSAIDs was carried out at multiple wavelengths such as 281, 255, 271 and 219 nm for INP, KTP, IBP and FNP respectively.

3.7 Synthesis of calixarenes

3.7.1 Schematic diagram for the preparation of *p*-tertbutylcalix[4]arene

The synthesis of *p*-tertbutylcalix[4]arene from *p*-tert-butylphenol via base induce synthesis of phenol are showed in Figure 3.1 as below.

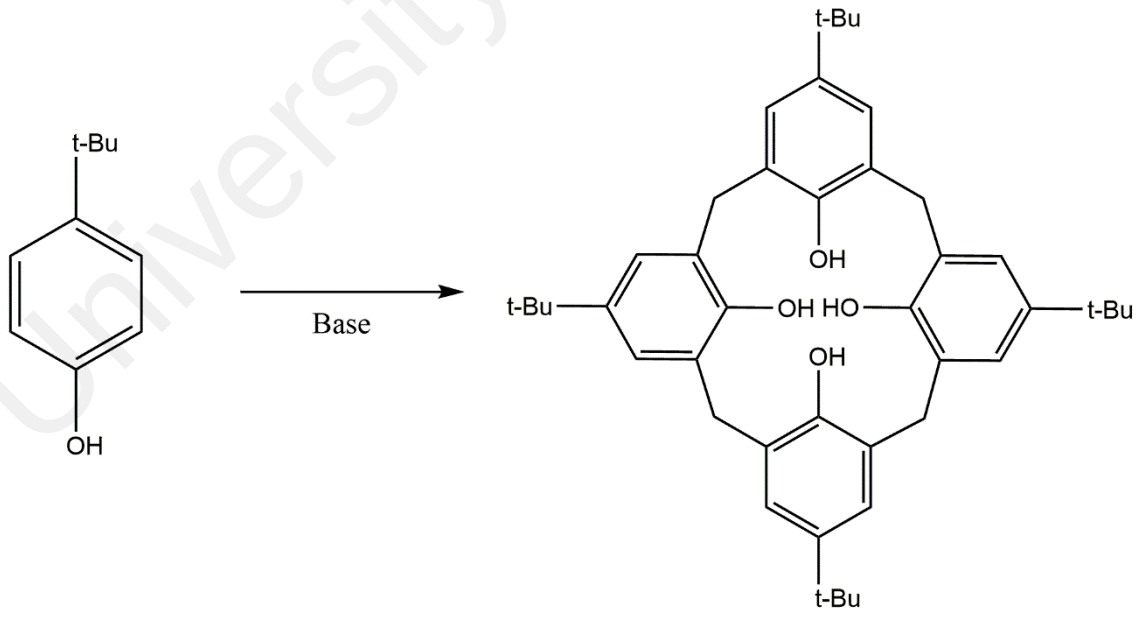

Figure 3.1: Schematic route for synthesis *p*-tertbutylcalix[4]arene from phenol

The synthesis of *p*-tertbutylcalix[4]arene was prepared according to Gutsche (2008). A mixture of *p*-tert-butylphenol, 37% of formaldehyde and sodium hydroxide (NaOH)

was heated for 4 h at temperature 110 - 120 °C to produce a thick viscous mass product. An amount of diphenyl ether was added to product and then heated in refluxing for 3 h. Then, reaction was cooled at room temperature and adequate amount of ethyl acetate was added to the mixture and stirred by using magnetic stirrer for 2 h. The crude product was separated by filtration and wash with deionized water until neutralize. The product was recrystallized from toluene to give 50% of glistering, white rhombs with melting point 342 - 344 °C.

3.8 Synthesis of new adsorbents

3.8.1 Synthesis of iron oxide nanoparticles

Iron oxide nanoparticles was prepared by using method reported by Kamboh (2013) with modification as following; 13.32 g of $FeCl_3.6H_2O$, 19.88 g of $FeCl_2.4H_2O$, 5 mL of HCl (5M), 40 mL of deionized water and 5 mL of ethanol were mixed in a flask followed by heating to 40 °C until complete dissolution of the salts. Then, the mixture was further for 2 h at room temperature. The suspension was immediately added to a 0.1 M ammonia solution and continued stirred for 2 h at room temperature. The product formed was separated from solution using external magnet and washed thoroughly with deionized water and dried under vacuum. The product was labelled as MNP adsorbent.

3.8.2 Synthesis of magnetic sporopollenin (MSp)

The magnetization of sporopollenin was carried out based method by Kamboh (2013) as follow; 13.32 g of $FeCl_3.6H_2O$, 19.88 g of $FeCl_2.4H_2O$, 5 mL of HCl (5M), 40 mL of deionized water and 5 mL of ethanol were mixed in a flask followed by heating to 40 °C until complete dissolution of the salts. Then 1.0 g of the freshly sporopollenin was re-dispersed in 30 mL of the prepared solution and stirred for 2 h at room temperature. The product suspension was filtered, and the filtrate was quickly washed with deionized water

and immediately transferred to a 0.1 M ammonia solution. After 2 h stirring at room temperature, the product was separated from solution using external magnet and washed thoroughly with deionized water and dried under vacuum. The product was labelled as MSp adsorbent.

3.8.3 Syntheses of Sp-TDI (1), Sp-TDI-βCD (2) and MSp-TDI-βCD (3)

The preparation of Sp-TDI (1), Sp-TDI-βCD (2) and **MSp-TDI-βCD (3)** are summarized in Figure 3.2 as below.

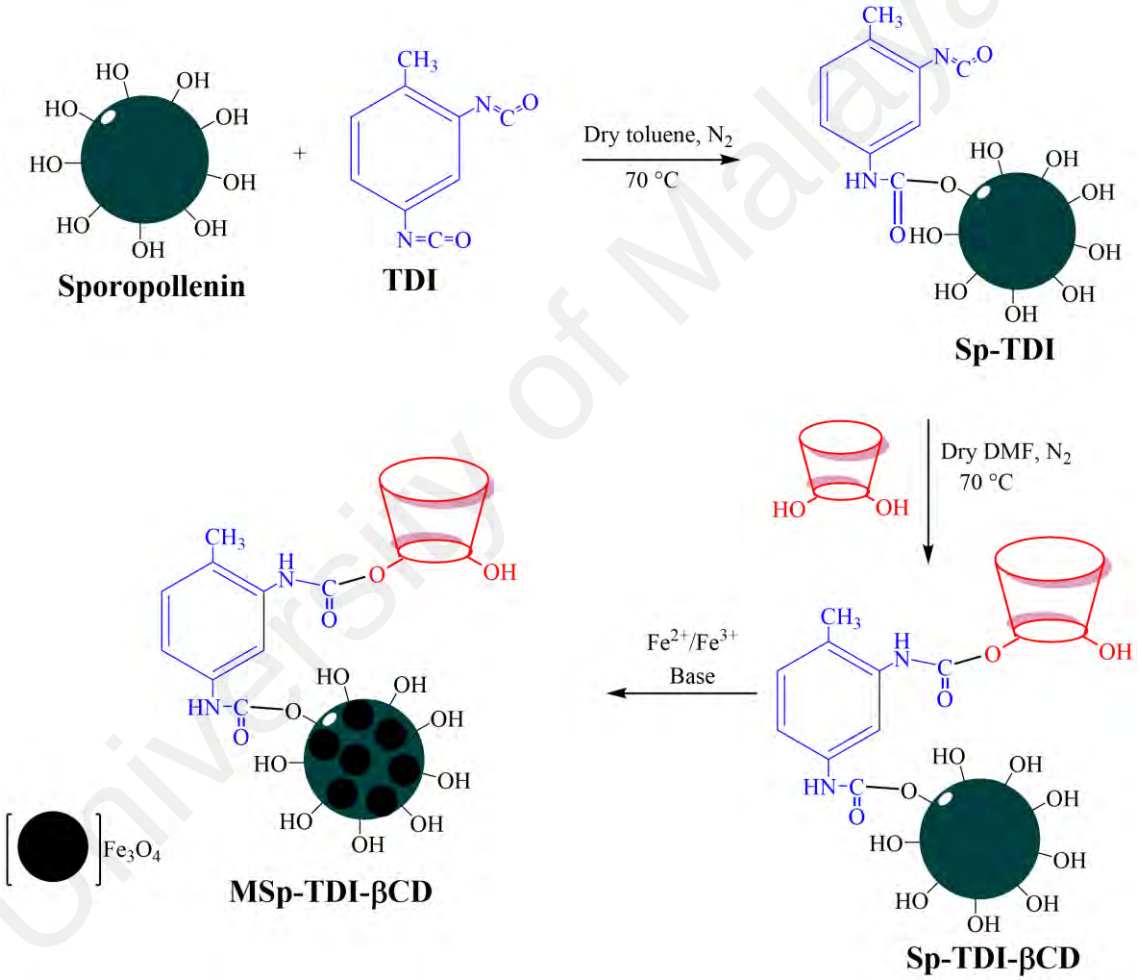

Figure 3.2: Schematic routes for the synthesis of **MSp-TDI-βCD** (**3**) adsorbent

3.8.3.1 Synthesis of Sp-TDI (1)

2.0 g of sporopollenin and 10 mL of TDI were added in 20 mL dry toluene and stirred by using magnetic stirrer under nitrogen gas at room temperature for 4 h. Then, the resultant product was separated by centrifugation at 4000 rpm for 5 min and sequentially

washed with dry toluene. The sample was dried, stored in desiccator and labelled as Sp-TDI (1).

3.8.3.2 Synthesis of Sp-TDI-βCD (2)

0.7 g of β-CD was dissolved in 20 mL of dry DMF, following the addition of 1.5 g of freshly prepared Sp-TDI (1). The reaction mixture was stirred under nitrogen atmosphere at 70 °C for 2 h. Then the resultant product was washed with excess acetone and deionized water for the removal of unreacted particles and dried under vacuum at 60 °C. The product was labelled as Sp-TDI-βCD (2).

3.8.3.3 Synthesis of MSp-TDI-βCD (3)

The magnetization of Sp-TDI-βCD (2) was carried out as follow; 13.32 g of $FeCl_3.6H_2O$, 19.88 g of $FeCl_2.4H_2O$, 5 mL of HCl (5M), 40 mL of deionized water and 5 mL of ethanol were mixed in a flask followed by heating to 40 °C until complete dissolution of the salts. Then 1.0 g of the freshly prepared Sp-TDI-βCD (2) was re-dispersed in 30 mL of the prepared solution and stirred for 2 h at room temperature. The product suspension was filtered, and the filtrate was quickly washed with deionized water and immediately transferred to a 0.1 M ammonia solution. After 2 h stirring at room temperature, the product was separated from solution using external magnet and washed thoroughly with deionized water and dried under vacuum. The product was labelled as **MSp-TDI-βCD** (**3**) adsorbent.

3.8.4 Syntheses of Sp-TDI-calix (4) and MSp-TDI-calix (5)

The preparation of Sp-TDI-calix (4) and **MSp-TDI-calix** (**5**) are summarized in Figure 3.3 as below.

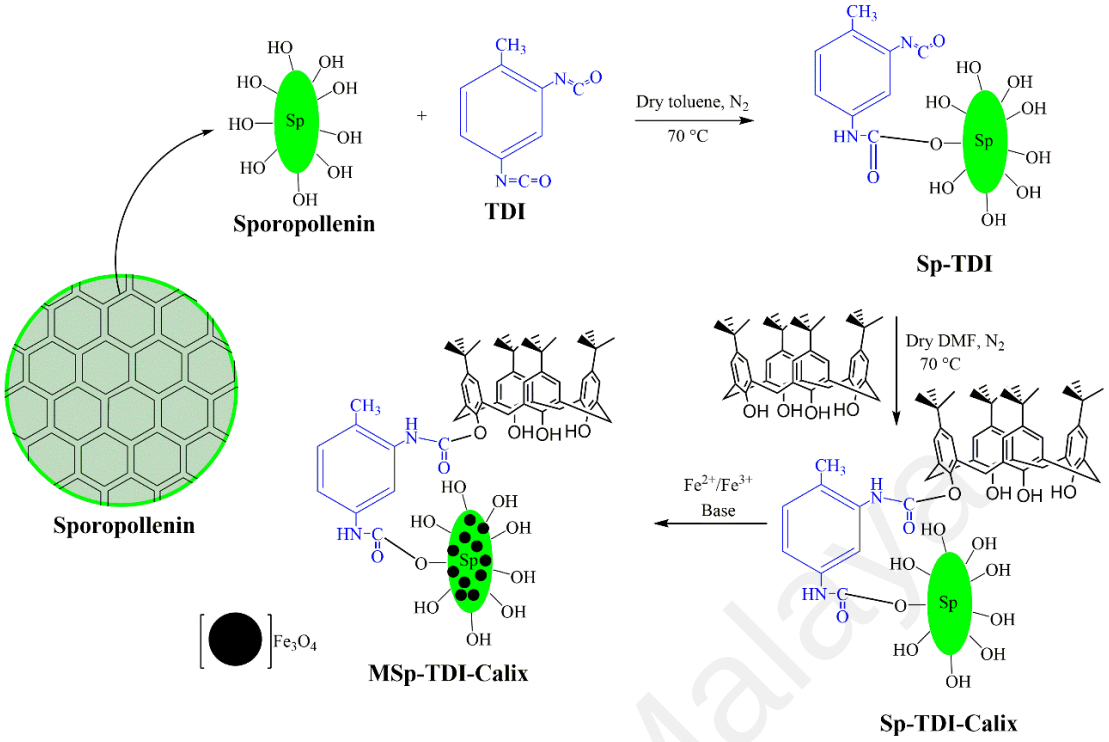

Figure 3.3: Schematic routes for the synthesis of **MSp-TDI-calix (5)** adsorbent

3.8.4.1 Synthesis of Sp-TDI-calix (4)

0.411 g of *p*-tertbutylcalix[4]arene was dissolved in 20 mL of dry DMF. Then, 1.5 g of Sp-TDI (1) was added to solution and stirred for 2 h at 70 °C using magnetic stirrer in presence of nitrogen gas. The resultant compound was washed with dichloromethane (DCM) and deionized water for remove all unnecessary particles absorbed on the surface of sample. The sample was dried and stored in desiccator and labelled as Sp-TDI-calix (4).

3.8.4.2 Synthesis of MSp-TDI-calix (5)

The magnetization of Sp-TDI-calix (4) was carried out as follow; 13.32 g of $FeCl_3.6H_2O$, 19.88 g of $FeCl_2.4H_2O$, 5 mL of HCl (5 M), 40 mL of water and 5 mL of ethanol were mixed in a flask followed by heating to 40 °C until complete dissolution of the salts. Then, 1.0 g of Sp-TDI-calix (4) was re-dispersed in 30 mL of the solution and stirred for 2 h at room temperature. The Sp-TDI-calix (4) suspension was filtered and the

filtrate was quickly washed with deionized water and immediately transfer into 0.1 M ammonia solution. After 2 h stirring at room temperature, resultant compound was separated from solution using external magnet and washed thoroughly with deionized water and dried under vacuum. The compound was labelled as **MSp-TDI-calix** (**5**) adsorbent.

3.9 Screening selectivity studies

To perform screening studies, 10 mg of different adsorbents (raw MNP, MSp, **MSp-TDI-βCD** and **MSp-TDI-calix)** was added to 10 mL mixture of NSAIDs (INP, KTP, IBP & FNP). The mixture was stirred for 10 min and the adsorbent was removed from the solution by applying external magnetic field neodymium magnet. The upper solution was decanted after few minutes. Then, 1.5 mL of acetonitrile (ACN) was added to elute NSAIDs adsorbed on adsorbents surface and continued stirred for 10 min. The collected eluate was exposed to nitrogen stream until dry and re-dissolved in 0.7 mL of acetonitrile. The sample was injected into HPLC for analysis.

3.10 MSPE procedure

3.10.1 Optimization parameters

Starting with adsorbent dosage, several assays were conducted through MSPE technique to achieve the optimum condition to extract NSAIDs from aqueous water samples. Therefore, sample volume, extraction and desorption time, volume and type of organic solvent, as well as solution pH were evaluated. Each evaluation, only one variable was verified at a time and repeated triplicate. The peak area in chromatographic analysis was used to evaluate the performance each parameter on the extraction of NSAIDs.

3.10.2 Adopted extraction conditions

3.10.2.1 MSPE extraction condition using MSp-TDI-βCD (3) adsorbent

10 mg **MSp-TDI-βCD** (**3**) adsorbent was added to 200 mL of deionized water spiked with mixture of INP, KTP, IBP & FNP with pH 4. The mixture was stirred vigorously for 30 min to make the adsorbent disperse uniformly in the solution. Then, the adsorbent was isolated from solution by using an external magnet. The solution became limpid and the upper solution was decanted after 5 min. Then, 1.5 mL of acetonitrile was added to elute the NSAIDs adsorbed on adsorbent surface and stirred for 30 min. The collected eluate was dried using stream nitrogen gas and re-dissolved in 0.7 mL of acetonitrile. Finally, 10 µL portion of the eluate was injected into HPLC for analysis.

3.10.2.2 MSPE extraction condition using MSp-TDI-calix (5) adsorbent

30 mg of **MSp-TDI-calix** (**5**) adsorbent was added to 200 mL of deionized water spiked sample (mixture of INP, KTP, IBP and FNP) at pH 4. The mixture was stirred vigorously for 30 min to make the adsorbent dispersed uniformly in the solution. Then, neodymium (Nd) magnet was used to separate the adsorbent from the solution. The solution became limpid and the upper solution was decanted after few minutes. Afterwards, 1.5 mL of acetonitrile was added to elute NSAIDs adsorbed on adsorbent surface and stirred for 10 min. The collected eluate was dried using stream nitrogen gas and re-dissolved in 0.7 mL of acetonitrile. Finally, 10 µL portion of the eluate was injected into HPLC for analysis.

3.10.3 Reusability study

Reusability study was conducted to determine the regeneration efficiency of adsorbent. Five cycles of MSPE technique under optimized condition was conducted and each cycle

the adsorbent was washed using acetonitrile to eluate remaining analyte at the adsorbent surface. At final step, the sample was injected into HPLC for further analysis.

3.10.4 Method validation

To validate the proposed technique, method validation parameters were conducted such as linearity, precision, limit of detection (LOD) and limit of quantification (LOQ) using optimized conditions for each adsorbent.

3.10.4.1 Linearity and precision

The linearity was conducted through standard calibration curve ranging from 0.5 to 500 ng/mL by diluting suitable amount of NSAIDs from 1000 µg/mL stock solution in methanol. The calibration curve was evaluated using six spiking concentration level of NSAIDs. Equation for linear regression can be expressed as equation 3.2 where *m* is slope of calibration curve and *c* is y- intercept. Coefficient of determination (R^2) for calibration curve was measured to show wellness a regression model fits the data obtained.

$$y = mx + C \tag{3.2}$$

In terms of precision, intermediate precision (inter-day) and repeatability (intra-day) were evaluate for sample solution under optimized conditions. Intermediate precision (inter-day) was measured in five replicates of samples for three days in a row. Meanwhile, repeatability (intra-day) was investigated in five replicates of samples on the same day. Result for these assessments were expressed in terms of relative standard deviation (% *RSD*) as expressed in equation 3.3 (Bhadra et al., 2011).

$$\% RSD = \frac{SD}{x} \times 100\% \quad (3.3)$$

Where x is mean value and SD in standard deviation of sample measured

3.10.4.2 Limit of detection (LOD) and limit of quantification (LOQ)

Detection limit and quantification limit were two main aspects to determine the lowest concentration of analyte in the sample that can be detected, and the lowest concentration can be quantitated with acceptable precision under optimized conditions respectively. The equation to calculate detection limit and quantification limit expressed as equation 3.4 and equation 3.5 below:

$$LOD = 3\frac{SD}{m} \quad (3.4)$$

$$LOQ = 10\frac{SD}{m} \quad (3.5)$$

Where SD is standard deviation of blank and m is slope from calibration curve.

3.10.5 Real sample application

To examine matrix effect and reliability of proposed method under optimized conditions, two level of concentration of NSAIDs were selected (10 ng/mL and 100 ng/mL) and were spiked into real sample water sample including tap, drinking and river water. The tap water was collected from analytical laboratory UM and drinking water was purchase from local store. River water was collected from Sungai Sendat, Selangor and was filtered through 0.22 um PTFE membrane to remove unnecessary particles and store at 4 °C prior to use. The sample pre-treatment MSPE of real samples for both adsorbents was mentioned in earlier chapter and further analysed using HPLC-DAD. The percentage

recovery of real samples for tested methods were calculated using equation 3.6 (Patnaik, 2017).

$$Recovery\ (\%\ R) = \frac{[C_s - C_{us}]}{[C_{sa}]} \times 100\% \tag{3.6}$$

Where C_s is the concentration of spiked sample; C_{us} is the concentration of unspiked sample and C_{sa} is the concentration of spiked sample added.

CHAPTER 4: RESULTS AND DISCUSSIONS

4.1 PART A: MOLECULAR MODELLING STUDIES

4.1.1 Geometry optimization of single molecules

Figure 4.1 and Figure 4.2 show the optimized structure of β-CD and *p*-tertbutylcalix. Based on optimization calculation, β-CD reported to have the optimization energy of -1450.9942 kcal/mol, meanwhile *p*-tertbutylcalix have optimization energy of -181.1182 kcal/mol. As compared to *p*-tertbutylcalix, β-CD tended to have lower and stronger optimization energy due to its stability. The presence of belt of hydrogen bond make it strong and stable structure. Seven intramolecular hydrogen belt bond form at secondary or wider cavity of β-CD. This existence of hydrogen bond has been reported to help stabilize the β-CD structure (Lawtrakul et al., 2003). The optimized structure of NSAIDs was illustrated in Figure 4.3. The optimization energy for INP, KTP, IBP and FNP were reported as -1.213540831 kcal/mol, -79.2612 kcal/mol, -99.5860 kcal/mol and -77.7355 kcal/mol respectively.

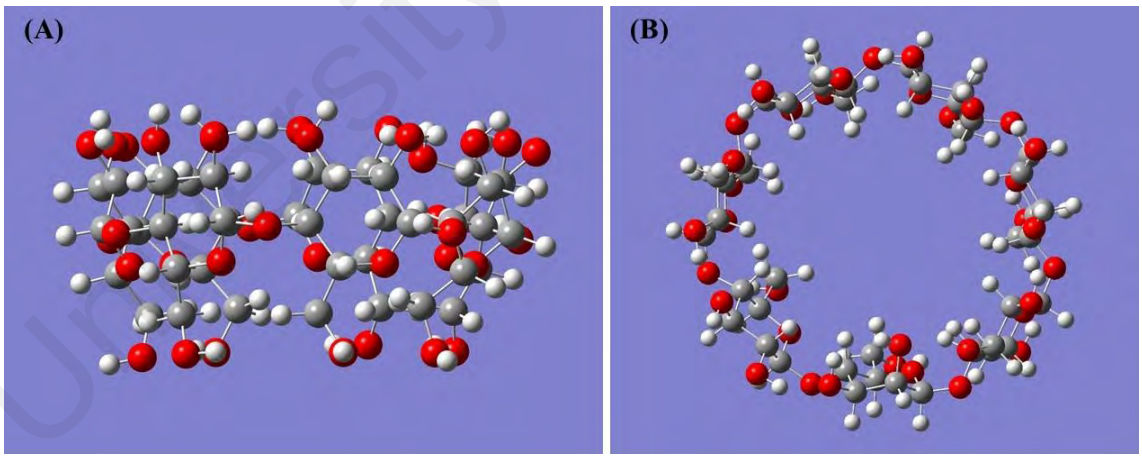

Figure 4.1: Optimized structure of β-CD (A) side view and (B) top view

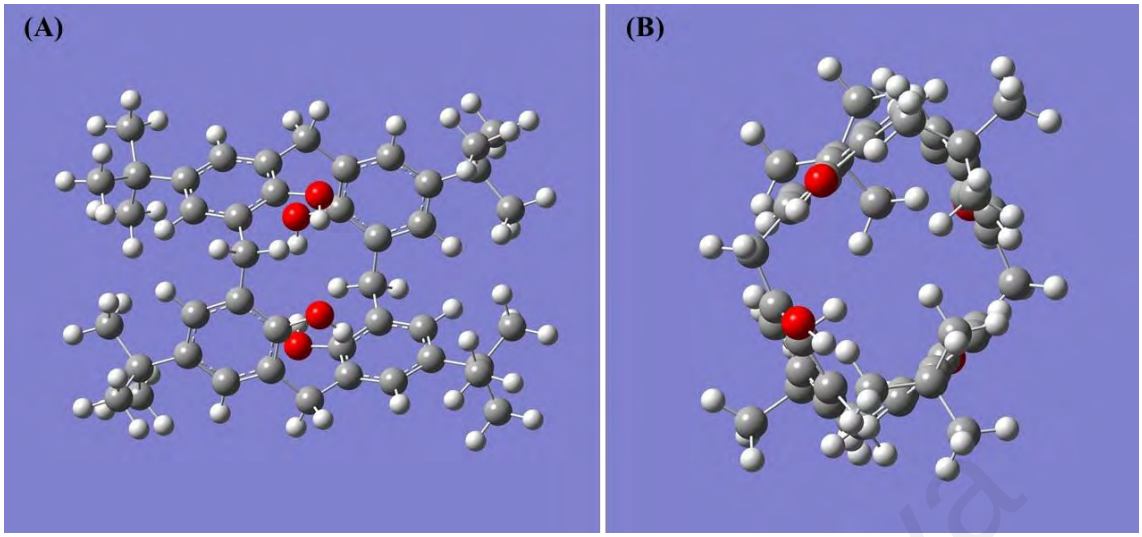

Figure 4.2: Optimized structure of *p*-tertbutylcalix (A) side view and (B) top view

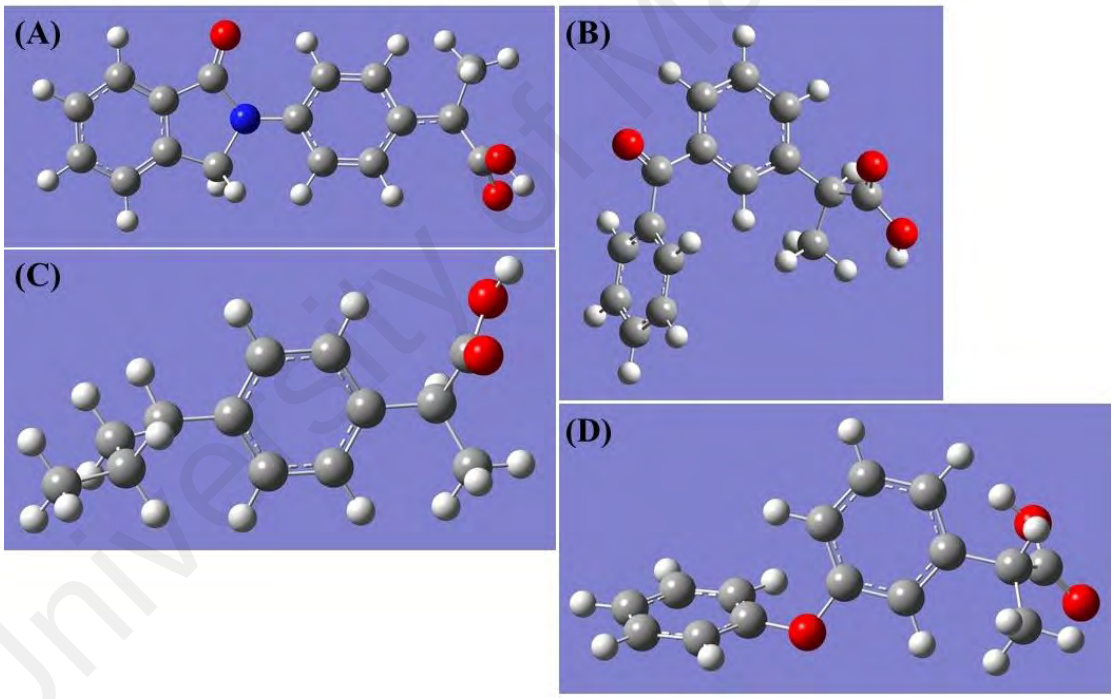

Figure 4.3: Optimized structure of NSAIDs (A) indoprofen; (B) ketoprofen; (C) ibuprofen and (D) fenoprofen

4.1.2 Molecular docking

Previous studied shows molecular docking not only use the most stable conformation to design a new receptor ligand complexes, but it also proved in identifying the binding sites on receptor and ligands (Deng et al., 2014; Sahihi & Ghayeb, 2014). In this

molecular simulation section, docking have been simulating to predict the best conformation for binding of two types of host β-CD and *p*-tertbutylcalix to NSAIDs guest molecules using binding free energy assessment. The energy was characterized by intermolecular energy which is van der Waals, hydrogen bonding, electrostatic energy and desolvation energy. More than that, internal and torsional free energy also have been included in calculation of energy. The equation used to calculate the docking energy and binding energy which is calculated by AutoDock are represented in Equation 4.1 and 4.2.

$$E_{docking} = Intermolecular\ energy + Internal\ free\ energy \quad (4.1)$$

$$E_{binding} = Intermolecular\ energy + Torsional\ energy \quad (4.2)$$

4.1.2.1 Binding free energy of NSAIDs with β-cyclodextrin and *p*-tertbutylcalix

The results of binding free energy of β-CD and *p*-tertbutylcalix to the individual NSAIDs guest molecule in the docking process are tabulated in Table 4.1. The low binding energy (more negative value) indicates that the host-guest structure is more favoured or stable. Every docking procedure generate nine modes which are the possible suitable binding sites for each NSAIDs with host molecule. The results show that the both β-CD and *p*-tertbutylcalix have a lowest binding free energy with INP of -6.6 kcal/mol and -6.5 kcal/mol respectively, followed towards KTP with binding energy of -5.4 kcal/mol and -5.6 kcal/mol respectively. For IBP, binding free energy with β-CD and *p*-tertbutylcalix was measured at -5.4 kcal/mol and -5.3 kcal/mol respectively. Finally, as for FNP, its shows binding free energy of guest molecule to β-CD and *p*-tertbutylcalix of -6.0 kcal/mol and -5.0 kcal/mol respectively.

Table 4.1: Binding energy from AutoDock Vina of β-CD and *p*-tertbutylcalix respect to NSAIDs

NSAIDs	Mode	Host	
		BCD	Calix
		Binding free energy (kcal/mol)	
INP	1	-6.6	-6.5
	2	-6.4	-6.0
	3	-6.2	-5.3
	4	-6.2	-5.3
	5	-6.1	-5.3
	6	-5.8	-5.1
	7	-5.6	-5.0
	8	-5.6	-5.0
	9	-5.5	-5.0
KTP	1	-5.4	-5.6
	2	-5.2	-5.4
	3	-5.1	-5.3
	4	-5.0	-5.2
	5	-5.0	-5.1
	6	-5.0	-5.0
	7	-4.8	-5.0
	8	-4.8	-5.0
	9	-4.8	-5.0
IBP	1	-5.4	-5.3
	2	-5.3	-5.2
	3	-5.1	-5.2
	4	-5.0	-5.2
	5	-5.0	-5.1
	6	-5	-4.9
	7	-4.9	-4.7
	8	-4.8	-4.5
	9	-4.7	-4.4
FNP	1	-6.0	-5.0
	2	-5.9	-4.9
	3	-5.9	-4.7
	4	-5.6	-4.7
	5	-5.5	-4.6
	6	-5.5	-4.5
	7	-5.5	-4.4
	8	-5.0	-4.3
	9	-4.8	-4.3

The differences in hydrogen bonding and van der Waals interaction makes variation in the binding free energies in every complexes molecule. The hydrogen bonding between the host and guest is crucial, thus it can decide the binding strength and location of β-CD and *p*-tertbutylcali*x* during interaction process. Based on the results, binding sites for NSAIDs towards β-CD is located inside the cavity, meanwhile as for *p*-tertbutylcalix NSAIDs is located outside the cavity of *p*-tertbutylcalix molecule. Figure 4.4 and Figure 4.5 show the suitable binding sites of NSAIDs with stable conformation towards β-CD and *p*-tertbutylcalix respectively.

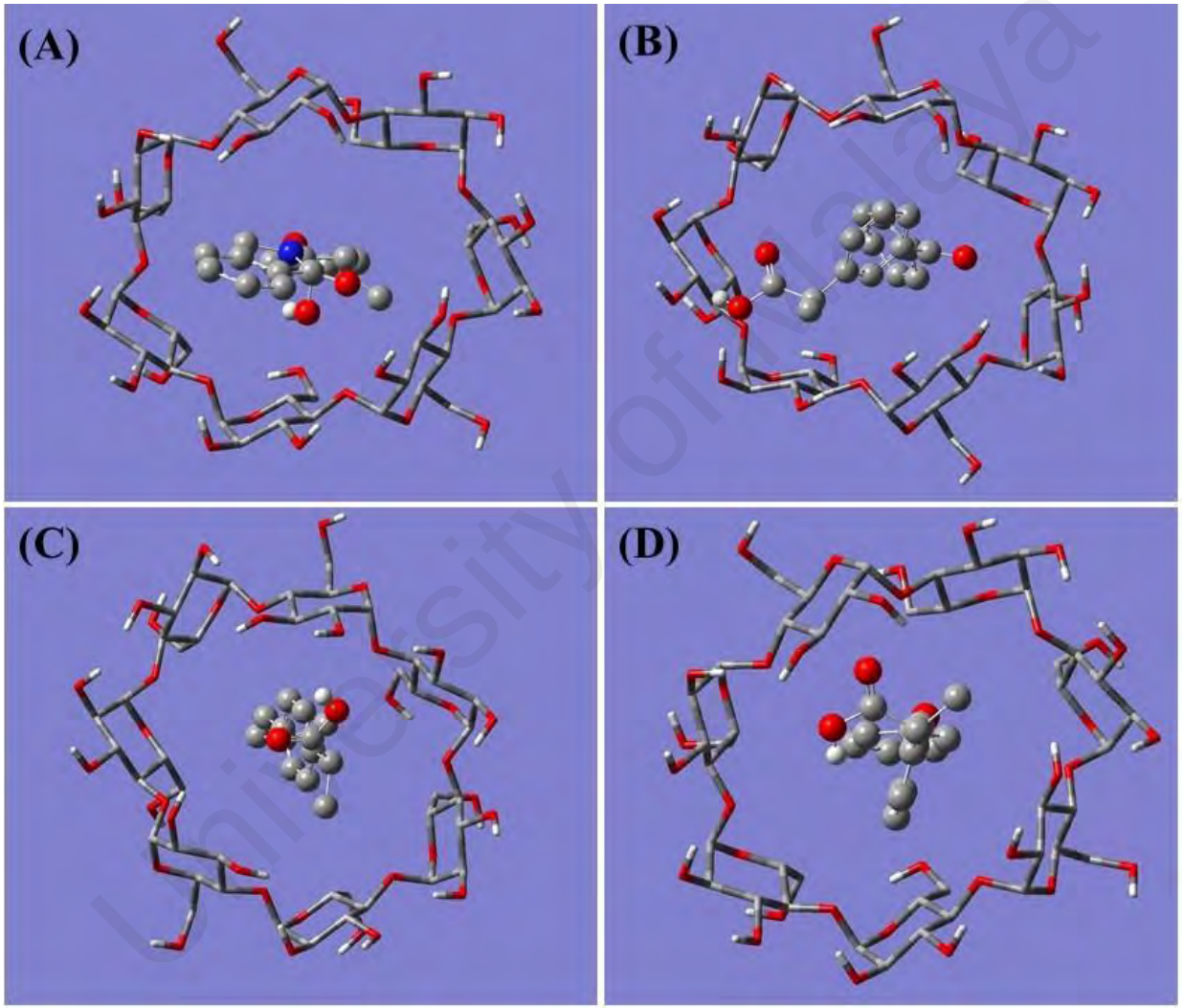

Figure 4.4: Suitable binding sites of NSAIDs (A) INP; (B) KTP; (C) IBP and (D) FNP with stable conformation towards β-CD

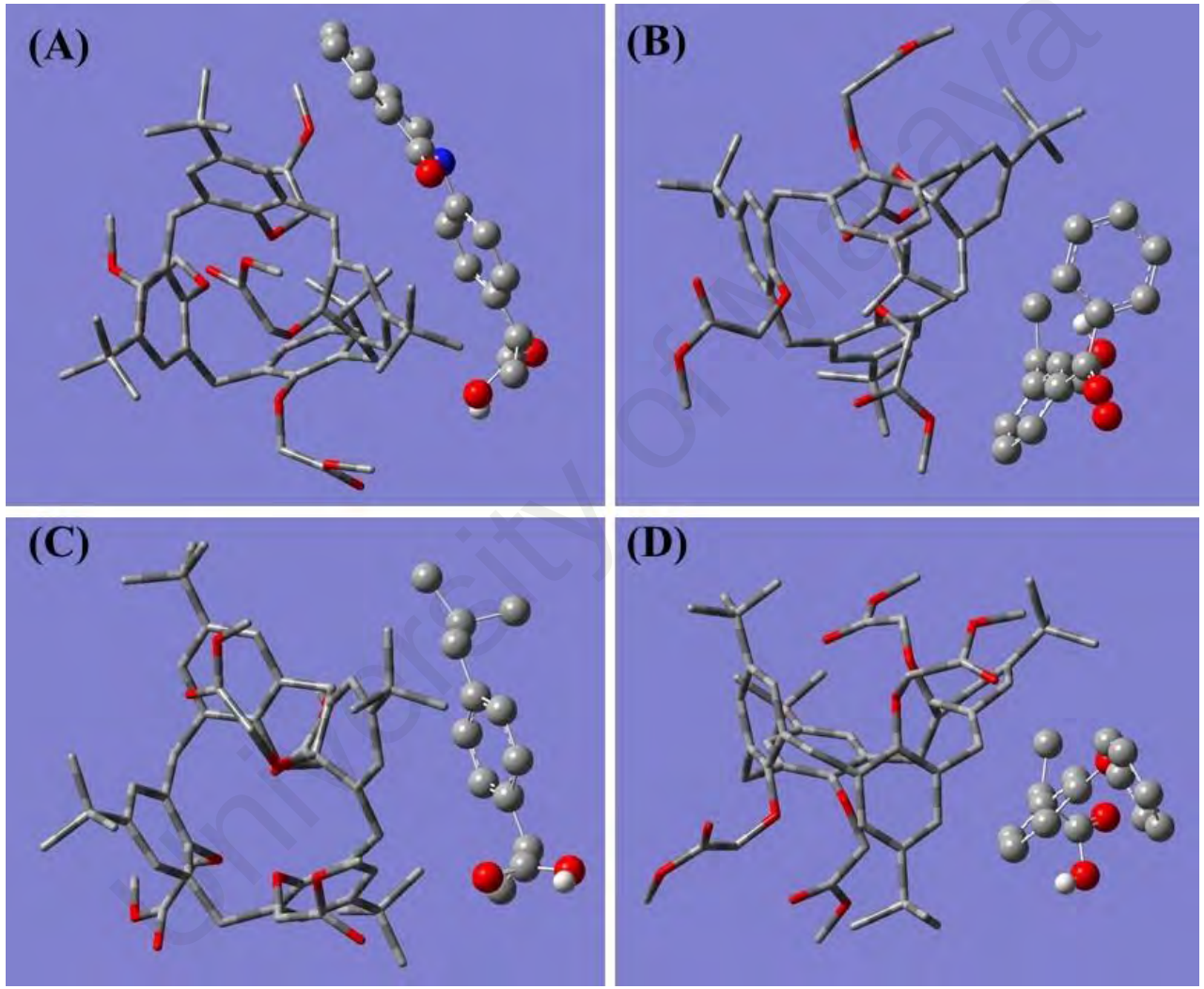

Figure 4.5: Suitable binding sites of NSAIDs (A) INP; (B) KTP; (C) IBP and (D) FNP with stable conformation towards *p*-tertbutylcalix

4.1.3 Molecular dynamics simulation

4.1.3.1 Structural and stability of NSAIDs toward host molecules

To investigate the stability of the host-guest formation of NSAIDs toward β-CD and *p*-tertbutylcalix respectively, the results were analyzed on the basis of root mean square deviations (RMSDs). The relative stability of guest molecule in complex system can be provided by RMSDs system. In biological molecules simulation, RMSDs have been used to determine the stability in many molecular dynamics (Gokara et al., 2014; Sahihi & Ghayeb, 2014; Wang et al., 2008). The RMSD values of β-CD complexes and *p*-tertbutylcalix complexes were plotted against the simulation time with respect to initial minimized structure as shown in Figure 4.6 and Figure 4.7 respectively. For β-CD complexes, all complexes stabilize after 50 ps along the trajectory at same simulation period except for β-CD-KTP and β-CD-IBP complexes it became unstable at 320 ps and 270 ps respectively. RMSD values rapidly increased between 320 ps to 340 ps suggesting conformational changes of ketoprofen in complex (Fatiha et al., 2015).

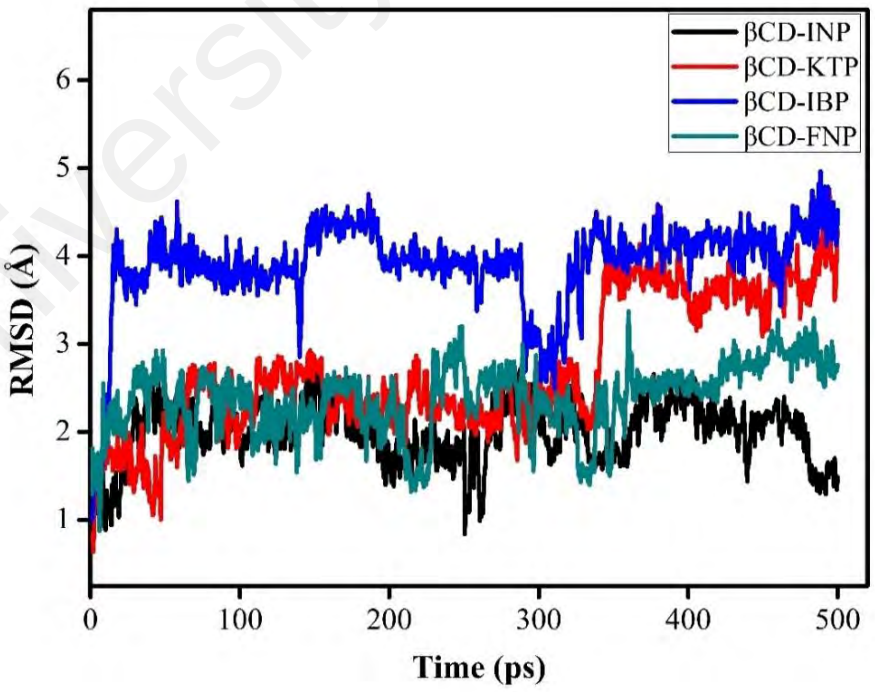

Figure 4.6: RMSD values of β-CD complexes

On the other hand, the *p*-tertbutylcalix complexes showed high RMSD values from starting point until 250 ps. Beyond 250 ps, all *p*-tertbutylcalix complexes starting to stable until end of trajectory simulation except for calix-KTP complex which is RMSD value changing from 4.0 Å to 10.0 Å. This indicated the complexes had reached the equilibrated state after 250 ps simulation and *p*-tertbutylcalix are capable to stabilize the structure of NSAIDs except for KTP molecule complex.

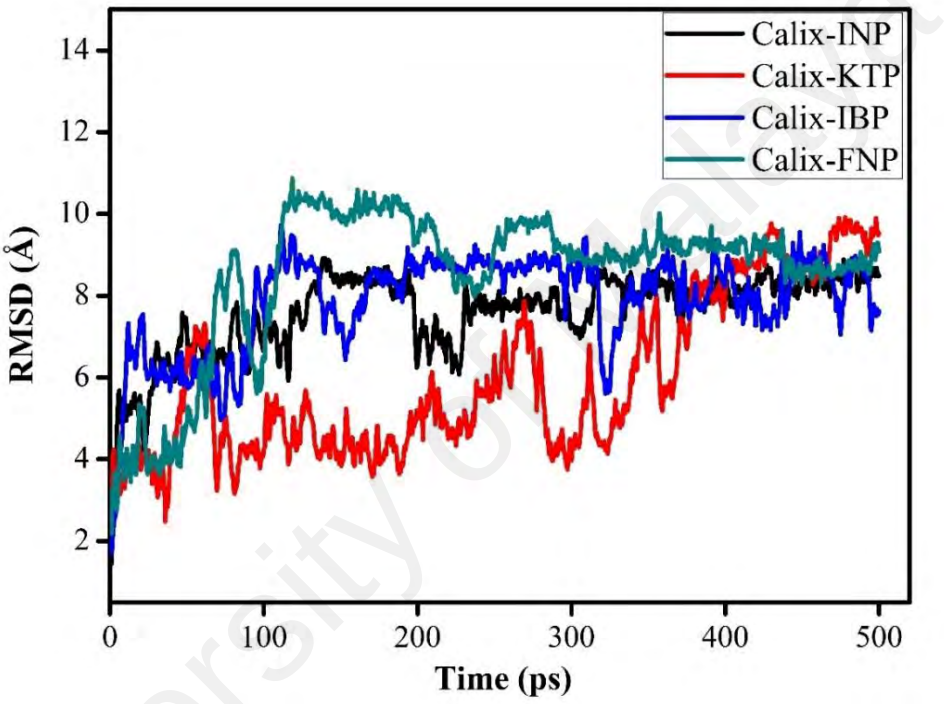

Figure 4.7: RMSD values of *p*-tertbutylcalix complexes

4.1.4 Quantum mechanics

4.1.4.1 Binding energy of complexes molecule

In this study, binding energy of complexes between β-CD and *p*-tertbutylcalix with NSAIDs was calculated. β-CD and *p*-tertbutylcalix acted as host molecules and encapsulated with NSAIDs. Several best conformations of complexes obtained from molecular dynamics were selected and calculated by using AM1 semi-empirical method. The process gives results the most stable structure and minimum energy for every

complex. The negative value indicates the interaction strength. The more negative value, the stronger interaction between the molecule (Terekhova & Kumeev, 2010). The result of lowest energy of every complex with individual NSAIDs are depicted in Figure 4.8 - 4.11 and Figure 4.12 - 4.15 for β-CD and *p*-tertbutylcalix complexes respectively. The minimum energy with most stable structure for β-CD and *p*-tertbutylcalix complexes towards INP, KTP, IBP and FNP are tabulated in Table 4.2.

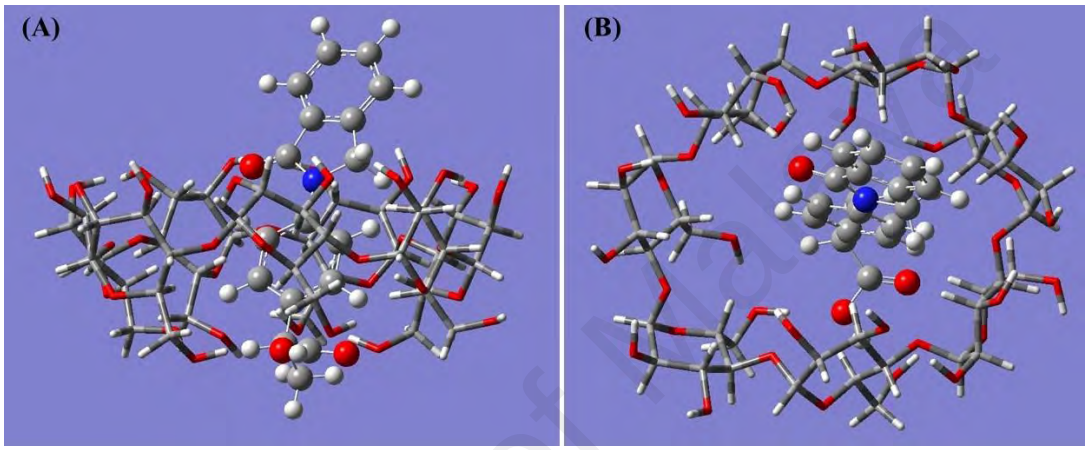

Figure 4.8: The lowest energy complex of β-CD with INP (A) side view and (B) top view

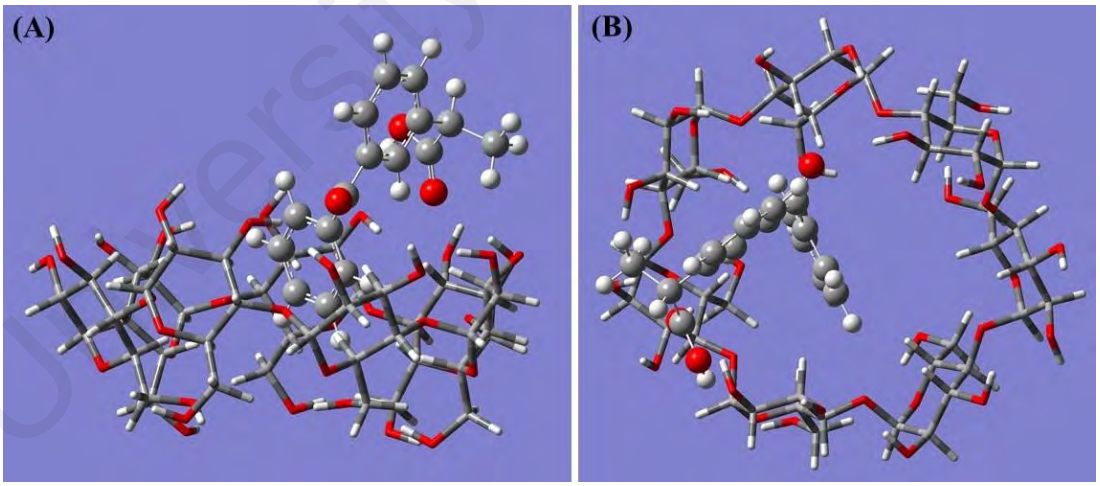

Figure 4.9: The lowest energy complex of β-CD with KTP (A) side view and (B) top view

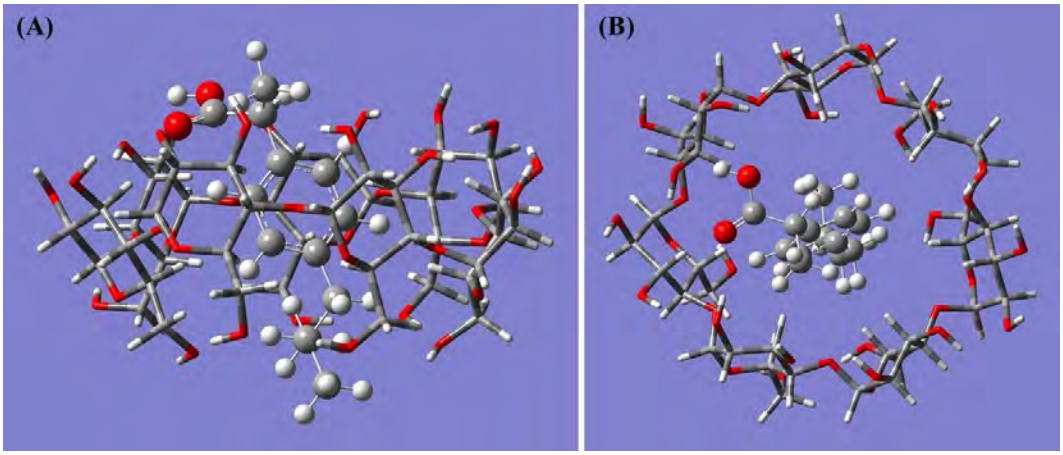

Figure 4.10: The lowest energy complex of β-CD with IBP (A) side view and (B) top view

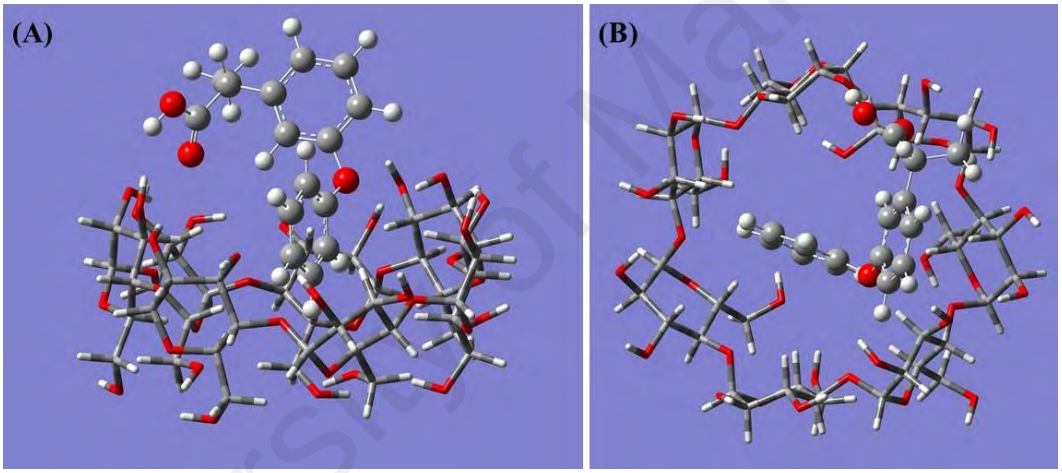

Figure 4.11: The lowest energy complex of β-CD with FNP (A) side view and (B) top view

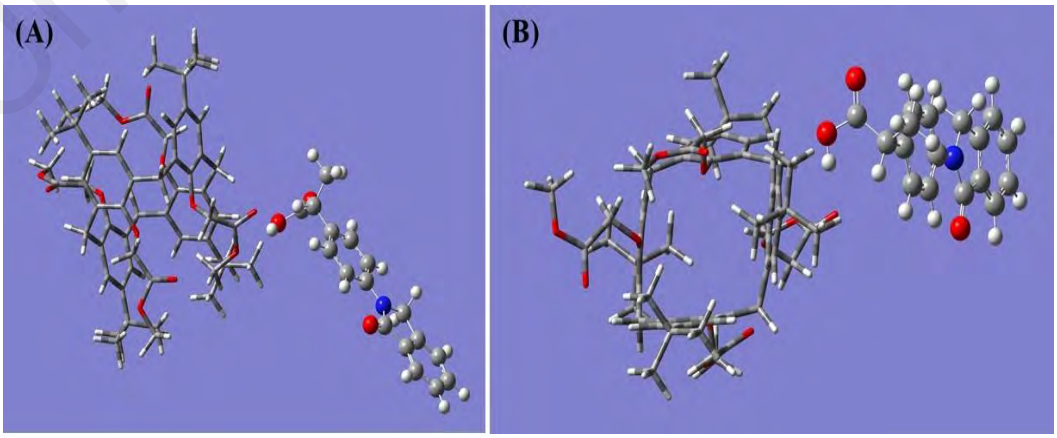

Figure 4.12: The lowest energy complex of *p*-tertbutylcalix with INP (A) side view and (B) top view

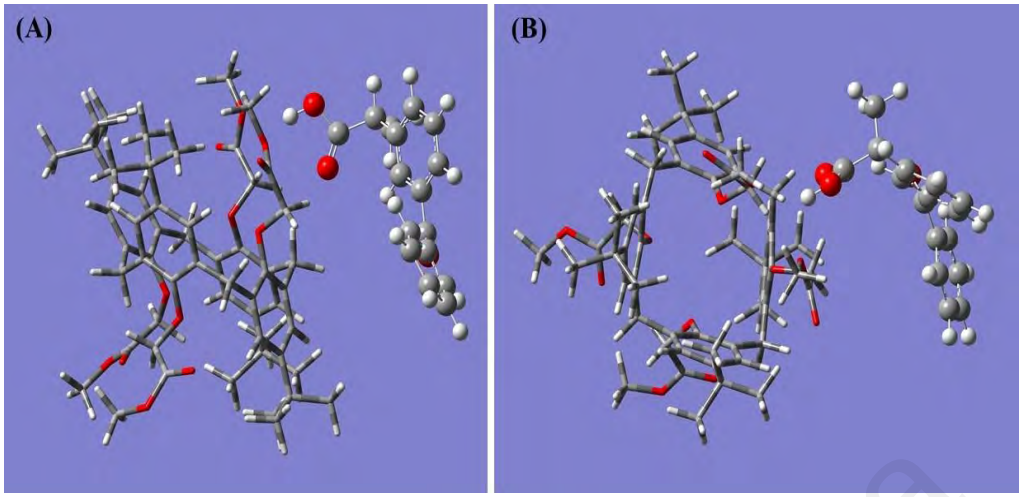

Figure 4.13: The lowest energy complex of *p*-tertbutylcalix with KTP (A) side view and (B) top view

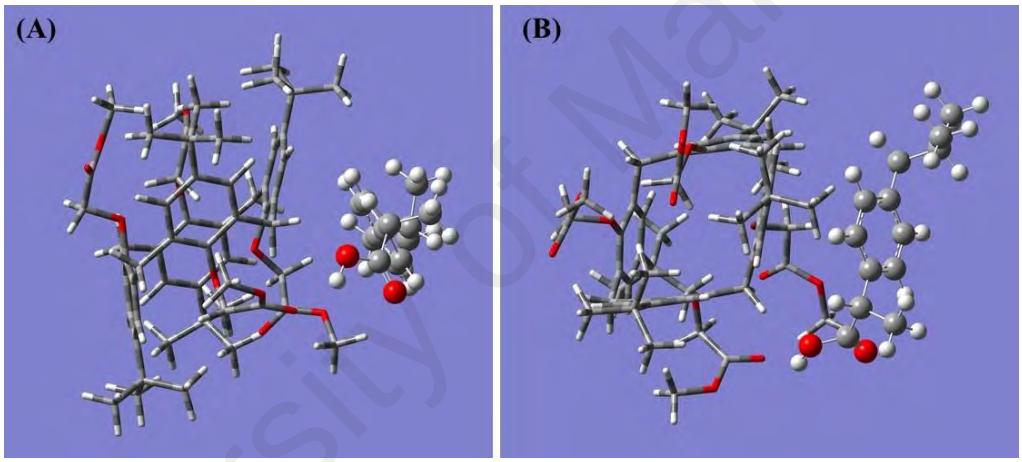

Figure 4.14: The lowest energy complex of *p*-tertbutylcalix with IBP (A) side view and (B) top view

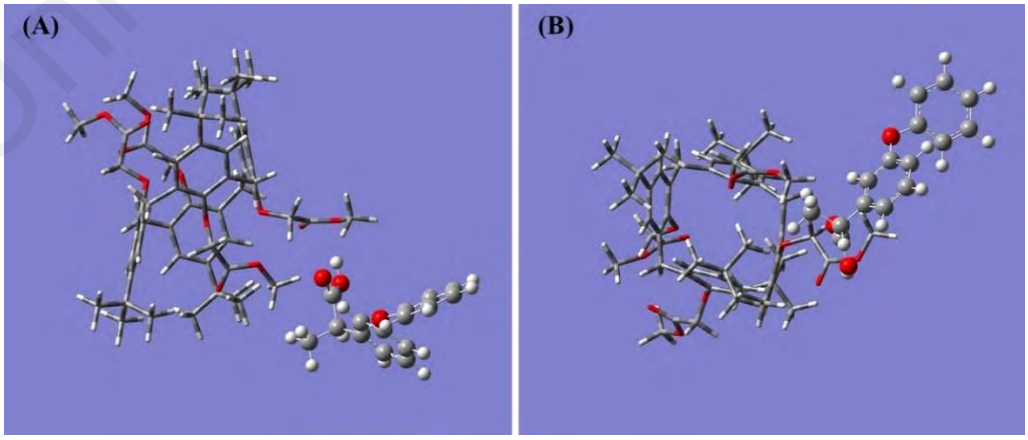

Figure 4.15: The lowest energy complex of *p*-tertbutylcalix with FNP (A) side view and (B) top view

Table 4.2: The lowest interaction energy using CHARMm force field for complexes

Complexes	Energy (Hartress)			Interaction energy (Hartress)	Interaction energy (kcal/mol)	VDW (kcal/mol)	EE (kcal/mol)
	Complex	Host	Guest				
β-CD-INP	-2.64	-2.56	0.003	-0.09	-56.22	-54.41	0.060
β-CD-KTP	-2.77	-2.62	-0.130	-0.03	-16.58	-56.56	0.030
β-CD-IBP	-2.82	-2.64	-0.160	-0.02	-13.15	-51.55	-0.040
β-CD-FNP	-2.78	-2.64	0.230	-0.37	-230.22	-53.71	-0.240
Calix-INP	-0.79	-0.68	-0.090	-0.01	-8.50	-32.36	-0.090
Calix-KTP	-0.83	-0.69	-0.130	-0.01	-5.57	-37.67	-0.002
Calix-IBP	-0.77	-0.62	-0.060	-0.09	-56.50	-36.26	0.020
Calix-FNP	-0.81	-0.68	-0.120	-0.13	-83.29	-30.57	-0.050

* **VDW**- Van der Waals energy
* **EE**- Electrostatic energy

4.1.5 Interaction between β-CD and *p*-tertbutylcalix at binding sites of NSAIDs molecules

This section will focus on the interaction of β-CD and *p*-tertbutylcalix with NSAIDs based on hydrogen bonding involve in the formation of complexes. The hydrogen bonds were analyzed at binding sites outer and inside of cavity of β-CD and *p*-tertbutylcalix. The hydrogen bond was measured by acceptor-donor atom distance of less than 3.5 Å (Buck & Karplus, 2001). With this description, the host-guest hydrogen bonding between β-CD and *p*-tertbutylcalix and NSAIDs complexation can be well determined. Figure 4.16 - 4.20 show the occupancy of hydrogen bond between them.

In β-CD complexes, β-CD-INP and β-CD-KTP complexes are observed to have the most occurrence of hydrogen bonding which five intermolecular bonds are exist between β-CD: INP and β-CD: KTP complex respectively. Meanwhile, for β-CD: IBP and β-CD: FNP complexes, the intermolecular hydrogen bond interaction was stronger in β-CD: FNP compared to β-CD: IBP which have four hydrogen bonding in β-CD: FNP towards three hydrogen bonding in β-CD: IBP. Fatiha (2015) and Muhammad & Adnan (2015) reported similar finding regarding hydrogen bond existed between complexation of β-CD and insulin (Fatiha et al., 2015; Muhammad & Adnan, 2015). For *p*-tertbutylcalix complexes, the intermolecular hydrogen bonding exist was fewer compared to β-CD complexes which are two hydrogen bonding in Calix-INP and Calix-KTP and only single hydrogen bonding measured in Calix-IBP and Calix-FNP. Most of intermolecular hydrogen bonding take part at carboxylic group of NSAIDs for both β-CD and *p*-tertbutylcalix complexes. These results consistently tally with simulation binding energy calculation in quantum mechanics showed β-CD complexes are stronger compared to *p*-tertbutylcalix complexes which give higher binding energy due to present of more hydrogen bonding. Due to this existing intermolecular force of attraction between

molecule, β-CD and *p*-tertbutylcalix have been chosen as receptor for the extraction of NSAIDs group. Table 4.3 summarize the occurrence of intermolecular hydrogen bonding with specific bond length in β-CD and *p*-tertbutylcalix complexes.

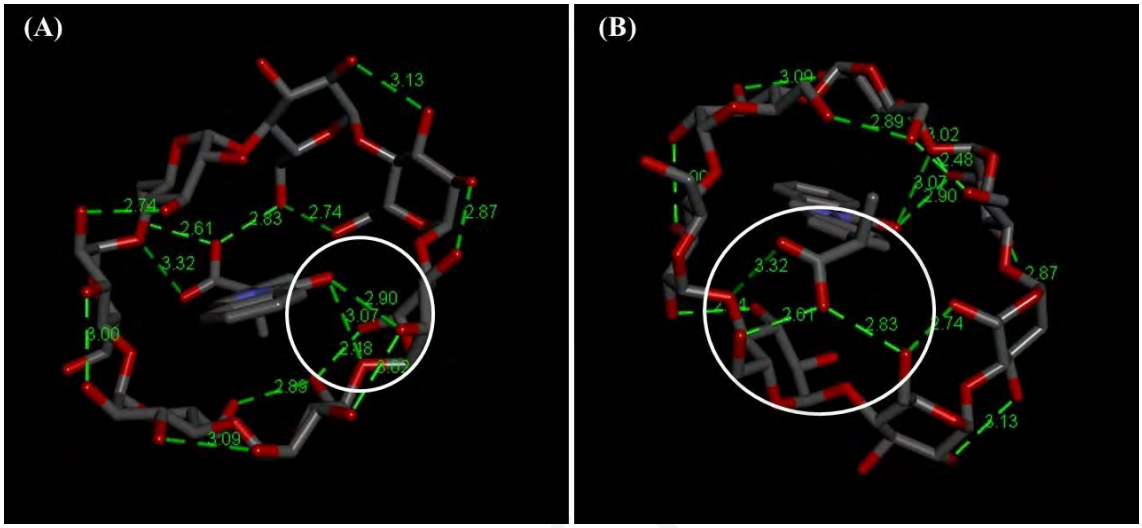

Figure 4.16: Hydrogen bond distance in angstrom between β-CD and INP (A) top view and (B) bottom view

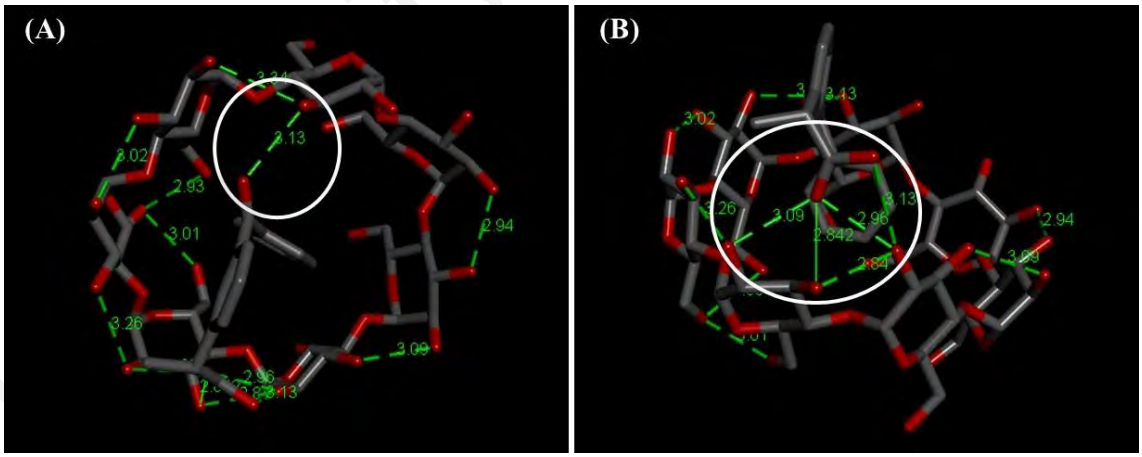

Figure 4.17: Hydrogen bond distance in angstrom between β-CD and KTP (A) top view and (B) side view

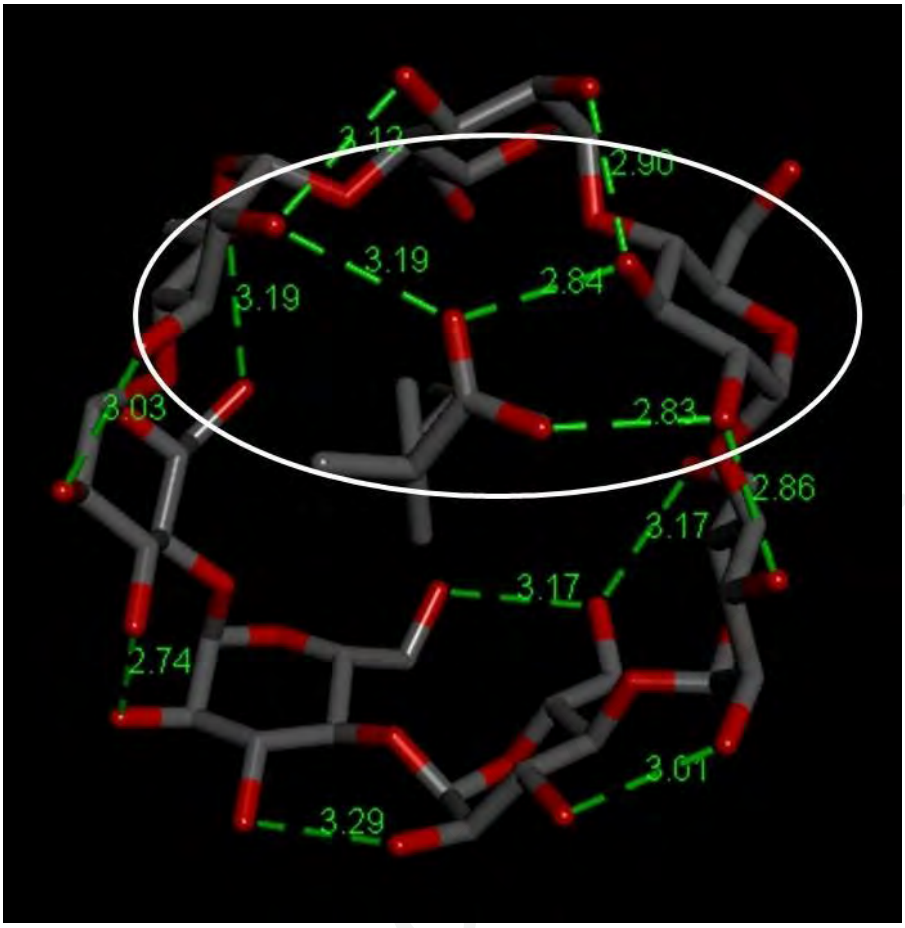

Figure 4.18: Hydrogen bond distance in angstrom distance in angstrom between β-CD and IBP

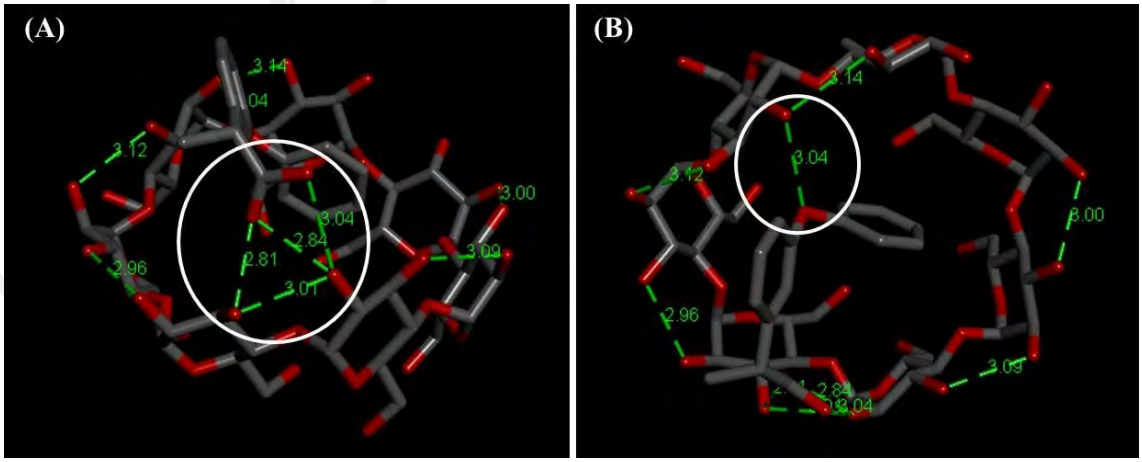

Figure 4.19: Hydrogen bond distance in angstrom between β-CD and FNP (A) top view and (B) side view

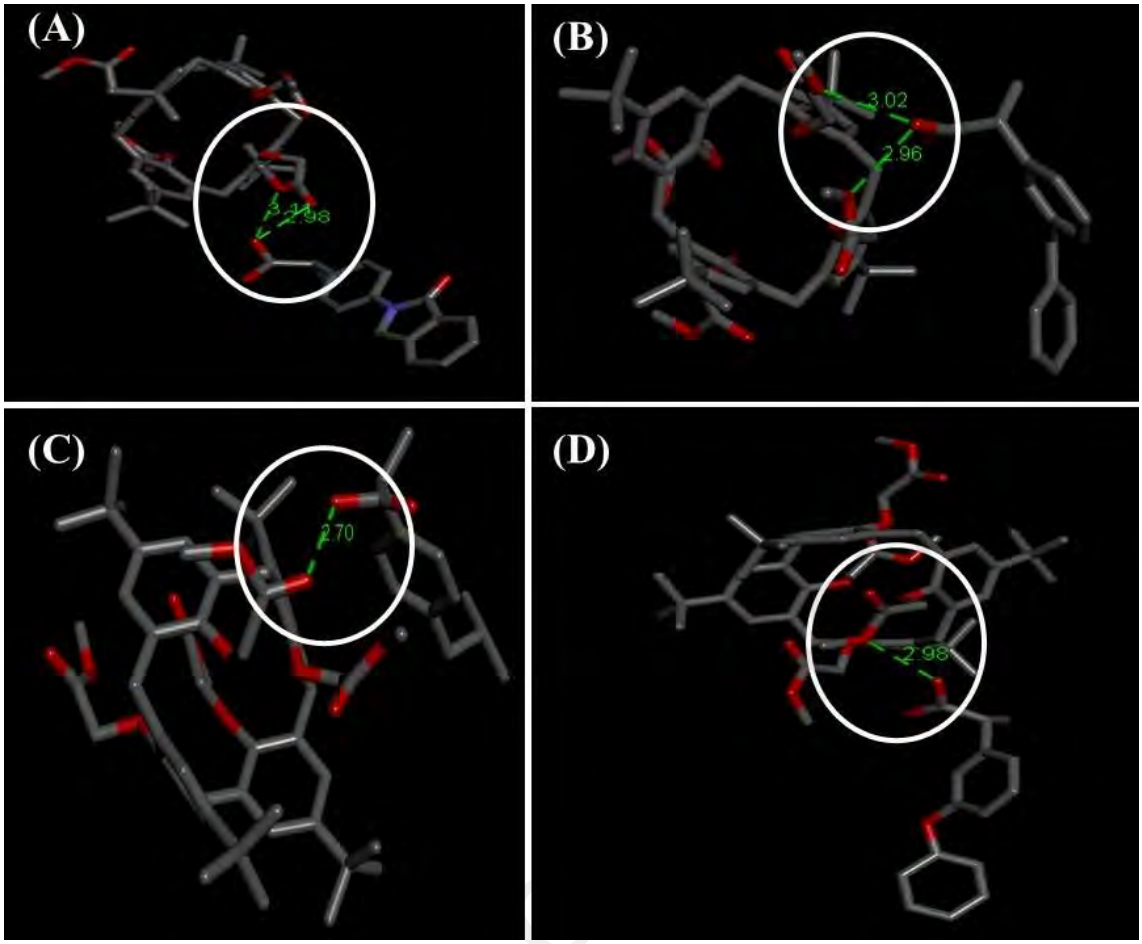

Figure 4.20: Hydrogen bond distance in angstrom between *p*-tertbutylcalix with (A) INP; (B) KTP; (C) IBP and (D) FNP

Table 4.3: Summary of hydrogen bonding occurrence in all complexes

Host	NSAID	Total of Hbond	Intermolecular Hbond	Distance (Å)
BCD	INP	5	O-H---O	2.90
			O-H---O	3.07
			O-H---O	2.61
			O-H---O	2.83
			O-H---O	3.32
	KTP	5	O-H---O	3.09
			O-H---O	2.96
			O-H---O	3.13
			O-H---O	2.84
			O-H---O	3.13
	IBP	3	O-H---O	3.19
			O-H---O	2.84
			O-H---O	2.83
	FNP	4	O-H---O	2.81
			O-H---O	2.84
			O-H---O	3.04
			O-H---O	3.04
***p*-tertbutylcalix**	INP	2	O-H---O	2.98
			O-H---O	3.11
	KTP	2	O-H---O	2.96
			O-H---O	3.02
	IBP	1	O-H---O	2.70
	FNP	1	O-H---O	2.98

4.2 PART B: EXPERIMENTAL STUDIES

4.2.1 Characterization of samples

The concept of this work is design and synthesis two types of new sporopollenin hybrid adsorbents functionalized with β-CD and *p*-tertbutylcalix[4]arene for magnetic solid phase extraction of non-steroidal anti-inflammatory drugs from water samples. Both synthesized adsorbents have been characterized by FTIR spectroscopy, X-ray diffraction (XRD), BET surface measurement and vibrating sample magnetometer (VSM). For morphological surface, the samples were characterized through field emission scanning electron microscopy (FESEM). The elementary analysis was confirmed by using energy dispersive X-ray spectroscopy (EDX).

The IR spectra of all synthesized adsorbents are shown in Figure 4.21. Raw sporopollenin showed some absorption bands at 1708, 1518, 1440 and 1112 cm^{-1}, respectively. These peaks indicate C=O, C=C, C-C and C-O stretching, respectively (Figure 4.21A). The following functionalization process of sporopollenin with TDI linker shows some additional bands around 2276, 1655 and 1516, 1603 and 1444 cm^{-1} indicate the presence of isocyanate group (N=C=O), NHCO carbamate linkage and aromatic TDI group, respectively (Figure 4.21B). The appearance of isocyanate at 2276 cm^{-1} clearly indicates the incorporation of isocyanate functionalities on the surface of sporopollenin. Additional peak at 1655 cm^{-1} and 1516 cm^{-1} for NHCO carbamate linkage groups stretching also confirmed the successful functionalization. In Figure 4.21(C), the disappearance of isocyanate group peaks (N=C=O) vibration at 2276 cm^{-1} was due to reaction between isocyanate group with β-CD. This is an evidence that β-CD is successfully bonded onto the surface of the Sp-TDI for the formation of Sp-TDI-βCD (Anne et al., 2018). Moreover, all significant peaks of β-CD in the range of 900 - 1709 cm^{-1} were present with a small shift. The magnetization process of Sp-TDI-βCD with

Fe_3O_4 MNPs and formation of **MSp-TDI-βCD** can be confirmed by the appearance of Fe-O stretching at around 562 cm^{-1} (Figure 4.21D).

The same concept applied for formation of Sp-TDI-calix and **MSp-TDI-calix**. IR spectrum for synthesized adsorbent of Sp-TDI-calix and **MSp-TDI-calix** were showed in Figure 4.21(E) and Figure 4.21(F). The disappearance of reserved isocyanate peak in Sp-TDI-calix is because of functionalization between Sp-TDI surface with *p*-tertbutylcalix[4]arene. Hence, it indicates *p*-tertbutylcalix[4]arene was successfully bonded onto the surface of the Sp-TDI (Mohammad, Mohamad, & Maah, 2010). Moreover, the appearance of bands at 1677 cm^{-1}, 1454 cm^{-1} and 1200 cm^{-1} correspond to C_{Ar}-C_{Ar} stretching, methylene bridge –CH_2- and C-C stretching respectively proved that *p*-tertbutylcalix[4]arene has been grafted on surface of sporopollenin. Finally, IR band at 566 cm^{-1} was associated with magnetite Fe_3O_4 band in **MSp-TDI-calix** indicates the adsorbent was successfully magnetite with Fe_3O_4. As summary, main IR frequencies with assignment peaks are shown in Table 4.4.

Table 4.4: Main IR frequencies with assignment peaks

Sample	Wavenumber (cm^{-1})	Assignment peaks
Sp	1708	C=O
	1518	C=C
	1440	C-C
	1112	C-O
Sp-TDI	2276	N-C=O
	1655, 1516	NHCO carbamate linkage
	1603, 1444	Aromatic TDI
Sp-TDI-βCD	1655, 1518	NHCO carbamate linkage
	1603, 1443	Aromatic TDI
	900-1700	β-CD
MSp-TDI-βCD	562	Fe-O
Sp-TDI-calix	1677	C_{Ar}-C_{Ar}
	1454	CH_2-CH_2
	1200	C-C
	1655, 1516	NHCO carbamate linkage
MSp-TDI-calix	566	Fe-O

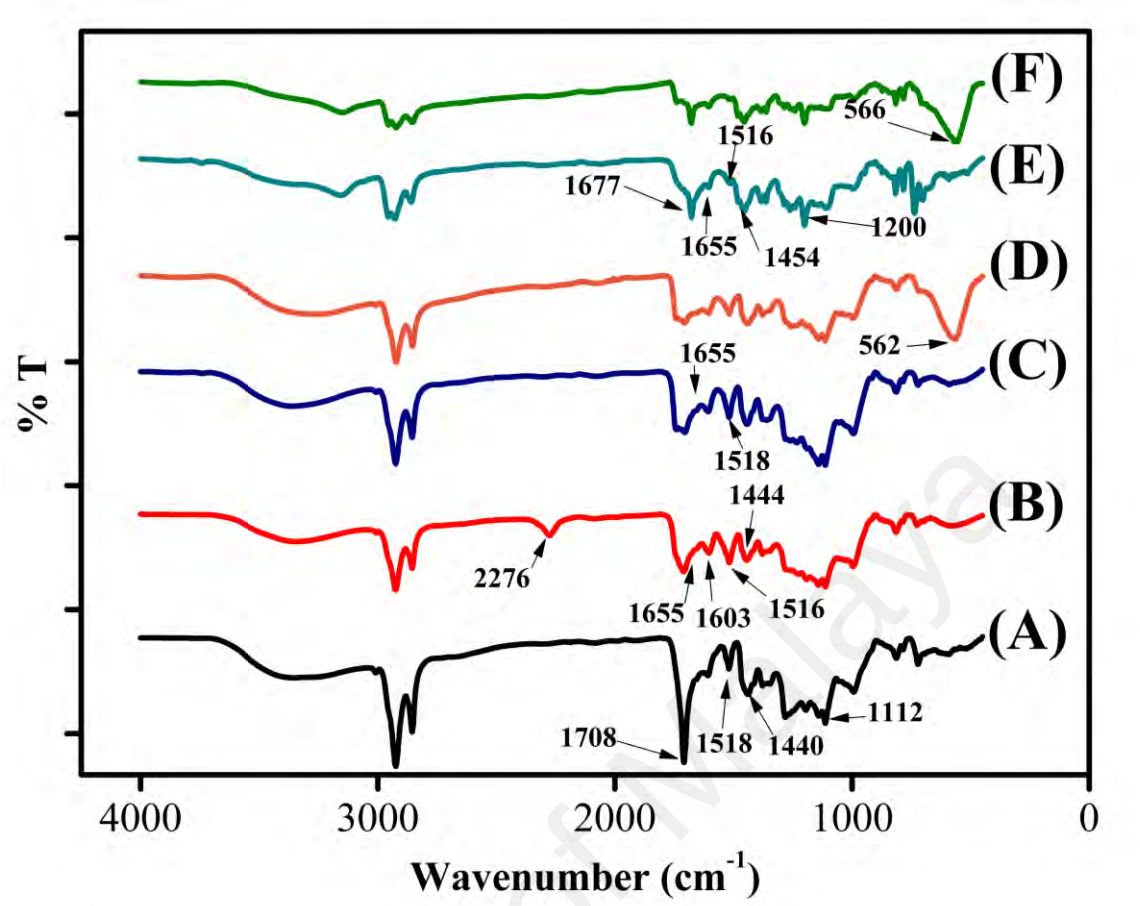

Figure 4.21: FTIR spectra of (A) sporopollenin; (B) Sp-TDI; (C) Sp-TDI-βCD; (D) **MSp-TDI-βCD**; (E) Sp-TDI-calix and (F) **MSp-TDI-calix**

The next characterization for validation of adsorbents formation was obtained through the X-ray diffraction (XRD) analysis. The XRD analyses were performed to measure the crystallinity of adsorbents. Sp and Sp-TDI exhibits broad diffraction peaks at ~25° which is typically observed for amorphous material as shown in Figure 4.22(A) and Figure 4.22 (B). Once β-CD was incorporated on the surface of Sp-TDI (Figure 4.22C), few diffraction peaks appear at ~10°-20° because of β-CD existed as crystalline form. Therefore, it indicates that β-CD functionalized at surface of Sp-TDI as well as improve the crystallinity properties of Sp-TDI. As for functionalized of *p*-tertbutylcalix[4]arene onto Sp-TDI surface, few diffraction peaks appear at ~10°-30° provided *p*-tertbutylcalix[4]arene successfully bonded onto surface of Sp-TDI. Moreover, the crystallinity of Sp-TDI-calix also has been improved by *p*-tertbutylcalix[4]arene by

appearance of few sharp and intense diffraction peaks as displayed in Figure 4.22(D). This make *p*-tertbutylcalix[4]arene was more suitable compound to improve crystallinity of Sp-TDI compared to β-CD. Six diffraction peaks of Fe_3O_4 were observed in **MSp-TDI-βCD** and **MSp-TDI-calix** as showed in Figure 4.22(E) and Figure 4.22(F). According to Joint Committee on Powder Diffraction Standards (JCPDS) reference pattern of magnetite (00-019-0629), these six diffractions pattern which are (220), (311), (400), (422), (511), and (440) related to cubic spine plane of Fe_3O_4 and confirming the presence of Fe_3O_4. It was also observed that no distinct diffraction peaks of β-CD and *p*-tertbutylcalix[4]arene appeared in **MSp-TDI-βCD** and **MSp-TDI-calix** respectively which indicated that the host molecules are distributed homogeneously without forming any phase separated crystal aggregates (Cao et al., 2013).

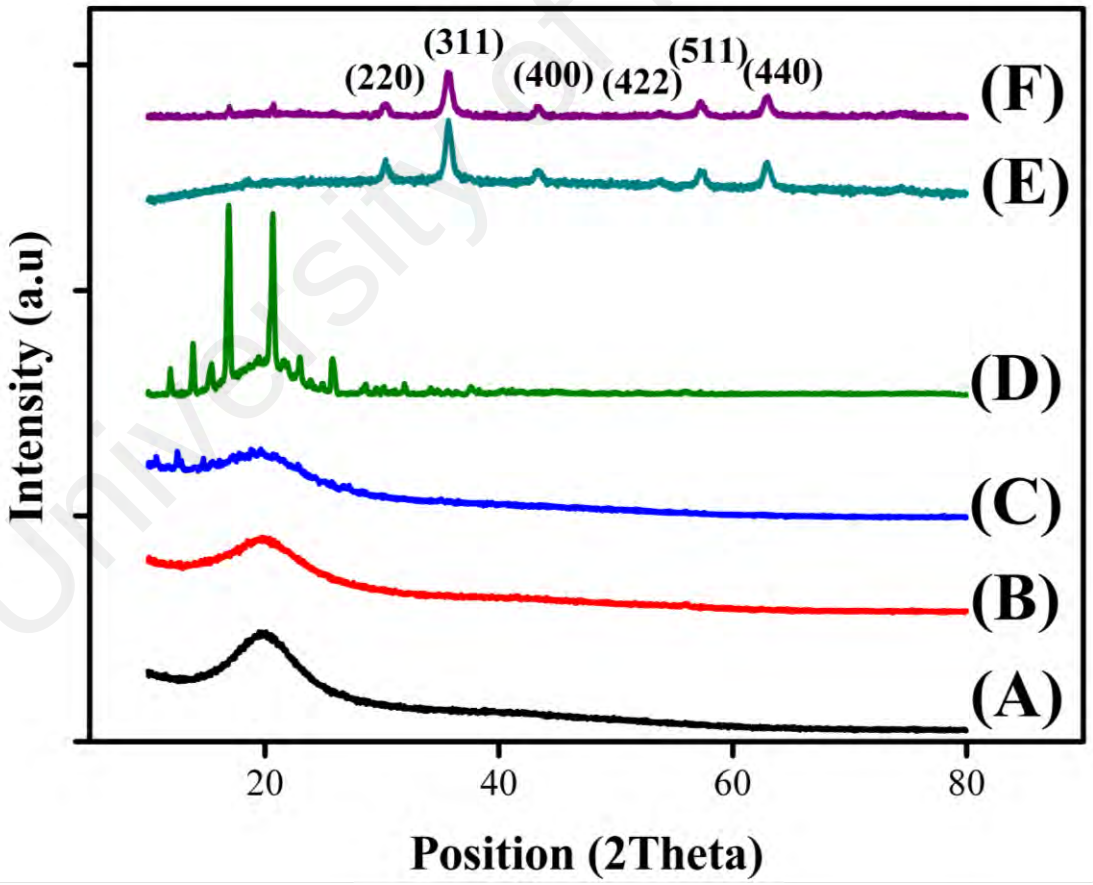

Figure 4.22: XRD spectra of (A) sporopollenin; (B) Sp-TDI; (C) Sp-TDI-βCD; (D) Sp-TDI-calix; (E) **MSp-TDI-βCD** and (F) **MSp-TDI-calix**

The structural and surface morphology of synthesized adsorbent was diagnostic through field emission scanning electron microscopy (FESEM). The FESEM images for sporopollenin, Sp-TDI-βCD, **MSp-TDI-βCD**, Sp-TDI-calix and **MSp-TDI-calix** are depicted in Figure 4.23. As illustrated in Figure 4.23(A), raw sporopollenin image showed a smooth morphology with open and uniform interconnected hexagonal hollowed structure surface. After functionalization with β-CD and *p*-tertbutylcalix[4]arene, the sporopollenin pores changes to be rough and bumpy surface filled with β-CD molecules and *p*-tertbutylcalix[4]arene respectively as showed in Figure 4.23(C) and Figure 4.23(E). As for Figure 4.23(D) and Figure 4.23 (F), it clearly showed that Fe_3O_4 particles were being occupied inside hollow surface of sporopollenin and each hollow structure remains unchanged after magnetization process. Hence, these images reveal that process of functionalization of β-CD and *p*-tertbutylcalix[4]arene onto surface of sporopollenin was successful and iron oxides also has embedded inside the pores of sporopollenin.

Combining FESEM morphological results and elemental composition by using energy dispersive x-ray give promising results in terms of formation of **MSp-TDI-βCD** and **MSp-TDI-calix** adsorbents. Before magnetization of Sp-TDI-βCD and Sp-TDI-calix, the nitrogen composition for both was 23.2% and 14.4% respectively as shown in Figure 4.24(A) and Figure 4.24(B). The presence of nitrogen from isocyanate group after functionalization of β-CD and *p*-tertbutylcalix[4]arene proved that this host molecule was bonded onto Sp-TDI surface. After the magnetization process, presence of iron element with composition of 18.8% and 33.8% for β-CD and *p*-tertbutylcalix[4]arene respectively suggesting the magnetic nanoparticles Fe_3O_4 was embedded at the surface of **MSp-TDI-βCD** and **MSp-TDI-calix** respectively as depicted in Figure 4.24(C) and Figure 4.24(D).

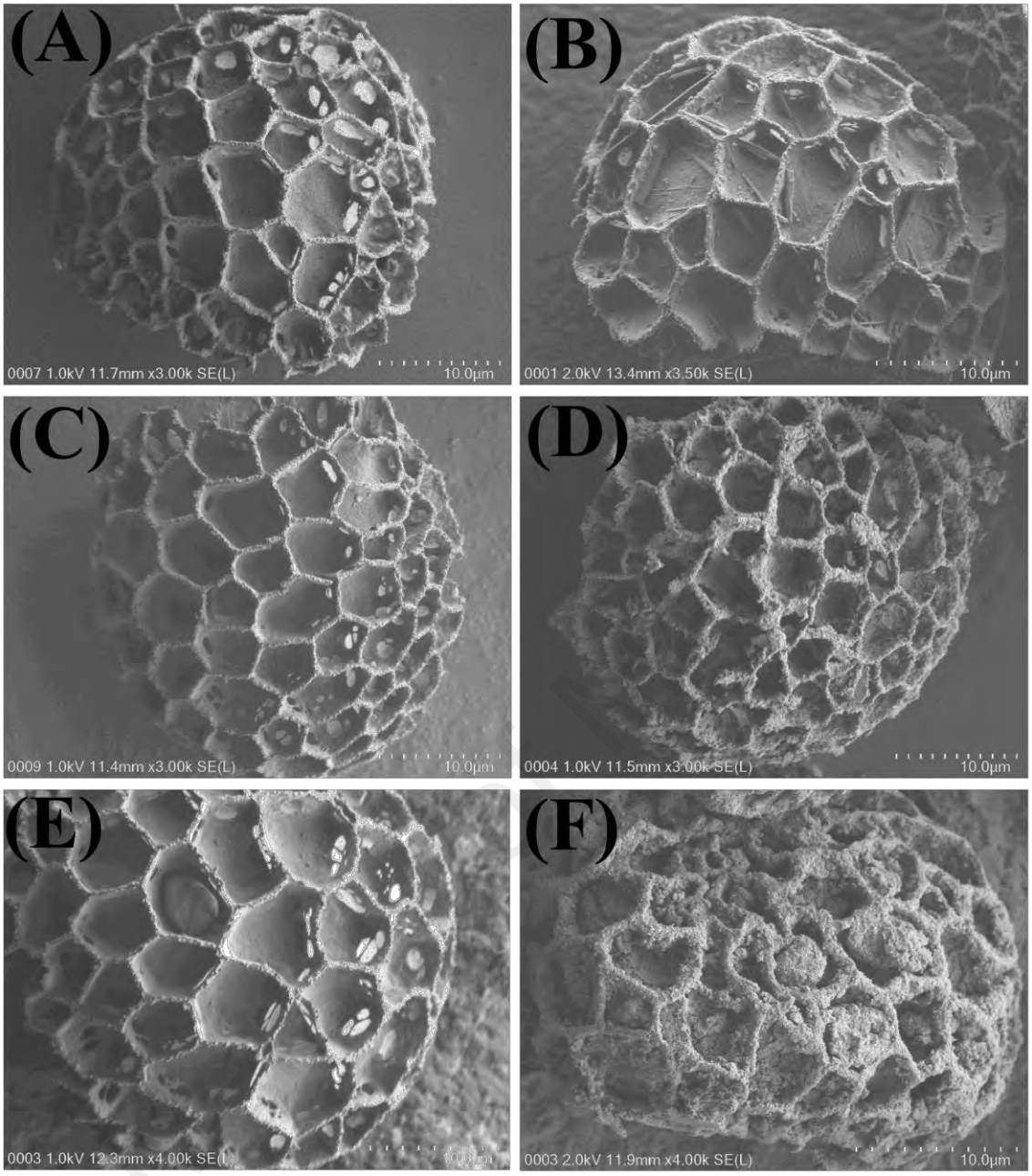

Figure 4.23: FESEM images of (A) Sporopollenin; (B) Sp-TDI; (C) Sp-TDI-βCD; (D) **MSp-TDI-βCD**; (E) Sp-TDI-calix and (F) **MSp-TDI-calix**

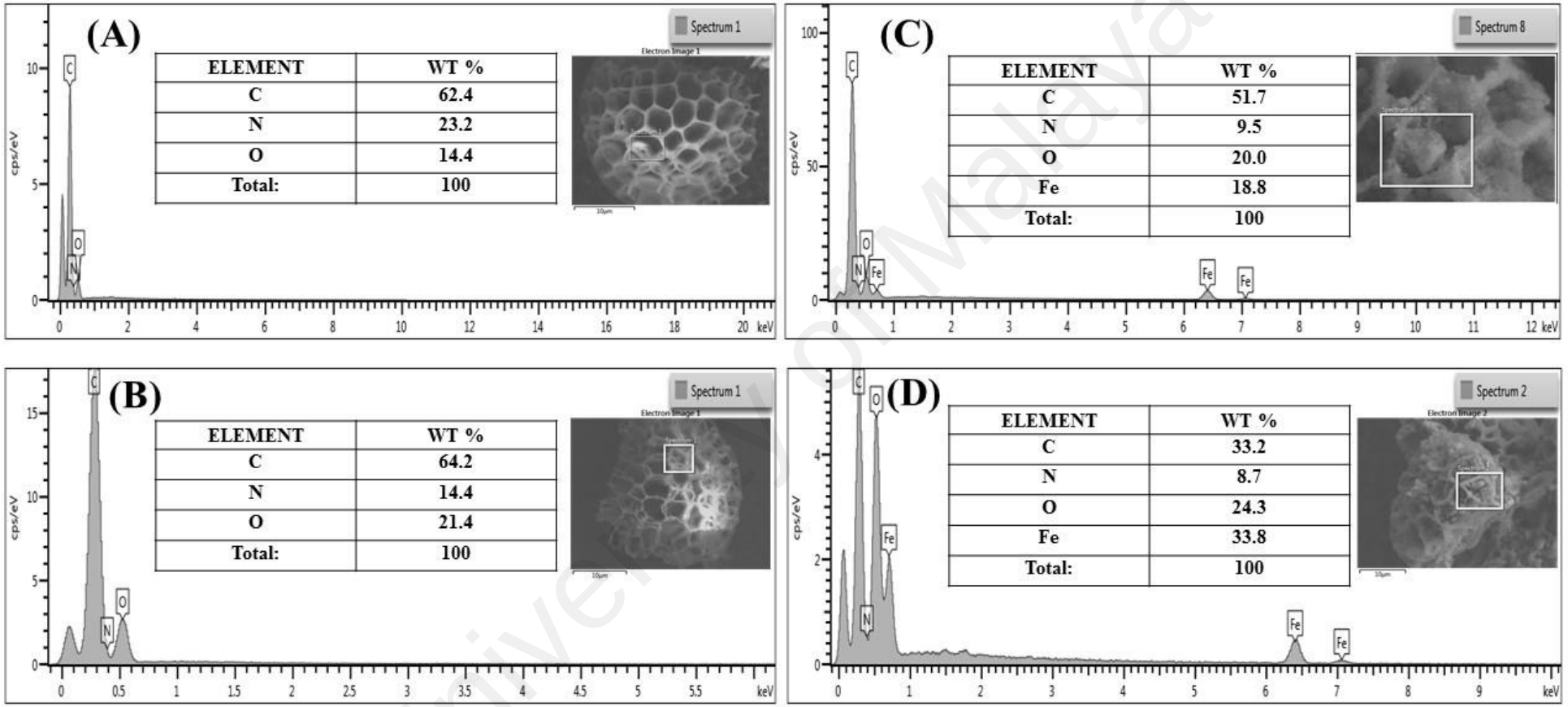

Figure 4.24: EDX spectra of (A) Sp-TDI-βCD; (B) Sp-TDI-calix; (C) **MSp-TDI-βCD** and (D) **MSp-TDI-calix**

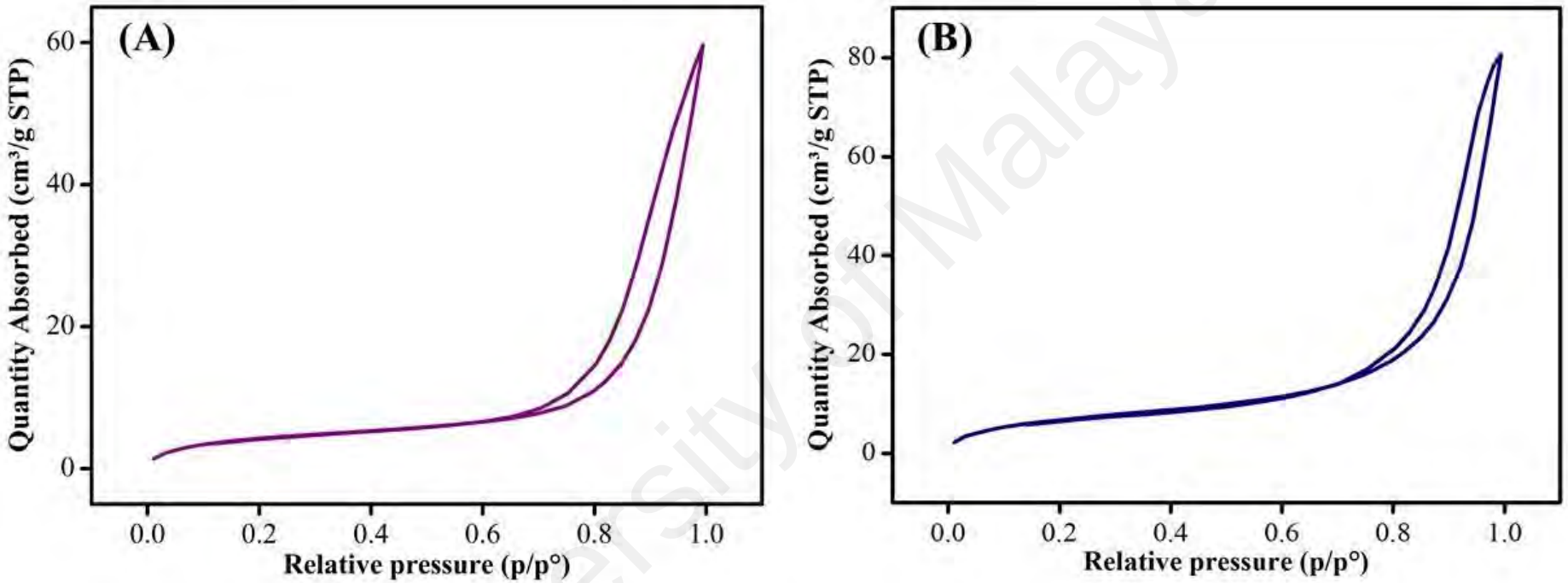

Figure 4.25: N_2 adsorption-desorption isotherms of (A) **MSp-TDI-βCD** and (B) **MSp-TDI-calix**

Figure 4.25 shows nitrogen adsorption-desorption isotherm of the adsorbent **MSp-TDI-βCD** and **MSp-TDI-calix**. Both of them exhibited close to type IV as defined by IUPAC classification with hysteresis loop in the range of 0.05 - 1.0 and suggesting that the adsorbent is basically mesoporous material with good pore connectivity (Farhadi et al., 2013). The specific surface area of the sample calculated by the BET is 16.5 m^2 g^{-1} for **MSp-TDI-βCD** and 26.5 m^2 g^{-1} for and **MSp-TDI-calix**. Besides, the pore size can be calculated from the surface area according to the equation $4V/S_{BET}$, where V is adsorption total pore volume and S_{BET} is the specific surface area of the **MSp-TDI-βCD** and **MSp-TDI-calix** respectively. The pore size calculated from the **MSp-TDI-βCD** surface area data is 22.3 nm meanwhile pore size for **MSp-TDI-calix** is 18.8 nm. The fluctuate trending between BET surface area in Sp-TDI-βCD and Sp-TDI-calix compared to raw sporopollenin from 2.27 to 2.73 m^2 g^{-1} and from 2.27 m^2/g to 2.08 m^2/g respectively due to adsorption sites has been covered by β-CD and *p*-tertbutylcalix[4]arene which has been immobilised on the surface of Sp-TDI and further hindered the N_2 molecules from accessing the binding site. Thus, it showed the β-CD and *p*-tertbutylcalix[4]arene were successfully bonded to Sp-TDI surface (Huang et al., 2010). After magnetization process, surface area, pore volume and pore size for both **MSp-TDI-βCD** and **MSp-TDI-calix** were increased rapidly. This proved magnetic nanoparticles enhanced the surface area by aggregation of particle and leads to enhancement of the spaces between the particles. Moreover, the improvement of these properties due to the dispersity of particles, thus enhance the adsorption capacity especially for large adsorbate molecule (Fan et al., 2011). Table 4.5 showed summary of pore size, pore volume and S_{BET} value for sporopollenin, Sp-TDI-βCD, **MSp-TDI-βCD**, Sp-TDI-calix and **MSp-TDI-calix**, respectively.

Table 4.5: Summary of pore size, pore volume and S_{BET} value for prepared adsorbents

Sample	Surface area ($m^2\ g^{-1}$)	Pore volume ($cm^3\ g^{-1}$)	Pore size (nm)
Sporopollenin	2.27	0.0014	2.60
Sp-TDI-βCD	2.73	0.0017	2.51
MSp-TDI-βCD	16.51	0.0922	22.3
Sp-TDI-calix	2.08	0.0017	3.26
MSp-TDI-calix	26.50	0.1250	18.8

The magnetism behaviour of **MSp-TDI-βCD** and **MSp-TDI-calix** was characterized by vibrating sample magnetometer (VSM) technique. Both **MSp-TDI-βCD** and **MSp-TDI-calix** displayed typical superparamagnetic behaviour as showed in Figure 4.26. The saturation magnetizations of analyse sample was 31.49 emu/g for **MSp-TDI-βCD** and as for **MSp-TDI-calix**, the saturation magnetization was 19.423 emu/g. Based on the results, its sufficient for both adsorbents to behaved as magnetic for separation since minimal magnetic separation reported was 16.30 emu/g (Cho et al., 2015). This properties make the adsorbent could be dispersed in water and separated by using neodymium magnet. The inset photos in Figure 4.26 show the adsorbent separation by using external magnetic field.

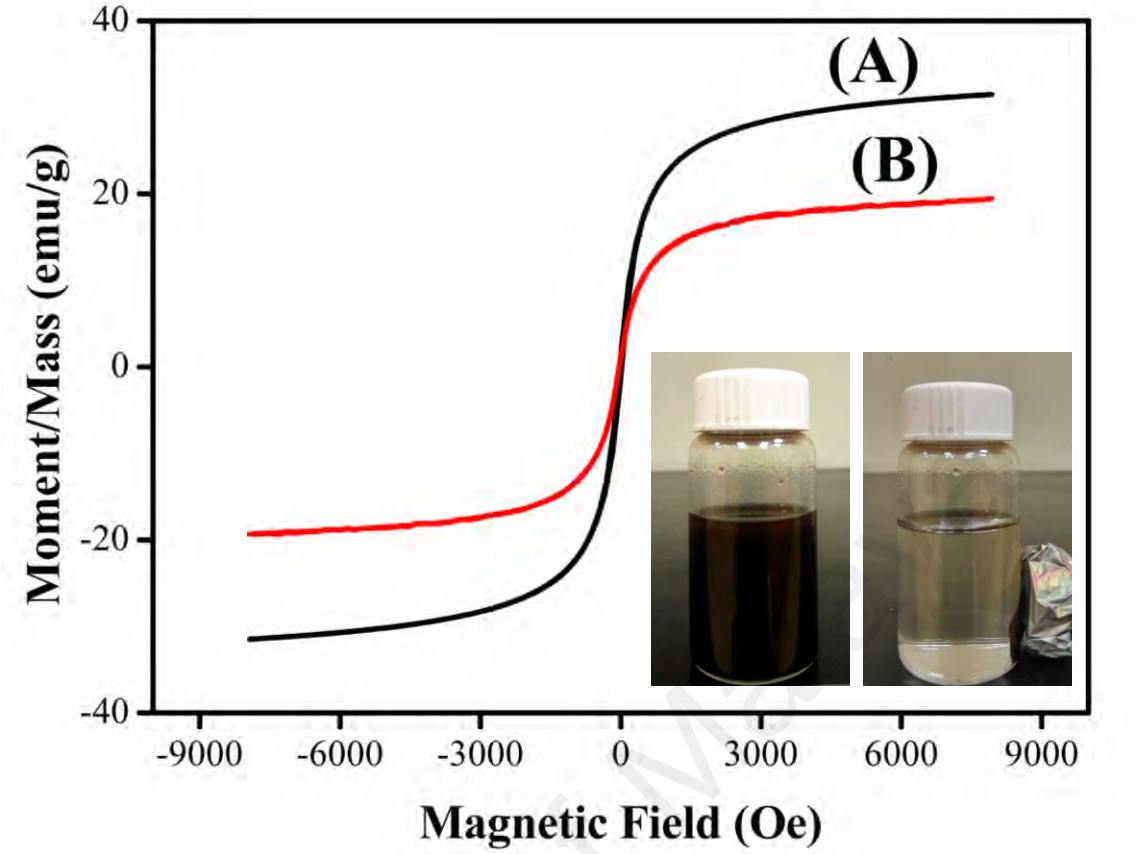

Figure 4.26: Magnetization curve of (A) **MSp-TDI-βCD** and (B) **MSp-TDI-calix**. The inset shows photographs of magnetic adsorbent dispersed in solution (left) and separated from water solution under an external magnetic field (right)

4.2.2 Applications of the MSp-TDI-βCD and MSp-TDI-calix

4.2.2.1 MSPE performance

(a) ***Screening study***

Preliminary sorption studies have been conducted to compare the performance of synthesized adsorbents with naked MNP and magnetic sporopollenin. The extraction efficiency of the adsorbents towards NSAIDs are illustrated in Figure 4.27. Among tested adsorbents, MNP showed lowest efficiency for all of the analytes studied. After introduction of sporopollenin to naked MNP, the extraction efficiency increased about 20% from initial concentration. Presence of sporopollenin makes the surface area increased and more accessible sites were available for NSAIDs adsorption. As for **MSp-**

TDI-βCD and **MSp-TDI-calix**, the presence of β-CD and *p*-tertbutylcalix[4]arene as a host molecules attached at the surface rapidly enhanced the selectively towards NSAIDs. Both host molecules were able to form inclusion complex with NSAIDs due to preserved cavity of both host during polymerization process. Even though hydrogen bonding existed between both host molecule and NSAIDs, but the highest adsorption was recorded for **MSp-TDI-calix** instead of **MSp-TDI-βCD**. This is because of presence of phenol group building up the structure of *p*-tertbutylcalix[4]arene. The extra π-π interaction formed between aromatic rings of phenol and aromatic rings of NSAIDs makes the interaction stronger in **MSp-TDI-calix** (Macias, Norton, & Evanseck, 2003). Meanwhile, β-CD existed as glucose and no additional molecular forces formed during the reaction between **MSp-TDI-βCD** and NSAIDs. Since **MSp-TDI-βCD** and **MSp-TDI-calix** showed the high peak area compared to naked MNP and MSp, it was selected for further MSPE extraction optimization.

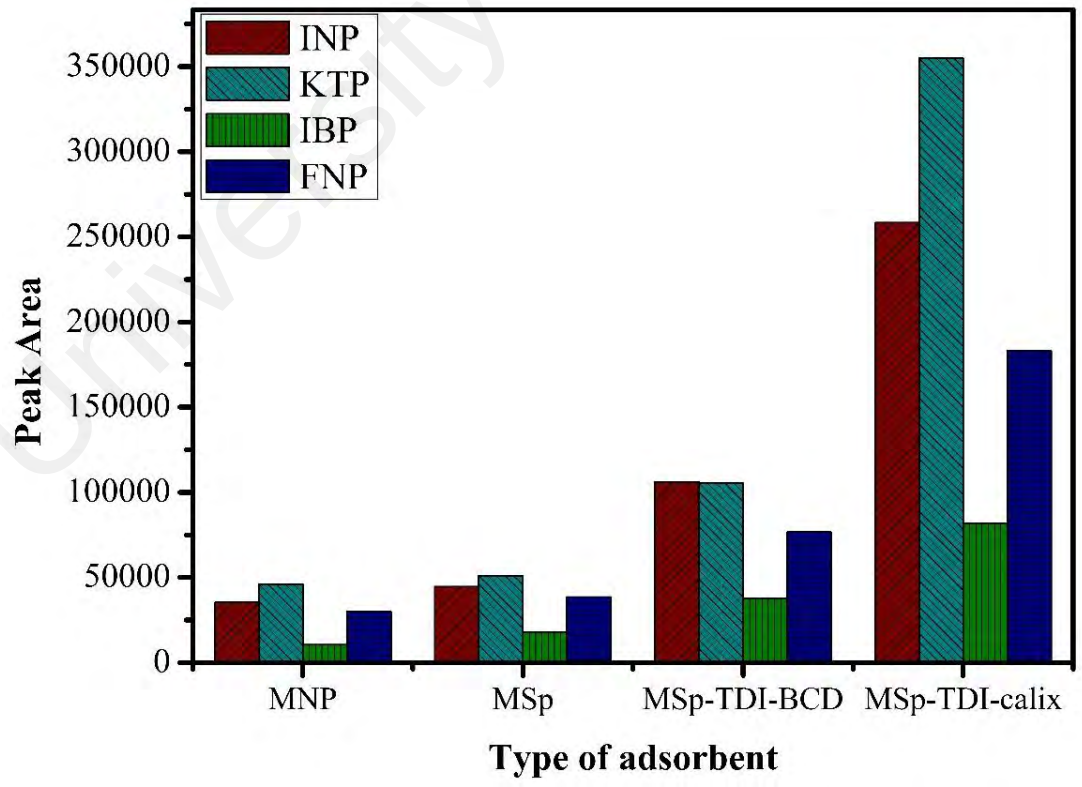

Figure 4.27: Preliminary sorption studied. Extraction condition: 10 mg adsorbent; 10 mL analytes solution; 10 min extraction and desorption time; 1.5 mL ACN elution

(b) ***Optimization parameters***

Several parameters such as adsorbent dosage, extraction and desorption time, type and volume organic solvent, sample volume and solution pH were evaluated in order to achieve optimal condition. These parameters mainly control the adsorbents surface characteristics and interaction between adsorbent/adsorbate. Therefore, extraction experiment was carried out using **MSp-TDI-βCD** and **MSp-TDI-calix** to study the effect of these parameters toward NSAIDs in water samples. Each trial was conducted using spiked standard solutions containing 1 µg/mL NSAIDs and each trial was performed in triplicated. At last, extraction efficiency was evaluated by using HPLC chromatography on each parameter studied towards NSAIDs.

Adsorbent dosage is the important parameter to improve the recovery of NSAIDs by the additional adsorption site of adsorbent. Six different amounts of dosage in the range of 5 mg to 50 mg was selected for both adsorbents and being optimized. Figure 4.28(A) showed optimum dosage of **MSp-TDI-βCD** was achieved at 10 mg meanwhile the optimum dosage for **MSp-TDI-calix** was measured at 30 mg as shown in Figure 4.28(B). The extraction efficiency of NSAIDs was starting to increase with increasing of adsorbents amount from 5 mg to 10 mg and 5 mg to 30 mg for **MSp-TDI-βCD** and **MSp-TDI-calix** respectively due to additional adsorption sites available for NSAIDs. Above this dosage, the extraction efficiency for both adsorbents were slightly equivalent or reduced compared to the optimum amount when the amount was increased to 50 mg. This is because an excessive amount of **MSp-TDI-βCD** and **MSp-TDI-calix** cannot encourage recovery significantly due to saturated active site and constantly saturated until adsorption equilibrium reaches (Rashidi et al., 2017). Therefore, 10 mg and 30 mg were setup as optimum dosage for **MSp-TDI-βCD** and **MSp-TDI-calix** respectively for all subsequent experiments.

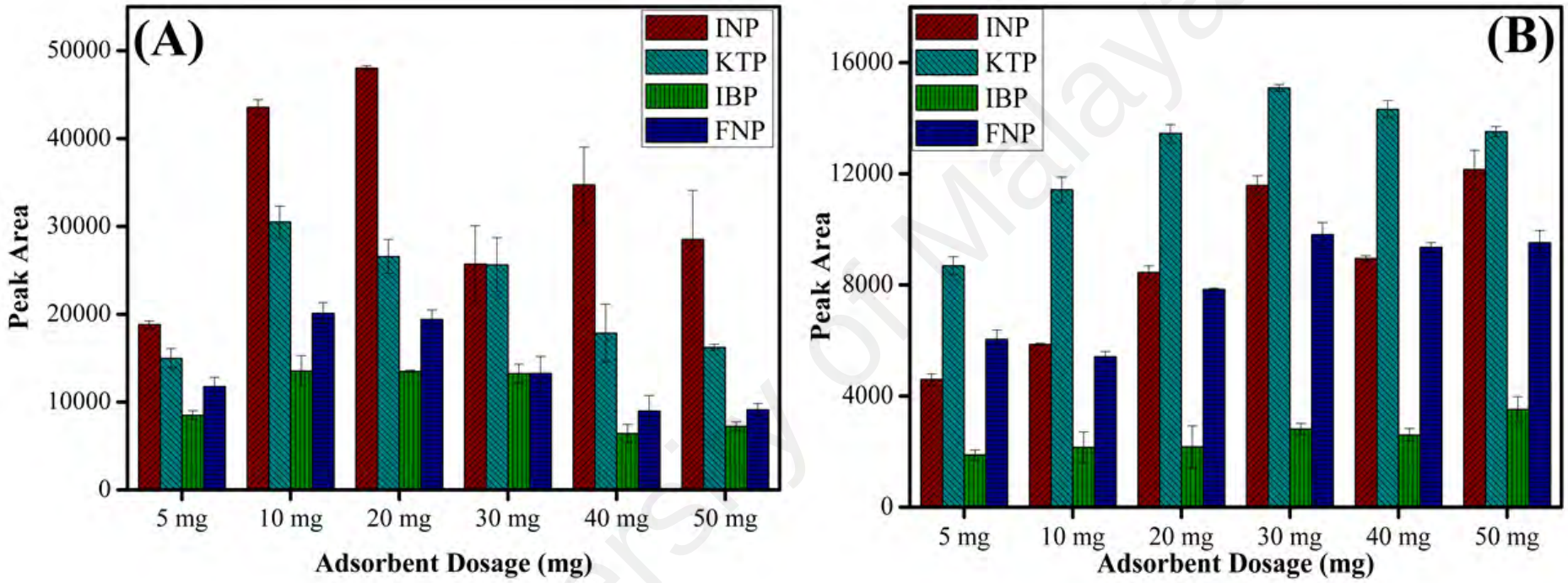

Figure 4.28: The effect of adsorbent dosage using (A) **MSp-TDI-βCD** and (B) **MSp-TDI-calix** for the extraction of NSAIDs using HPLC-DAD. HPLC conditions: acidified (1% with acetic acid) water/acetonitrile (50:50 v/v) as a mobile phase at a flow rate of 1 mL min^{-1}, the HPLC column temperature was set at 40 °C, the sample injection volume was 10 µL, the DAD detection for the selected NSAIDs was carried out at multiple wavelengths i.e., 281, 255, 271 and 219 nm for INP, KTP, IBP and FNP respectively

To attain the maximum NSAIDs adsorption on the surface of adsorbent, the sufficient contact time was required. The ideal extraction time was needed to obtain good enrichment performance as equilibrium was attained. However, if the extraction time was taking too long, it will squander much time and efficiency decreased. Thus, the extraction time were studied in the range of 5 min to 60 min for both adsorbent. As presented in Figure 4.29(A) and Figure 4.29(B), the maximum extraction efficiency was obtained at 30 min of extraction time for both adsorbent **MSp-TDI-βCD** and **MSp-TDI-calix**. After 30 min, extraction efficiency was decreased until reached 60 min. The reason of this observation is because of availability of vacant adsorption sites for NSAIDs during initial stage of adsorption process (Anne et al., 2018). After certain period of time, these vacant adsorption sites were occupied, and the extraction equilibrium was achieved between the aqueous phase and the adsorbent after 60 min. Therefore, 30 min was adequate to absorb all analytes fully.

In the same way, desorption time profile was studied for NSAIDs by varying the time from 5 min to 60 min for both adsorbent **MSp-TDI-βCD** and **MSp-TDI-calix**. As illustrated in Figure 4.30(A), **MSp-TDI-βCD** took about 30 min to desorb NSAIDs whereas **MSp-TDI-calix** acquired 10 min to completely desorb NSAIDs from adsorbent as shown in Figure 4.30(B). Above these desorption time for both adsorbent, extraction efficiency was not increase significantly. Re-adsorption of NSAIDs from the adsorbent surface may cause this observation and lower the extraction efficiency since MSPE is based on equilibrium driven process. Nevertheless, **MSp-TDI-calix** give shorter desorption time might be due to less number of hydrogen bond exist in **MSp-TDI-calix** compared to **MSp-TDI-βCD**. Thus, short time is required to extract the target analytes from the adsorbent surface Hence, 30 min and 10 min was sufficient and acceptable to fully eluted absorbed NSAIDs at the surface of adsorbent.

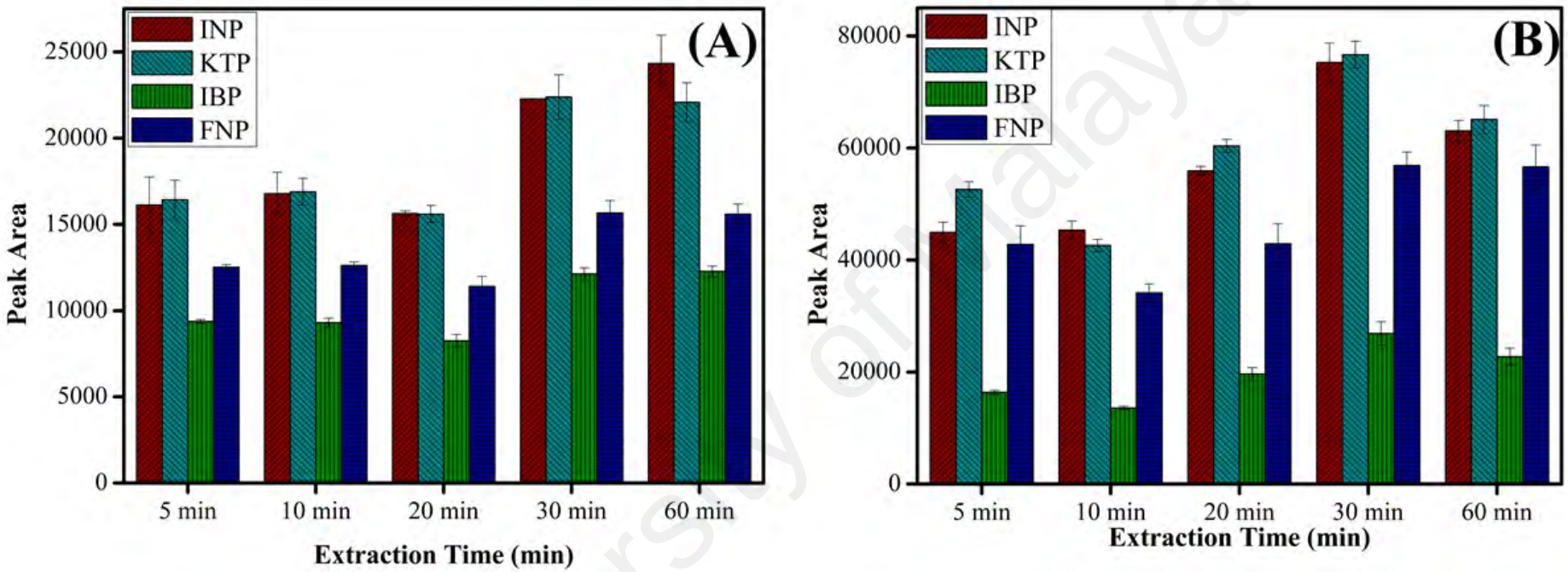

Figure 4.29: The effect of extraction time using (A) **MSp-TDI-βCD** and (B) **MSp-TDI-calix** for the extraction of NSAIDs using HPLC-DAD. HPLC conditions: acidified (1% with acetic acid) water/acetonitrile (50:50 v/v) as a mobile phase at a flow rate of 1 mL min^{-1}, the HPLC column temperature was set at 40 °C, the sample injection volume was 10 µL, the DAD detection for the selected NSAIDs was carried out at multiple wavelengths i.e., 281, 255, 271 and 219 nm for INP, KTP, IBP and FNP respectively

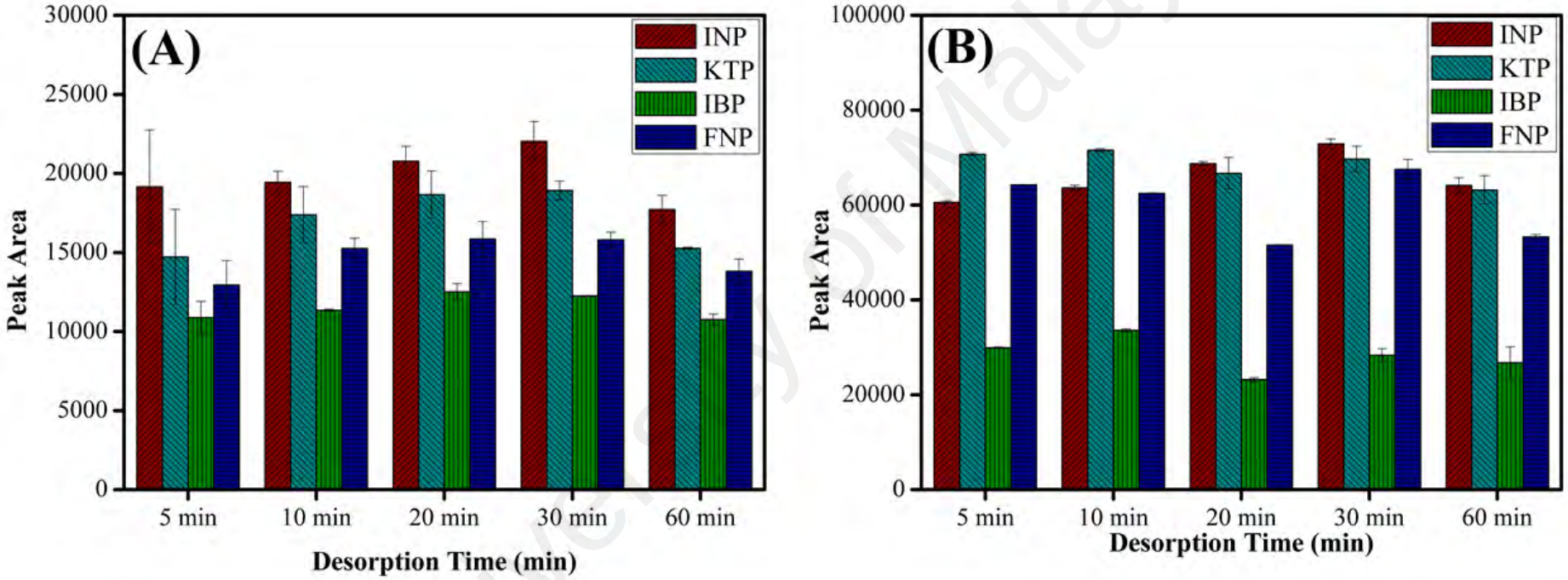

Figure 4.30: The effect of desorption time using (A) **MSp-TDI-βCD** and (B) **MSp-TDI-calix** for the extraction of NSAIDs using HPLC-DAD. HPLC conditions: acidified (1% with acetic acid) water/acetonitrile (50:50 v/v) as a mobile phase at a flow rate of 1 mL min^{-1}, the HPLC column temperature was set at 40 °C, the sample injection volume was 10 µL, the DAD detection for the selected NSAIDs was carried out at multiple wavelengths i.e., 281, 255, 271 and 219 nm for INP, KTP, IBP and FNP respectively

The next parameter needed to be optimized is type of organic solvent. It is to ensure the absorbed NSAIDs desorbed back after the extraction process to in order to recover the adsorbent. This stage is clearly the important point to entire extraction process and it is dependent upon the targeted analytes and its interaction with the adsorbent surface material and the selection of organic solvent to be used in the desorption process. To examine the influence of organic solvent on the extraction efficiency of NSAIDs, seven types of organic solvents was used which is methanol, acetonitrile, toluene, *n*-hexane, dichloromethane, dimethyl fluoride, ethyl acetate, and chloroform. Figure 4.31(A) and Figure 4.31(B) depict that the profile of type organic solvent used on desorption of NSAIDs by **MSp-TDI-βCD** and **MSp-TDI-calix** respectively. Both graph showed acetonitrile is the excellent candidate as desorption solvent with maximum extraction efficiency compared to another solvent. These phenomena can be explained by molecular interaction between analytes and sorbent surface. The intermolecular forces may occur between adsorbents and NSAIDs are hydrogen bonding, dipole-dipole interaction, π-π interaction and also van der Waals forces (Rozi, 2018). The organic eluent disrupts the retentive intermolecular forces between sorbent surface and analyte. Methanol is expected to give strong eluent on polar polymeric sorbent, but for instance acetonitrile give excellent eluent effect on sorbent surface compared with methanol. This is because methanol has strong polar eluent strength and it is unable to disrupt on non-polar interaction site. Acetonitrile is mid to polar-apolar eluent strength that can be disrupt the binding mechanism at polar and non-polar site sorbent surface. Nonpolar solvent as *n*-hexane give poor eluent capability due to its non-polar characteristic to disrupt the polar interaction. Therefore, acetonitrile was chosen as organic solvent for desorption of NSAIDs subsequently.

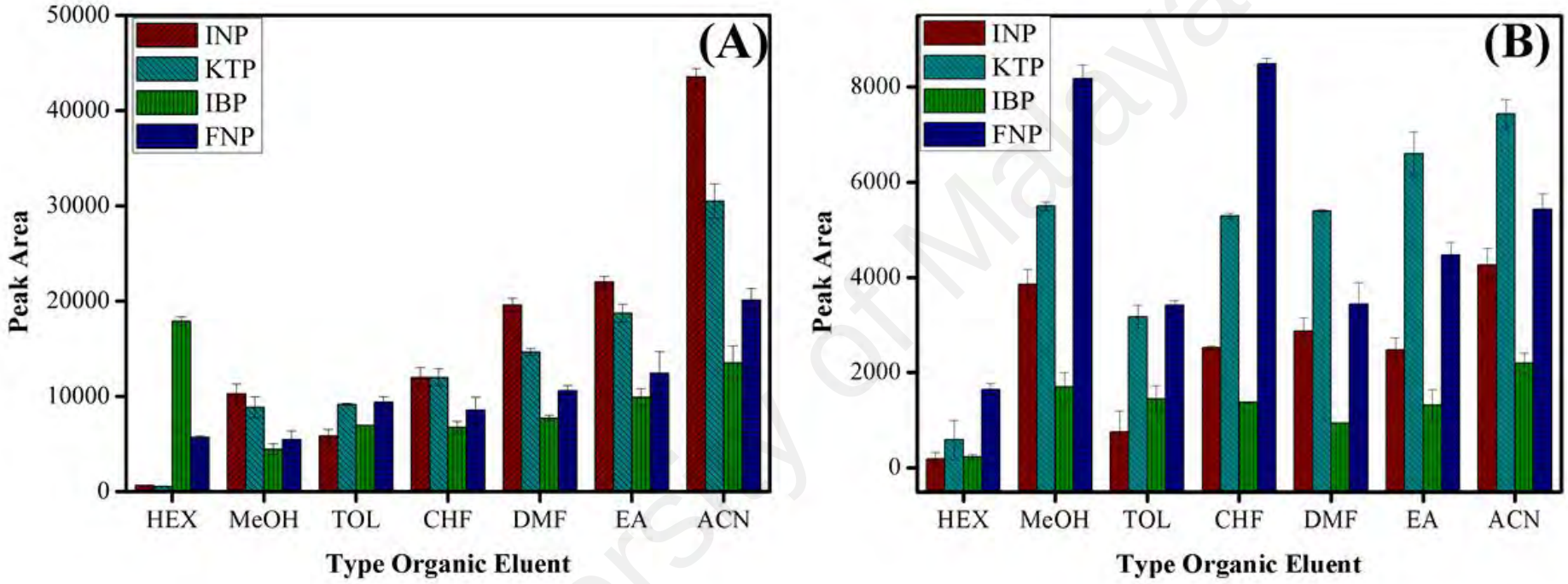

Figure 4.31: The effect of organic eluent types using (A) **MSp-TDI-βCD** and (B) **MSp-TDI-calix** for the extraction of NSAIDs using HPLC-DAD. HPLC conditions: acidified (1% with acetic acid) water/acetonitrile (50:50 v/v) as a mobile phase at a flow rate of 1 mL min^{-1}, the HPLC column temperature was set at 40 °C, the sample injection volume was 10 µL, the DAD detection for the selected NSAIDs was carried out at multiple wavelengths i.e., 281, 255, 271 and 219 nm for INP, KTP, IBP and FNP respectively

In addition to type organic solvent was used, the effect of its volume on the extraction efficiency also was investigated in the range of 0.5 mL to 3.0 mL for **MSp-TDI-βCD** and **MSp-TDI-calix** as presented in Figure 4.32(A) and Figure 4.32(B) respectively. For both adsorbent, the highest extraction efficiency was attained by using 1.5 mL of acetonitrile. By increasing the volume of acetonitrile, the extraction efficiency was increase until it reached optimum volume of 1.5 mL. Beyond this amount, the extraction efficiency starting to decrease because of dilution factor. The concentration of NSAIDs will diluted when high amount of organic used to elute all analytes fully. The optimum 1.5 mL of acetonitrile was suitable amount to be used in further trial.

During analysis of real sample, the concentration of targeted analyte basically lower than analytical instrument detection limit range. Sample volume plays important rule to recover the targeted analytes. High enrichment factor and high sensitivity can be obtained by using large sample volume (Korrani et al., 2016). Thus, six different volume of water samples ranging from 20 - 250 mL were evaluated. From Figure 4.33(A) and Figure 4.33(B), the peak area increased by increase of sample volume and the highest peak area with 200 mL sample volume was obtained for **MSp-TDI-βCD** and **MSp-TDI-calix**. However, beyond 200 mL sample volume the peak area is decrease significantly in **MSp-TDI-βCD** probably due to the breakthrough volume being exceeded (Rahim et al., 2016). Therefore, 200 mL of sample volume was selected as ideal and sufficient volume for further extraction of NSAIDs in water samples for both adsorbents.

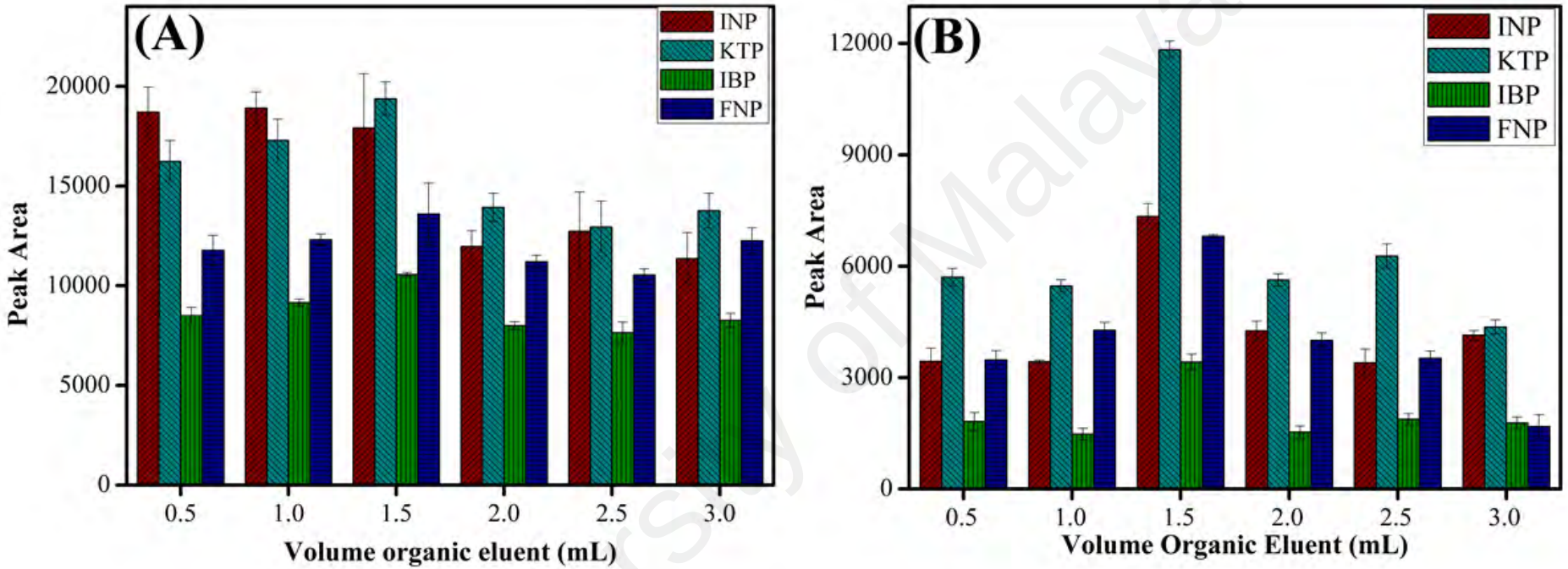

Figure 4.32: The effect of organic eluent volume using (A) **MSp-TDI-βCD** and (B) **MSp-TDI-calix** for the extraction of NSAIDs using HPLC-DAD. HPLC conditions: acidified (1% with acetic acid) water/acetonitrile (50:50 v/v) as a mobile phase at a flow rate of 1 mL min^{-1}, the HPLC column temperature was set at 40 °C, the sample injection volume was 10 µL, the DAD detection for the selected NSAIDs was carried out at multiple wavelengths i.e., 281, 255, 271 and 219 nm for INP, KTP, IBP and FNP respectively

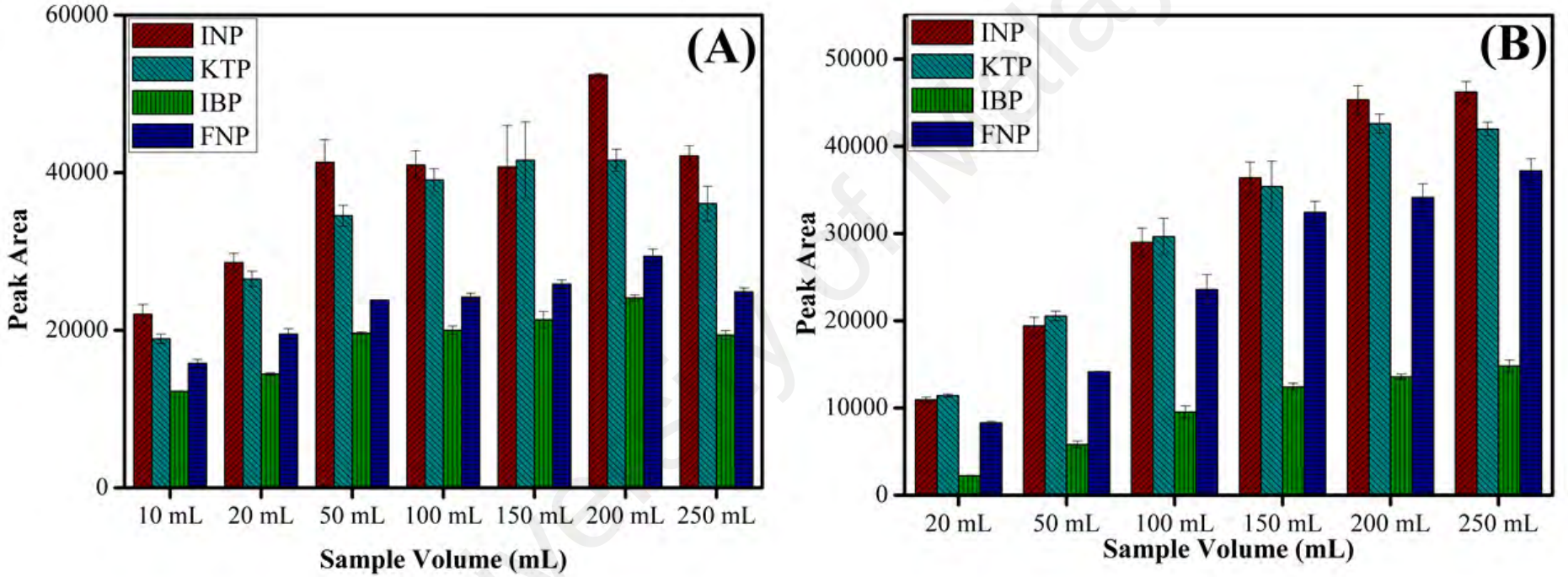

Figure 4.33: The effect of sample volume using (A) **MSp-TDI-βCD** and (B) **MSp-TDI-calix** for the extraction of NSAIDs using HPLC-DAD. HPLC conditions: acidified (1% with acetic acid) water/acetonitrile (50:50 v/v) as a mobile phase at a flow rate of 1 mL min^{-1}, the HPLC column temperature was set at 40 °C, the sample injection volume was 10 µL, the DAD detection for the selected NSAIDs was carried out at multiple wavelengths i.e., 281, 255, 271 and 219 nm for INP, KTP, IBP and FNP respectively

The sample pH is most important factor influencing the extraction efficiency of an analytes. The effectiveness of adsorption is highly dependent on the pH of the medium, since diversity in pH prompts variations in the surface properties of the adsorbent and in the degree of ionization of the selected NSAIDs molecules. Thus, the effect of solution pH on the extraction of selected NSAIDs was investigated using **MSp-TDI-βCD** and **MSp-TDI-calix** as an adsorbent at a pH of 2 - 10 as presented in Figure 4.34(A) and Figure 4.34(B). Results indicated that for both adsorbent, acidic medium is more suitable for the extraction of the selected NSAIDs and maximum extraction efficiency for selected NSAIDs was measured at pH 4. The highest extraction efficiency for the selected NSAIDs can be explained in terms of pKa values. The studied NSAIDs has pK_a value in the range of 3.66 - 4.88. The pH zero-point charge (pH_{zpc}) for both adsorbent was determined at value 6.0. At pH < pK_a value, the four NSAIDs mostly existed in deprotonated forms. The adsorbent surface exists in protonated form, which resulted in intermolecular forces such as hydrogen bonding, π-π interaction and Van der Waals interaction between analytes and adsorbent surface. Hence, higher extraction efficiency was obtained. However, beyond of pH 4, the peak area decreased rapidly. At pH > 6, the extraction efficiency was low for targeted analytes due to electrostatic repulsion between NSAIDs and the adsorbent surface. The NSAIDs molecule was transformed to anionic form, while the adsorbent surface also changed to deprotonated surface. The extraction is affected in a negative way in which strong repulsive force occurred between negative adsorbent surface and anionic targeted analytes leading the existed intermolecular forces severely weakened (Fan et al., 2011). Hence, pH 4 was selected for subsequent experiment.

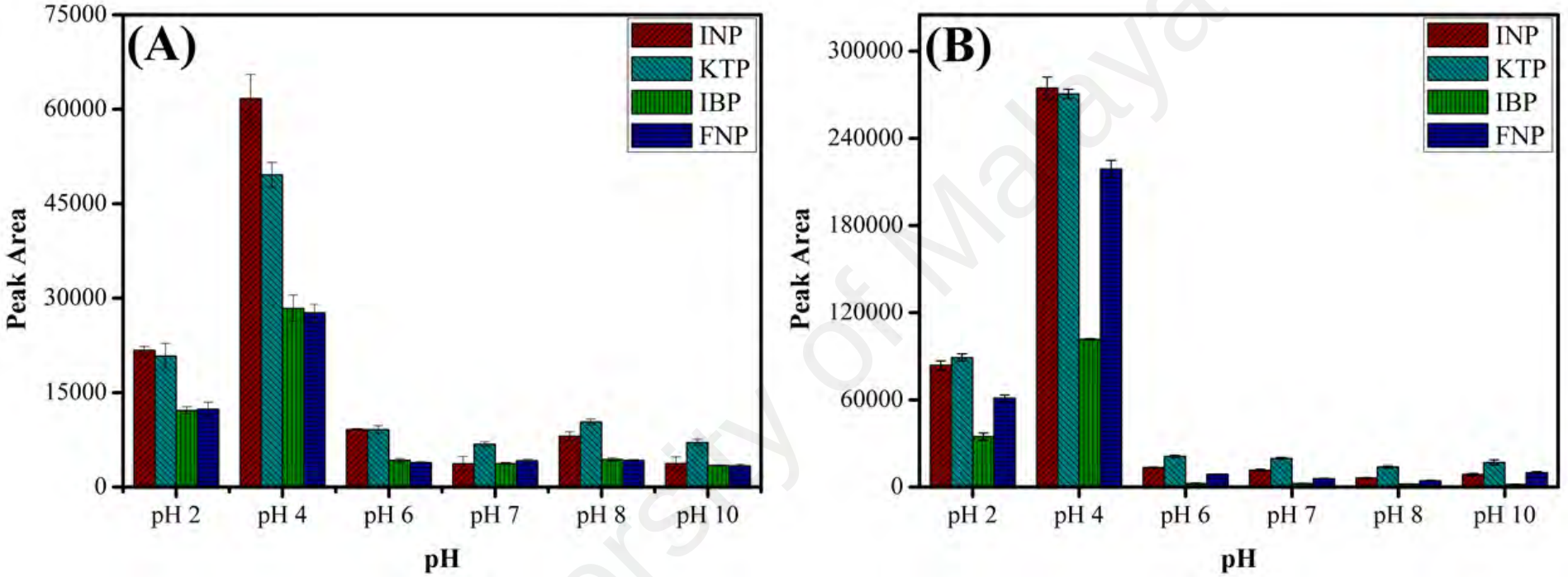

Figure 4.34: The effect of pH solution using (A) **MSp-TDI-βCD** and (B) **MSp-TDI-calix** for the extraction of NSAIDs using HPLC-DAD. HPLC conditions: acidified (1% with acetic acid) water/acetonitrile (50:50 v/v) as a mobile phase at a flow rate of 1 mL min^{-1}, the HPLC column temperature was set at 40 °C, the sample injection volume was 10 µL, the DAD detection for the selected NSAIDs was carried out at multiple wavelengths i.e., 281, 255, 271 and 219 nm for INP, KTP, IBP and FNP respectively

The reusability properties of the adsorbent are critical factors for practical use. Hence, reusability investigations of **MSp-TDI-βCD** and **MSp-TDI-calix** were conducted up to five cycles as shown in Figure 4.35 (A) and Figure 4.35(B) respectively. After each cycle, the adsorbent was washed with acetonitrile before the next MSPE application. The extraction efficiency persisted stable after five recycles, which indicated the **MSp-TDI-βCD** and **MSp-TDI-calix** magnetic particles were mechanically stable and possessed good reusability.

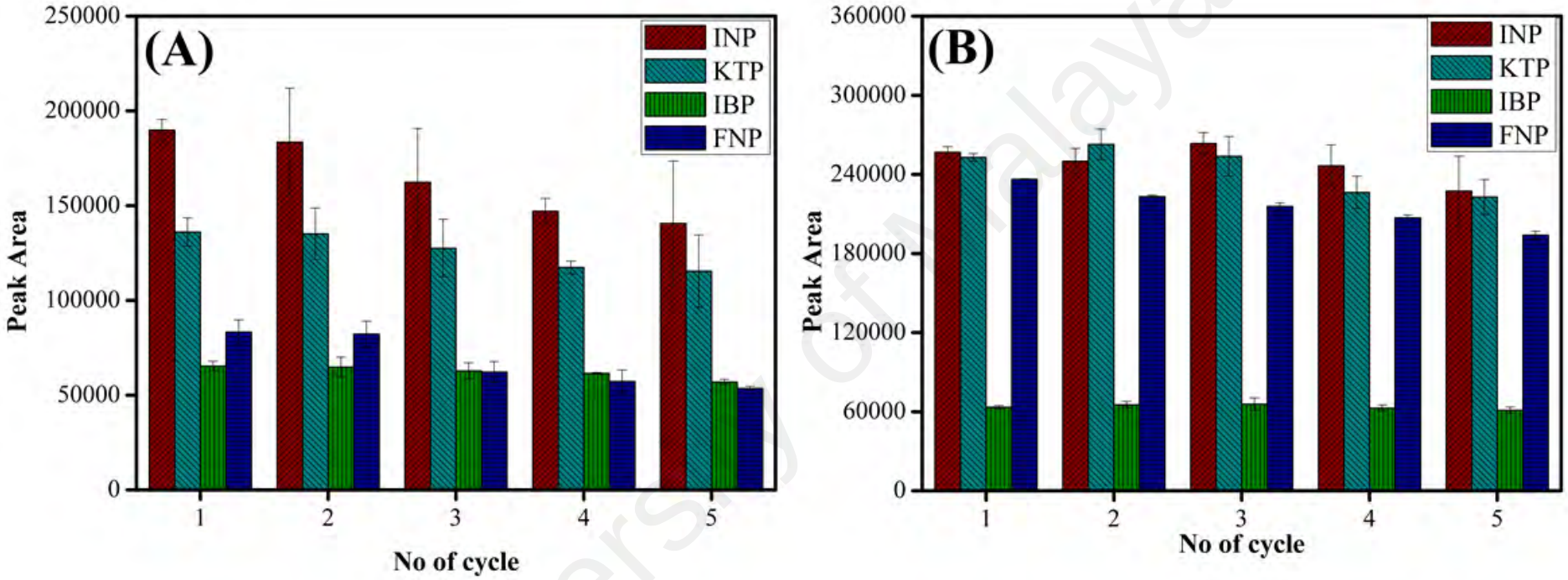

Figure 4.35: The reusability of adsorbents using (A) **MSp-TDI-βCD** and (B) **MSp-TDI-calix** for the extraction of NSAIDs using HPLC-DAD. HPLC conditions: acidified (1% with acetic acid) water/acetonitrile (50:50 v/v) as a mobile phase at a flow rate of 1 mL min^{-1}, the HPLC column temperature was set at 40 °C, the sample injection volume was 10 µL, the DAD detection for the selected NSAIDs was carried out at multiple wavelengths i.e., 281, 255, 271 and 219 nm for INP, KTP, IBP and FNP respectively

Based on optimized discussion, there are two optimal conditions for extraction of studied NSAIDs which is 10 mg of **MSp-TDI-βCD**, 200 mL sample volume, 1.5 mL of acetonitrile, 30 min of extraction and desorption time, and solution pH 4. For second adsorbent, the optimized conditions were 30 mg of **MSp-TDI-calix**, 200 mL sample volume, 30 min of extraction time and 10 min of desorption time, 1.5 mL of acetonitrile and sample pH 4. In order to validate the proposed MSPE method for extraction of studied NSAIDs, several statistical analysis experiments were conducted such as linearity, limit of quantification (LOQ), limit of detection (LOD) and precision. Analytical performance figures of merits are tabulated in Table 4.6. Linearity was defined as the ability of method to provide test result that are directly proportional to analyte concentration within a given range and usually reported as variance of the slope of the regression line. In this study, calibration curve was constructed at six level of concentration in the range of 0.5 - 500 ng/mL. A linear regression was obtained with good coefficient of determination $R^2 \geq 0.99$ for **MSp-TDI-βCD** and $R^2 \geq 0.99$ for **MSp-TDI-calix** respectively.

Limit of detection (LOD) and limit of quantification (LOQ) were also measured in this study. LOD was defined as the lowest concentration of an analyte in the sample able to be detected but not necessarily quantified. LOD was measured based on signal to noise ratio with formula of 3*SD/*m* where *SD* is standard deviation of the samples and *m* is slope of graph. In this study, LOD for selected NSAIDs were obtained to be 0.16 - 0.37 ng/mL for **MSp-TDI-βCD** adsorbent. Meanwhile, LOD for **MSp-TDI-calix** also were found in the range of 0.06 - 0.27 ng/mL. As for LOQ, it defined as the lowest concentration of an analyte in a sample that can be quantified with acceptable precision and accuracy. LOQ can be calculated same as LOD with formula of 10*SD/*m*. LOQ for selected NSAIDs based on **MSp-TDI-βCD** and **MSp-TDI-calix** adsorbent were calculated in the range of 0.53 - 1.22 ng/mL and 0.20 - 0.89 ng/mL respectively.

Precision was conducted in this study and it defines as the closeness of agreement among individual test results from repeated analyses of same samples. Precision was calculated in terms of repeatability for intra-day (five consecutives replicates on same day) and intermediate precision for inter-day (five consecutives replicates for three days). Repeatability refers to the ability of the method to generate the same results over a short time interval under identical conditions. Intermediate precision defines as agreement between the results from within same laboratory variation due to random events that might normally occur such as different analyst, different instrument or different days of experiment. In present study, the results were expressed as percentage relative standard deviation (RSD%). The selected NSAIDs shows the good precision with range of %*RSD* in between 2.1 - 5.5% for intra-day ($n = 5$) and 2.5 - 4.0% for inter-days ($n = 15$) for **MSp-TDI-βCD** adsorbent. As for **MSp-TDI-calix**, it shows improved RSD% compared than first adsorbent in range of 2.4 - 3.9% for intra-days ($n = 5$) and 2.5 - 3.2% for inter-days ($n = 15$).

Table 4.6: Qualitative data of the proposed MSPE method

Adsorbent	Analyte	Linearity (ng/mL)	R^2	LOD (ng/mL)	LOQ (ng/mL)	Precision	
						Intraday (RSD% $n = 5$)	Interday (RSD% $n = 15$)
MSp-TDI-βCD	INP	0.5 - 500	0.99	0.16	0.53	4.7	2.7
	KTP	0.5 - 500	0.99	0.18	0.59	5.5	4.0
	IBP	0.5 - 500	0.99	0.37	1.22	2.1	2.5
	FNP	0.5 - 500	0.99	0.17	0.58	5.5	3.3
MSp-TDI-calix	INP	0.5 - 500	0.99	0.07	0.25	2.4	2.5
	KTP	0.5 - 500	0.99	0.06	0.20	3.2	2.8
	IBP	0.5 - 500	0.99	0.27	0.89	3.9	3.1
	FNP	0.5 - 500	0.99	0.11	0.37	2.4	3.2

Tap, drinking and river water was chosen as real water samples matrices for the extraction of selected NSAIDs to assess the reliability of proposed method using both adsorbent **MSp-TDI-βCD** and **MSp-TDI-calix**. All real water samples were prepared by spiking four selected NSAIDs; INP, KTP, IBP and FNP at the concentration of 100 ng/mL and 10 ng/mL under optimized conditions in order to determine the sample matrix effect. Prior to the analysis, the blank samples were analysed to ensure the absent of selected NSAIDs in the real water samples. Figure 4.36 represents of spiked real water sample containing 100 ng/mL of selected NSAIDs compared with non-spiked samples for both adsorbents. All results were tabulated in Table 4.7 shows satisfactory recovery of selected NSAIDs for both adsorbent. For tap water analysis, MSPE proposed method gives acceptable recovery of selected NSAIDs for **MSp-TDI-βCD** in the range of 99.7 - 123.6% with RSDs (n = 5) ranging from 2.9 - 9.7%. Meanwhile, for **MSp-TDI-calix** gives better recovery in the range of 88.1 - 115.8% with RSD (n = 5) of 1.6 - 4.6%. As for drinking water analysis, tested method represents the satisfactory recoveries for selected NSAIDs for **MSp-TDI-βCD** ranging 99.7 - 123.6 % with RSDs (n = 5) of 2.9 - 9.7%. For **MSp-TDI-calix**, the recovery achieved in the range of 91.9 - 107.9% with RSDs (n = 5) from 1.9 - 4.6%.

Finally, as for river water sample, the present method gives tremendous recovery of selected NSAIDs for both adsorbent with excellent RSDs in the range of 97.3 - 123.5 with RSDs (n = 5) of 2.1% - 12.4% and 94.3% - 115.8% with RSDs (n = 5) from 1.8 - 4.5% for **MSp-TDI-βCD** and **MSp-TDI-calix** respectively. Based on the results attained, the excellent recoveries in three different sample matrices at trace level for selected NSAIDs shows the MSPE method can be classified as high potential technique for pre-concentration of samples. Moreover, based on Figure 4.36 (A-C)(i), no NSAIDs were detected in non-spiked real samples for both adsorbents.

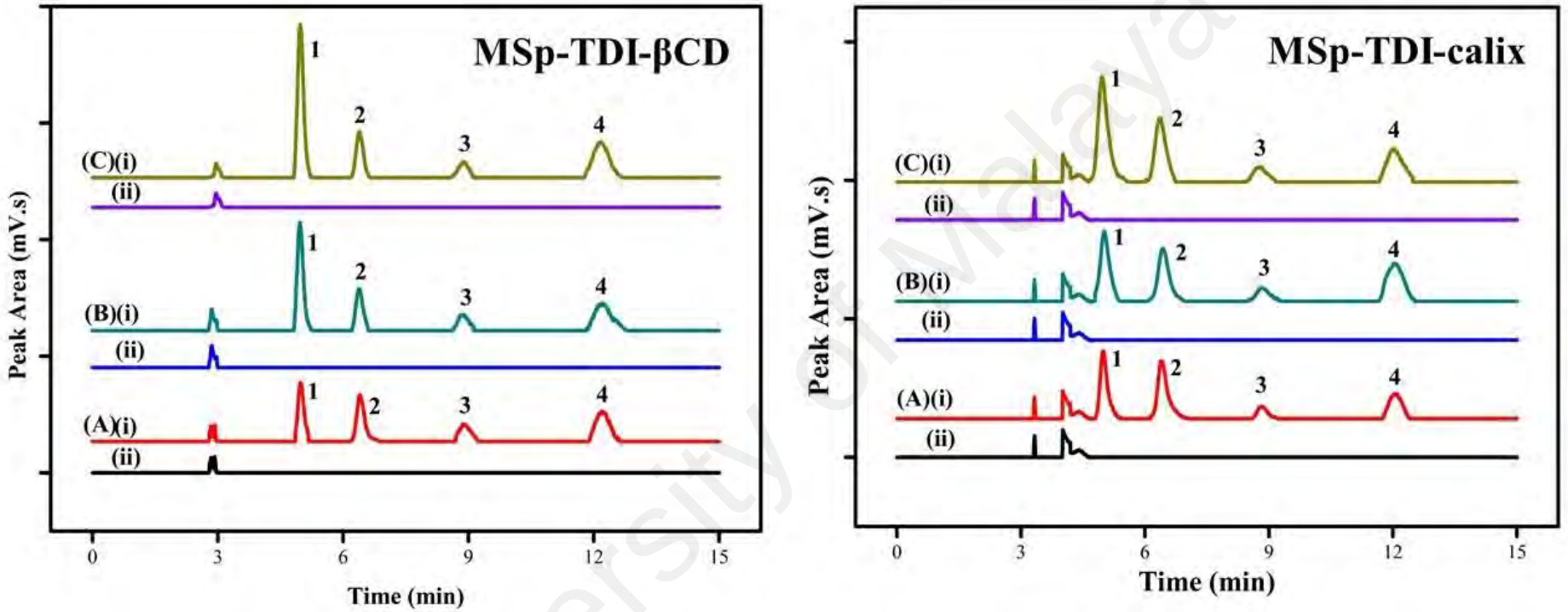

Figure 4.36: HPLC chromatograms of water samples (spiked with 100 ng/mL of each NSAIDs) using the proposed **MSp-TDI-βCD** and **MSp-TDI-calix** MSPE method; (A)(i) spiked tap water; (A)(ii) non-spiked tap water; (B)(i) spiked drinking water; (B)(ii) non-spiked drinking water; (C)(i) spiked river water; (C)(ii) non-spiked river water. Peak identification: (1) INP, (2) KTP, (3) IBP and (4) FNP

Table 4.7: Percentage relative recovery and RSD (n = 5) of NSAIDs in spiked water samples extracted with **MSp-TDI-βCD** and **MSp-TDI-calix**

Adsorbent	Analyte	Spiked (ng/mL)	Tap water (n = 5)		Drinking Water (n = 5)		River Water (n = 5)	
			Recovery (%)	RSD (%)	Recovery (%)	RSD (%)	Recovery (%)	RSD (%)
MSp-TDI-βCD	INP	10	123.6	9.5	92.9	4.1	112.8	4.2
		100	106.3	3.7	117.7	4.9	121.8	3.3
	KTP	10	115.6	8.6	92.5	9.6	123.5	5.6
		100	112.8	4.0	103.5	8.4	97.3	3.4
	IBP	10	109.4	8.2	113.7	12.3	103.4	9.4
		100	112.4	5.3	120.8	8.4	121.9	2.1
	FNP	10	99.7	9.7	99.6	9.7	108.3	12.4
		100	118.5	2.9	110.3	1.9	98.9	7.7

Table 4.7, continued

Adsorbent	Analyte	Spiked (ng/mL)	Tap water (*n* = 5)		Drinking Water (*n* = 5)		River Water (*n* = 5)	
			Recovery (%)	RSD (%)	Recovery (%)	RSD (%)	Recovery (%)	RSD (%)
MSp-TDI-calix	INP	10	92.4	3.6	104.6	1.9	103.6	4.0
		100	99.6	4.1	107.9	4.0	103.3	1.8
	KTP	10	88.1	2.1	107.8	2.1	98.2	2.2
		100	97.4	1.6	105.7	4.6	106.5	3.2
	IBP	10	109.8	4.6	105.2	3.0	94.3	4.5
		100	110.7	1.8	94.3	4.3	115.8	1.9
	FNP	10	103.5	4.4	96.2	2.6	97.2	3.5
		100	103.2	4.3	91.9	3.6	107.0	3.2

The proposed magnetic solid phase extraction (MSPE) technique based **MSp-TDI-βCD** and **MSp-TDI-calix** was compared with previous reported studies on determination of NSAIDs from various of sample matrices using same technique with different types of adsorbents. The purpose of comparison is to evaluate the effectiveness of develop method compared to other published studies in terms of linearity, percentage recovery, %RSD and LODs as shown in Table 4.8. The previous results shown that the uses of MSPE method were used intensively in various sample matrices including blood, human plasma and urine, as well as water and sewage water. Based on the results, our proposed method with applying our synthesized adsorbent shows excellent LOD and better %RSD compared to another studied making our synthesized adsorbents sensitive and selective for extraction of NSAIDs. Good recovery also was attained at accepted range level makes our synthesized adsorbents and technique as potential adsorbent and efficient method to encounter and eliminates all matrix effect in real samples. Moreover, simple preparation of **MSp-TDI-βCD** and **MSp-TDI-calix** as well as application of host-guest concept is the main advantages for selecting the adsorbent of MSPE method to determination of NSAIDs in water samples.

Table 4.8: Comparison of the developed MSPE adsorbent with other literature MSPE adsorbents for determination of NSAIDs in various sample matrices

Matrix	Type of analytes	Adsorbent	Technique	Linearity (ng/mL)	Recovery (%)	RSD%	LODs (ng/mL)	Ref
Urine and sewage	**NSAIDs**	MNPs modified with cetyltrimethyl-ammonium bromide (CTAB)	MSPE/HPLC DAD	7 - 200	91 - 97	3.98 - 9.83	2 - 7	(Sharifabadi et al., 2014)
Human plasma	**NSAIDs**	1-butyl-3-methylimidazolium bromide-INPs	MSPE/HPLC UV	10000 - 500000	98.7 - 100	0.4 - 0.8	1.5 - 5.8	(Ali et al., 2016)
Blood	**NSAIDs**	Fe_3O_4@SiO_2@IL	MSPE/HPLC UV	0.5 - 100	92 - 97	8.0 - 10.2	0.2 - 0.5	(Amiri et al., 2016)
Water and river water	**NSAIDs**	C_{18}/Diol-Fe_3O_4 MNPs	MSPE/HPLC UV	5 - 800	NR	NR	0.42 - 1.44	(Yuan Luo,2015)
Water	**NSAIDs**	MS-CNPrTEOS	MSPE/HPLC UV	1 - 1000	85.1 - 106.4	1.0 - 5.6	0.21 - 0.51	(Wahib et al., 2018)
Tap, drinking and river water	**NSAIDs**	**MSp-TDI-βCD**	**MSPE/HPLC DAD**	**0.5 - 500**	**92.5 - 123.6**	**1.9 - 12.4**	**0.1 - 0.4**	**Current study**
Tap, drinking and river water	**NSAIDs**	**MSp-TDI-calix**	**MSPE/HPLC DAD**	**0.5 - 500**	**88 - 116**	**1.6 - 4.6**	**0.06 - 0.26**	**Current study**

CHAPTER 5: CONCLUSION AND FUTURE RECOMMENDATIONS

5.1 Conclusion

The novel adsorbents cyclodextrin and calixarene framework functionalized bio-polymeric spores of sporopollenin hybrid magnetic materials have been synthesized in order to enhancing the extraction performance towards pharmaceutical pollutants. In the present study, **MSp-TDI-βCD** and **MSp-TDI-calix** were successfully characterized and used as a new MSPE adsorbent for the fast, simple and efficient extraction and enrichment of selected NSAIDs in environmental water samples prior to HPLC determination. Highly efficient and excellent extraction efficiency were achieved during extraction process for **MSp-TDI-βCD** and **MSp-TDI-calix**. For real water determination in tap, drinking and river water analysis, high recovery rates and acceptable RSDs for **MSp-TDI-βCD**, and **MSp-TDI-calix**. Hydrogen bonding, π-π interaction and van der Waals forces existed between functionalized adsorbent with selected NSAIDs were predicted as a main factors for high extraction efficiency during MSPE process. Another advantages such as effective regeneration and stability up to five cycles and superior performance of the adsorbent indicates its applicability to be employed as a potential adsorbent for extraction of selected NSAIDs.

For molecular modelling simulation section, the interaction between selected NSAIDs with β-CD and *p*-tertbutylcalix were investigated using several computational method which are molecular docking, molecular dynamics and quantum molecular mechanics semi-empirical AM1 method. Based on molecular docking simulation, the possible binding sites for NSAIDs – β-CD was located at inside cavity of β-CD, meanwhile binding sites for NSAIDs - *p*-tertbutylcalix was located at outer cavity of *p*-tertbutylcalix. The molecular dynamics simulation further confirmed the stability of all complex studied and showed that structural rearrangements in order to stabilize the whole complexation system. The dynamics of each selected NSAIDs molecule in cavity for each β-CD and *p*-

tertbutylcalix showed variation for both complexation systems. Each selected NSAIDs was stably bound on the each of host cavity except for β-CD-KTP and calix-KTP. As for quantum molecular mechanics semi-empirical AM1 method, it gives most stable and minimum energy for each of complexes formed. The contribution of intermolecular hydrogen bonding interaction was proven to act as the main assist for the formation of complexes. More hydrogen bond formed in β-CD complexes compared to *p*-tertbutylcalix complexes.

As a conclusion, based on molecular simulation and experimental approaches, it is believed that the synthesized adsorbent of **MSp-TDI-βCD** and **MSp-TDI-**calix and also the application of host-guest interaction of complexation technique of selected NSAIDs with β-CD and *p*-tertbutylcalix could be an alternative technique for the pre-concentrate, enrichment and extraction of NSAIDs from aqueous environmental matrices.

5.2 Recommendations for future research

The recommendation for future research is as follows:

a. From synthesis perspective, the sporopollenin could be functionalized with other type of host molecule by using current or other type of linker so it can be employed for another sample preparation.
b. In application aspects, the MSPE technique could be tried with other organic contaminants such as poly aromatic hydrocarbon (PAH) due presence of aromatic ring or other suitable contaminants that close to local environmental problems.
c. The free energies involved between NSAIDs with β-CD and *p*-tertbutylcalix in the complexation could be further examined by further energy study such as molecular mechanics Poisson-Boltzmann surface area (MM - PBSA).

REFERENCES

Abbasi, S., Haeri, S. A., & Sajjadifar, S. (2019). Bio-dispersive liquid liquid microextraction based on nano rhamnolipid aggregates combined with molecularly imprinted-solid phase extraction for selective determination of paracetamol in human urine samples followed by HPLC. *Microchemical Journal*, *146*, 106–114.

Abd Rahim, M., Wan Ibrahim, W. A., Ramli, Z., Sanagi, M. M., & Aboul-Enein, H. Y. (2016). New sol-gel hybrid material in solid phase extraction combined with liquid chromatography for the determination of non-steroidal anti-inflammatory drugs in water samples. *Chromatographia*, *79*, 421–429.

Abd Wahib, S. M., Wan Ibrahim, W. A., Sanagi, M. M., Kamboh, M. A., & Abdul Keyon, A. S. (2018). Magnetic sporopollenin-cyanopropyltriethoxysilane-dispersive micro-solid phase extraction coupled with high performance liquid chromatography for the determination of selected non-steroidal anti-inflammatory drugs in water samples. *Journal of Chromatography A*, *1532*, 50–57.

Agrawal, Y. K., Pancholi, J. P., & Vyas, J. M. (2009). Design and synthesis of calixarene. *Journal of Scientific & Industrial Research*, *68*, 745–768.

Ahmad, N. F., Kamboh, M. A., Nodeh, H. R., Halim, S. N. B. A., & Mohamad, S. (2017). Synthesis of piperazine functionalized magnetic sporopollenin: a new organic-inorganic hybrid material for the removal of lead(II) and arsenic(III) from aqueous solution. *Environmental Science and Pollution Research*, *24*, 21846–21858.

Ahrer, W., Scherwenk, E., & Buchberger, W. (2001). Determination of drug residues in water by the combination of liquid chromatography or capillary electrophoresis with electrospray mass spectrometry. *Journal of Chromatography A*, *910*, 69–78.

Akceylan, E., Bahadir, M., & Yilmaz, M. (2009). Removal efficiency of a calix[4]arene-based polymer for water-soluble carcinogenic direct azo dyes and aromatic amines. *Journal of Hazardous Materials*, *162*, 960–966.

Akrami, M., Khoobi, M., Khalilvand-Sedagheh, M., Haririan, I., Bahador, A., Faramarzi, M. A., … Shafiee, A. (2015). Evaluation of multilayer coated magnetic nanoparticles as biocompatible curcumin delivery platforms for breast cancer treatment. *RSC Advances*, *5*, 88096–88107.

Albrecht, M. (2007). Supramolecular chemistry - General principles and selected examples from anion recognition and metallosupramolecular chemistry. *Naturwissenschaften*, *94*, 951–966.

Ali, I., Kulsum, U., AL-Othman, Z. A., & Saleem, K. (2016). Analyses of nonsteroidal anti-inflammatory drugs in human plasma using dispersive nano solid-phase extraction and high-performance liquid chromatography. *Chromatographia*, *79*, 145–157.

Alinezhad, H., Amiri, A., Tarahomi, M., & Maleki, B. (2018). Magnetic solid-phase extraction of non-steroidal anti-inflammatory drugs from environmental water samples using polyamidoamine dendrimer functionalized with magnetite nanoparticles as a sorbent. *Talanta*, *183*, 149–157.

Allport, D. C., Gilbert, D. S., & Outterside, S. M. (1998). *MDI and TDI: Safety, Health & Environment, A Source Book and Practical Guide*. Sussex, England: John Wiley & Son Ltd.

Alvira, E. (2017). Molecular dynamics study of the factors influencing the β-cyclodextrin inclusion complex formation of the isomers of linear molecules. *Journal of Chemistry*, *2017*, 1–9.

Amiri, M., YadollahYamini, Safari, M., & Asiabi, H. (2016). Magnetite nanoparticles coated with covalently immobilized ionic liquids as a sorbent for extraction of non-steroidal anti-inflammatory drugs from biological fluids. *Microchimica Acta*, *183*, 2297–2305.

Anne, J. M., Y. H. Boon, B. Saad, M. Miskam, M. M. Yusoff, M. S. Shahriman, … M. Raoov. (2018). b-Cyclodextrin conjugated bifunctional isocyanate linker polymer for enhanced removal of 2,4-dinitrophenol from environmental waters. *Royal Society Open Science*, *5*, 180942-180964.

Ariga, K., & Kunitake, T. (2006). *Supramolecular Chemistry — Fundamentals and Applications*. Verlag Berlin Heidelberg, Germany: Springer.

Arslan, M., Sayin, S., & Yilmaz, M. (2013). Removal of carcinogenic azo dyes from water by new cyclodextrin-immobilized iron oxide magnetic nanoparticles. *Water, Air, and Soil Pollution*, *224*, 1–9.

Asgharinezhad, A. A., Mollazadeh, N., Ebrahimzadeh, H., Mirbabaei, F., & Shekari, N. (2014). Magnetic nanoparticles based dispersive micro-solid-phase extraction as a novel technique for coextraction of acidic and basic drugs from biological fluids and waste water. *Journal of Chromatography A*, *1338*, 1–8.

Ashton, D., Hilton, M., & Thomas, K. V. (2004). Investigating the environmental transport of human pharmaceuticals to streams in the United Kingdom. *Science of the Total Environment*, *333*, 167–184.

Atanassova, M., & Kurteva, V. (2016). Synergism as a phenomenon in solvent extraction of 4f-elements with calixarenes. *RSC Advances*, *6*, 11303–11324.

Ayar, A., Gezici, O., & Küçükosmanoğlu, M. (2007). Adsorptive removal of methylene blue and methyl orange from aqueous media by carboxylated diaminoethane sporopollenin: On the usability of an aminocarboxilic acid functionality-bearing solid-stationary phase in column techniques. *Journal of Hazardous Materials*, *146*, 186–193.

Badruddoza, A. Z. M., Hidajat, K., & Uddin, M. S. (2010). Synthesis and characterization of β-cyclodextrin-conjugated magnetic nanoparticles and their uses as solid-phase artificial chaperones in refolding of carbonic anhydrase bovine. *Journal of Colloid and Interface Science*, *346*, 337–346.

Badruddoza, A. Z. M., Junwen, L., Hidajat, K., & Uddin, M. S. (2012). Selective recognition and separation of nucleosides using carboxymethyl-β-cyclodextrin functionalized hybrid magnetic nanoparticles. *Colloids and Surfaces B: Biointerfaces*, *92*, 223–231.

Badruddoza, A. Z. M., Tay, A. S. H., Tan, P. Y., Hidajat, K., & Uddin, M. S. (2011). Carboxymethyl-β-cyclodextrin conjugated magnetic nanoparticles as nano-adsorbents for removal of copper ions: Synthesis and adsorption studies. *Journal of Hazardous Materials*, *185*, 1177–1186.

Bai, L., Mei, B., Guo, Q. Z., Shi, Z. G., & Feng, Y. Q. (2010). Magnetic solid-phase extraction of hydrophobic analytes in environmental samples by a surface hydrophilic carbon-ferromagnetic nanocomposite. *Journal of Chromatography A*, *1217*, 7331–7336.

Bakhshaei, S., Kamboh, M. A., Nodeh, H. R., Zain, S., Rozi, S. K. M., Mohamad, S., & Mohialdeen, I. A. M. (2016). Magnetic solid phase extraction of polycyclic aromatic hydrocarbons and chlorophenols based on cyano-ionic liquid functionalized magnetic nanoparticles and their determination by HPLC-DAD. *RSC Advances*, *6*, 77047–77058.

Barrier, S. (2008). *Physical and chemical properties of sporopollenin exine particles* (Doctoral thesis, University of Hull). Retrieved on 12th February 2019 from https://hydra.hull.ac.uk/resources/hull:6412

Barrier, S., Rigby, A. S., Diego-Taboada, A., Thomasson, M. J., Mackenzie, G., & Atkin, S. L. (2010). Sporopollenin exines: A novel natural taste masking material. *LWT - Food Science and Technology*, *43*, 73–76.

Behbahani, M., Salarian, M., Bagheri, A., Tabani, H., Omidi, F., & Fakhari, A. (2014). Synthesis, characterization and analytical application of Zn(II)-imprinted polymer as an efficient solid-phase extraction technique for trace determination of zinc ions in food samples. *Journal of Food Composition and Analysis*, *34*, 81–89.

Belenguer-Sapiña, C., Pellicer-Castell, E., El Haskouri, J., Guillem, C., Simó-Alfonso, E. F., Amorós, P., & Mauri-Aucejo, A. (2018). Design, characterization and comparison of materials based on β and γ cyclodextrin covalently connected to microporous silica for environmental analysis. *Journal of Chromatography A*, *1563*, 10–19.

Bell, B. (2018). *Advancing the application of analytical techniques in the biological chemistry of sporopollenin: towards novel plant physiological tracers in Quaternary palynology* (Doctoral thesis, The University of Manchester). Retrieved on 12th May 2018 from https://www.research.manchester.ac.uk/portal/en/theses/advancing-the-application-of-analytical-techniques-in-the-biological-chemistry-of-sporopollenin-towards-novel-plant-physiological-tracers-in-quaternary-palynology(59605f2b-642a-4ea9-8921-4c926217e6f2).html

Bengtsson, M., & Oksman, K. (2006). The use of silane technology in crosslinking polyethylene/wood flour composites. *Composites Part A: Applied Science and Manufacturing*, *37*, 752–765.

Bernard, S., Benzerara, K., Beyssac, O., Balan, E., & Brown, G. E. (2015). Evolution of the macromolecular structure of sporopollenin during thermal degradation. *Heliyon*, *1*, 1–28.

Beveridge, J. S., Stephens, J. R., & Williams, M. E. (2011). The use of magnetic nanoparticles in analytical chemistry. *Annual Review of Analytical Chemistry*, *4*, 251–273.

Bhadra, S., Das, S. C., Roy, S., Arefeen, S., & Rouf, A. S. S. (2011). Development and validation of RP-HPLC method for quantitative estimation of vinpocetine in pure and pharmaceutical dosage forms. *Chromatography Research International*, *2011*, 1–7.

Biagi, R. F. G. (2012). *Characterization and synthesis of cyclodextrin inclusion complexes and their applications as fluorescent probes for sensing biomacromolecules by characterization and synthesis of cyclodextrin inclusion* (Doctoral thesis, University of Toronto). Retrieved on 13th February 2019 from https://tspace.library.utoronto.ca/handle/1807/34016

Blackwell, L. J. (2007). *Sporopollenin Exines as a Novel Drug Delivery System* (Doctoral thesis, University of Hull). Retrieved on 12th February 2019 from https://hydra.hull.ac.uk/resources/hull:7162

Bodor, N., & Buchwald, P. (2002). Theoretical insights into the formation, structure, and energetics of some cyclodextrin complexes. *Journal of Inclusion Phenomena*, *44*, 9–14.

Botsi, A., Yannakopoulou, K., Hadjoudis, E., & Waite, J. (1996). AM1 calculations on inclusion complexes of cyclomaltoheptaose (β-cyclodextrin) with 1,7-dioxaspiro[5.5]undecane and nonanal, and comparison with experimental results. *Carbohydrate Research*, *283*, 1–16.

Bound, J. P., & Voulvoulis, N. (2005). Household disposal of pharmaceuticals as a pathway for aquatic contamination in the United Kingdom. *Environmental Health Perspectives*, *113*, 1705–1711.

Breslow, R. (1995). Biomimetic chemistry and artificial enzymes: Catalysis by design. *Accounts of Chemical Research*, *28*, 146–153.

Breslow, R., Czarniecki, M. F., Emert, J., & Hamaguchi, H. (1980). Improved acylation rates within cyclodextrin complexes from flexible capping of the cyclodextrin and from adjustment of the substrate geometry. *Journal of the American Chemical Society*, *102*, 762–770.

Brocos, P., Díaz-Vergara, N., Banquy, X., Pérez-Casas, S., Costas, M., & Piñeiro, Á. (2010). Similarities and differences between cyclodextrin-sodium dodecyl sulfate host-guest complexes of different stoichiometries: Molecular dynamics simulations at several temperatures. *Journal of Physical Chemistry B*, *114*, 12455–12467.

Brooks, J., Grant, P. R., Muir, M., Giljzel, P. Van, & Shaw, G. (1971). *Sporopollenin*. Berkeley Square, London: Academic Press.

Brooks, J., & Shaw, G. (1978). Sporopollenin: A review of its chemistry, palaeochemistry and geochemistry. *Grana*, *17*, 91–97.

Buck, M., & Karplus, M. (2001). Hydrogen bond energetics: A simulation and statistical analysis of N-methyl acetamide (NMA), water, and human lysozyme. *Journal of Physical Chemistry B*, *105*, 11000–11015.

Buser, H., Poiger, T., & Muller, M. D. (1998). Occurrence and fate of the pharmaceutical drug diclofenac in surface waters. *Environmental Science & Technology*, *32*, 3449–3456.

Cao, H., He, J., Deng, L., & Gao, X. (2009). Fabrication of cyclodextrin-functionalized superparamagnetic Fe_3O_4/amino-silane core-shell nanoparticles via layer-by-layer method. *Applied Surface Science*, *255*, 7974–7980.

Chalasani, R., & Vasudevan, S. (2012). Cyclodextrin functionalized magnetic iron oxide nanocrystals: A host-carrier for magnetic separation of non-polar molecules and arsenic from aqueous media. *Journal of Materials Chemistry*, *22*, 14925–14931.

Chalasani, R., & Vasudevan, S. (2013). Cyclodextrin-functionalized Fe_3O_4@TiO2: Reusable, magnetic nanoparticles for photocatalytic degradation of endocrine-disrupting chemicals in water supplies. *ACS Nano*, *7*, 4093–4104.

Chandrasekharan, N., & Simmons, D. L. (2004). Protein family review. The cyclooxygenases. *Genome Biology*, *5*, 241–247.

Chen, J., Cao, S., Zhu, M., Xi, C., Zhang, L., Li, X., … Chen, Z. (2018). Fabrication of a high selectivity magnetic solid phase extraction adsorbent based on β-cyclodextrin and application for recognition of plant growth regulators. *Journal of Chromatography A*, *1547*, 1–13.

Chen, J., & Zhu, X. (2015). Ionic liquid coated magnetic core/shell Fe_3O_4@SiO_2 nanoparticles for the separation / analysis of linuron in food samples. *Spectrochimica Acta Part A: Molecular and Biomolecular Spectroscopy*, *137*, 456–462.

Chen, L., & Li, B. (2013). Magnetic molecularly imprinted polymer extraction of chloramphenicol from honey. *Food Chemistry*, *141*, 23–28.

Chen, L., Liu, J., Zeng, Q., Wang, H., Yu, A., Zhang, H., & Ding, L. (2009). Preparation of magnetic molecularly imprinted polymer for the separation of tetracycline antibiotics from egg and tissue samples. *Journal of Chromatography A*, *1216*, 3710–3719.

Cho, E., Tahir, M. N., Choi, J. M., Kim, H., Yu, J. H., & Jung, S. (2015). Novel magnetic nanoparticles coated by benzene- and β-cyclodextrin-bearing dextran, and the sorption of polycyclic aromatic hydrocarbon. *Carbohydrate Polymers*, 133, 221-228.

Costi, E. M., Goryacheva, I., Sicilia, M. D., Rubio, S., & Pérez-Bendito, D. (2008). Supramolecular solid-phase extraction of ibuprofen and naproxen from sewage based on the formation of mixed supramolecular aggregates prior to their liquid chromatographic/photometric determination. *Journal of Chromatography A*, *1210*, 1–7.

Cragg, P. J. (2005). *A Practical Guide to Supramolecular Chemistry*. West Sussex, England: John Wiley & Sons Ltd.

Dai, Y., Wang, Q., Zhang, X., Jia, S., Zheng, H., Feng, D., & Yu, P. (2010). Molecular docking and QSAR study on steroidal compounds as aromatase inhibitors. *European Journal of Medicinal Chemistry*, *45*, 5612–5620.

Dalvand, A., Nabizadeh, R., Reza Ganjali, M., Khoobi, M., Nazmara, S., & Hossein Mahvi, A. (2016). Modeling of reactive blue 19 azo dye removal from colored textile wastewater using L-arginine-functionalized Fe_3O_4 nanoparticles: Optimization, reusability, kinetic and equilibrium studies. *Journal of Magnetism and Magnetic Materials*, *404*, 179–189.

Dam, H. H., Reinhoudt, D. N., & Verboom, W. (2007). Multicoordinate ligands for actinide/lanthanide separations. *Chemical Society Reviews*, *36*, 367–377.

David, A., & Pancharatna, K. (2009). Developmental anomalies induced by a non-selective COX inhibitor (ibuprofen) in zebrafish (Danio rerio). *Environmental Toxicology and Pharmacology*, *27*, 390–395.

De Andrade, J. R., Oliveira, M. F., Da Silva, M. G. C., & Vieira, M. G. A. (2018). Adsorption of Pharmaceuticals from Water and Wastewater Using Nonconventional Low-Cost Materials: A Review. *Industrial and Engineering Chemistry Research*, *57*, 3103–3127.

Deng, F., Xie, M., Zhang, X., Li, P., Tian, Y., Zhai, H., & Li, Y. (2014). Combined molecular docking, molecular dynamics simulation and quantitative structure-activity relationship study of pyrimido[1,2-c][1,3]benzothiazin-6- imine derivatives as potent anti-HIV drugs. *Journal of Molecular Structure*, *1067*, 1–13.

Deng, X., Li, W., Ding, G., & Chen, X. (2018). Enantioselective separation of: RS-mandelic acid using β-cyclodextrin modified Fe_3O_4@SiO_2/Au microspheres. *Analyst*, *143*, 2665–2673.

Díaz-Cruz, M. S., López De Alda, M. J., & Barceló, D. (2003). Environmental behavior and analysis of veterinary and human drugs in soils, sediments and sludge. *Trends in Analytical Chemistry*, *22*, 340–351.

Diego-Taboada, A., Beckett, S. T., Atkin, S. L., & Mackenzie, G. (2014). Hollow pollen shells to enhance drug delivery. *Pharmaceutics*, *6*, 80–96.

Du, X., He, J., Zhu, J., Sun, L., & An, S. (2012). Ag-deposited silica-coated Fe_3O_4 magnetic nanoparticles catalyzed reduction of *p*-nitrophenol. *Applied Surface Science*, *258*, 2717–2723.

Du, X., Zhang, X., Jiang, C., Zhang, W., & Yang, L. (2018). The trace detection of nitrite ions using neutral red functionalized SH-β-cyclodextrin @Au nanoparticles. *Sensors (Switzerland)*, *18*, 681–692.

Dyab, A. K. F., Abdallah, E. M., Ahmed, S. A., & Rabee, M. M. (2016). Fabrication and characterisation of novel natural lycopodium clavatum sporopollenin microcapsules loaded in-situ with nano-magnetic humic acid-metal complexes. *Journal of Encapsulation and Adsorption Sciences*, *6*, 109–131.

Eduard Musin. (2013). *Adsorption Modeling* (Bachelor thesis, Mikkeli University of Applied Sciences). Retrieved on 18th February 2019 from https://www.theseus.fi/bitstream/handle/10024/69655/Musin_Eduard.pdf?sequence=1&isAllowed=y

Erdemir, S., Bahadir, M., & Yilmaz, M. (2009). Extraction of carcinogenic aromatic amines from aqueous solution using calix[n]arene derivatives as carrier. *Journal of Hazardous Materials*, *168*, 1170–1176.

Ewing, T. J. A., Makino, S., Skillman, A. G., & Kuntz, I. D. (2001). DOCK 4.0 : Search strategies for automated molecular docking of flexible molecule databases. *Journal of Computer-Aided Molecular Design*, *15*, 411–428.

Fan, H., Chen, Z., Blinker, C. J., Clawson, J., & Alam, T. (2005). Synthesis of organo-silane functionalized nanocrystal micelles and their self-assembly. *Journal of the American Chemical Society*, *127*, 13746–13747.

Fan, J., Zhang, J., Zhang, C., Ren, L., & Shi, Q. (2011). Adsorption of 2,4,6-trichlorophenol from aqueous solution onto activated carbon derived from loosestrife. *Desalination*, *267*, 139–146.

Fan, L., Zhang, Y., Luo, C., Lu, F., Qiu, H., & Sun, M. (2012). Synthesis and characterization of magnetic β-cyclodextrin-chitosan nanoparticles as nano-adsorbents for removal of methyl blue. *International Journal of Biological Macromolecules*, *50*, 444–450.

Fan, W., Mao, X., He, M., Chen, B., & Hu, B. (2014). Development of novel sol-gel coatings by chemically bonded ionic liquids for stir bar sorptive extraction - Application for the determination of NSAIDS in real samples. *Analytical and Bioanalytical Chemistry*, *406*, 7261–7273.

Faraji, M. (2016). Recent analytical applications of magnetic nanoparticles. *Nanochemistry Research*, *1*, 264–290.

Farhadi, S., Safabakhsh, J., & Zaringhadam, P. (2013). Synthesis, characterization, and investigation of optical and magnetic properties of cobalt oxide (Co_3O_4) nanoparticles. *Journal of Nanostructure in Chemistry*, *3*, 69–77.

Farré, M., Petrovic, M., Gros, M., Kosjek, T., Martinez, E., Heath, E., … Barceló, D. (2008). First interlaboratory exercise on non-steroidal anti-inflammatory drugs analysis in environmental samples. *Talanta*, *76*, 580–590.

Fatiha, E., Rohana, M., Muhammad, A., Mohammad, A., Basyaruddin, M., & Rahman, A. (2015). Theoretical investigation on insulin dimer-β-cyclodextrin interactions using docking and molecular dynamics simulation. *Journal of Inclusion Phenomena and Macrocyclic Chemistry*, *84*, 1–10.

Feng, L. (2014). *Advanced Oxidation Processes for The Removal of Residual Non-Steroidal Anti- Inflammatory Pharmaceuticals from Aqueous Systems* (Doctoral thesis, Université Paris-Est). Retrieved on 18th February 2019 from https://tel.archives-ouvertes.fr/tel-00952080/document

Fent, K., Weston, A. A., & Caminada, D. (2006). Ecotoxicology of human pharmaceuticals. *Aquatic Toxicology*, *76*, 122–159.

Fermeglia, M., Ferrone, M., Lodi, A., & Pricl, S. (2003). Host-guest inclusion complexes between anticancer drugs and β-cyclodextrin: Computational studies. *Carbohydrate Polymers*, *53*, 15–44.

Fetter, R. C., Salek, J. S., Sikorski, C. T., Kumaravel, G., & Lin, F. T. (1990). Cooperative binding by aggregated mono-6-(alkylamino)-β-cyclodextrins. *Journal of the American Chemical Society*, *112*, 3860–3868.

Fick, J., Söderström, H., Lindberg, R. H., Phan, C., Tysklind, M., & Larsson, D. G. J. (2009). Contamination of surface, ground, and drinking water from pharmaceutical production. *Environmental Toxicology and Chemistry*, *28*, 2522–2527.

Filby, A. L., Neuparth, T., Thorpe, K. L., Owen, R., Galloway, T. S., & Tyler, C. R. (2007). Health impacts of estrogens in the environment, considering complex mixture effects. *Environmental Health Perspectives*, *115*, 1704–1710.

Fiori, J., Pasquini, B., Caprini, C., Orlandini, S., Furlanetto, S., & Gotti, R. (2018). Chiral analysis of theanine and catechin in characterization of green tea by cyclodextrin-modified micellar electrokinetic chromatography and high performance liquid chromatography. *Journal of Chromatography A*, *1562*, 115–122.

Flippin, J. L., Huggett, D., & Foran, C. M. (2007). Changes in the timing of reproduction following chronic exposure to ibuprofen in Japanese medaka, Oryzias latipes. *Aquatic Toxicology*, *81*, 73–78.

Floresta, G., & Rescifina, A. (2019). Metyrapone-β-cyclodextrin supramolecular interactions inferred by complementary spectroscopic/spectrometric and computational studies. *Journal of Molecular Structure*, *1176*, 815–824.

Frisch, M. J., Trucks, G. W., Schlegel, H. B., Scuseria, G. E., Robb, M. A., Cheeseman, J. R., … Petersson, G. A. (2009). Gaussian 09 program. *Gaussian Inc., Wallingford, CT*.

Frömming, K.-H., & Szejtli, J. (1993). *Cyclodextrins in Pharmacy*. Berlin, Germany: Kluwer Academic.

Garth-greeves, A. (2016). *The Detection of Non-Steroidal Anti-Inflammatory Drugs in Keratinous Matrices* (Doctoral thesis, Anglia Ruskin University). Retrieved on 18th February 2019 from https://arro.anglia.ac.uk/701347/

Gebauer, S., Friebe, S., Gübitz, G., & Krauss, G. J. (1998). High performance liquid chromatography on calixarene-bonded silica gels. II. Separations of regio-and stereoisomers on *p*-tert-butylcalix[n]arene phases. *Journal of Chromatographic Science*, *36*, 383–387.

Gentili, A. (2007). LC-MS methods for analyzing anti-inflammatory drugs in animal-food products. *Trends in Analytical Chemistry*, *26*, 595–608.

Gezici, O., & Bayrakci, M. (2015). Calixarene-engineered surfaces and separation science. *Journal of Inclusion Phenomena and Macrocyclic Chemistry*, *83*, 1–18.

Ghosh, S., Badruddoza, A. Z. M., Uddin, M. S., & Hidajat, K. (2011). Adsorption of chiral aromatic amino acids onto carboxymethyl-β-cyclodextrin bonded Fe_3O_4/SiO_2 core – shell nanoparticles. *Journal of Colloid And Interface Science*, *354*, 483–492.

Gill, C. S., Price, B. A., & Jones, C. W. (2007). Sulfonic acid-functionalized silica-coated magnetic nanoparticle catalysts. *Journal of Catalysis*, *251*, 145–152.

Gironès, J., Pimenta, M. T. B., Vilaseca, F., de Carvalho, A. J. F., Mutjé, P., & Curvelo, A. A. S. (2007). Blocked isocyanates as coupling agents for cellulose-based composites. *Carbohydrate Polymers*, *68*, 537–543.

Gokara, M., Malavath, T., Kalangi, S. K., Reddana, P., & Subramanyam, R. (2014). Unraveling the binding mechanism of asiatic acid with human serum albumin and its biological implications. *Journal of Biomolecular Structure and Dynamics*, *32*, 1292–1302.

Goodsell, D. S., & Olson, A. J. (1990). Automated docking of substrates to proteins by simulated annealing. *Proteins: Structure, Function and Genetics*, *8*, 195–202.

Grigera, J. R., Ca, E. R., & Rosa, S. De. (1998). Computer simulation of the cyclodextrin–phenylalanine complex. *Carbohydrate Research*, *310*, 253–259.

Gummin, D. D., Mowry, J. B., Spyker, D. A., Brooks, D. E., Fraser, M. O., & Banner, W. (2017). 2016 Annual Report of the American Association of Poison Control Centers' National Poison Data System (NPDS): 34th Annual Report. *Clinical Toxicology*, *55*, 1072–1252.

Gungor, O., Yilmaz, A., Memon, S., & Yilmaz, M. (2008). Evaluation of the performance of calix[8]arene derivatives as liquid phase extraction material for the removal of azo dyes. *Journal of Hazardous Materials*, *158*, 202–207.

Gutsche, C. D. (2000). *Calixarenes for Separations*. *American Chemical Society Symposium Series* (Vol. 757). Washington, DC: American Chemical Society.

Gutsche, C. D. (2008). *Calixarenes An Introduction*. Cambridge, UK: RSC Publishing.

Gutsche, C. D., Iqbal, M., & Stewart, D. (1986). Calixarenes. 18. Synthesis Procedures for *p*-tert-butylcalix[4]arene. *Journal of Organic Chemistry*, *51*, 742–745.

Gutsche, C. D., & Lin, L.-G. (1986). Calixarenes 12: The synthesis of functionalized calixarenes. *Tetrahedron*, *42*, 1633–1640.

Hamad, S. A., Dyab, A. F. K., Stoyanov, S. D., & Paunov, V. N. (2011). Encapsulation of living cells into sporopollenin microcapsules. *Journal of Materials Chemistry*, *21*, 18018–18023.

Hanessian, S., Benalil, A., Simard, M., & Bélanger-Gariépy, F. (1995). Crystal structures and molecular conformations of mono-6-azido-6-deoxy α-cyclodextrin and mono-2-O-allyl-α-cyclodextrin-The formation of polymeric helical inclusion complexes. *Tetrahedron*, *51*, 10149–10158.

Harrowfield, J. M., Mocerino, M., Peachey, B. J., Skelton, B. W., & White, A. H. (1996). Rare-earth-metal solvent extraction with calixarene phosphates. *Journal of the Chemical Society - Dalton Transactions*, *8*, 1687–1699.

Hedges, A. R. (1998). Industrial applications of cyclodextrins. *Chemical Reviews*, *98*, 2035–2044.

Heidari, H., & Razmi, H. (2012). Multi-response optimization of magnetic solid phase extraction based on carbon coated Fe_3O_4 nanoparticles using desirability function approach for the determination of the organophosphorus pesticides in aquatic samples by HPLC-UV. *Talanta*, *99*, 13–21.

Hemsley, A. R., Barrie, P. J., Chaloner, W. G., & Scott, A. C. (1993). The composition of sporopollenin and its use in living and fossil plant systematics. *Grana*, *32*, 2–11.

Hernando, M. D., Mezcua, M., Fernández-Alba, A. R., & Barceló, D. (2006). Environmental risk assessment of pharmaceutical residues in wastewater effluents, surface waters and sediments. *Talanta*, *69*, 334–342.

Hertel, M. P., Behrle, A. C., Williams, S. A., Schmidt, J. A. R., & Fantini, J. L. (2009). Synthesis of amine, halide, and pyridinium terminated 2-alkyl-*p*-tert-butylcalix[4]arenes. *Tetrahedron*, *65*, 8657–8667.

Hirai, T., Matsumoto, S., & Kishi, I. (1997). Simultaneous analysis of several non-steroidal anti-inflammatory drugs in human urine by high-performance liquid chromatography with normal solid-phase extraction. *Journal of Chromatography B: Biomedical Applications*, *692*, 375–388.

Hospital, A., Goñi, J. R., Orozco, M., & Gelpí, J. L. (2015). Molecular dynamics simulations : Advances and applications. *Advances and Applications in Bioinformatics and Chemistry*, *8*, 37–47.

Hou, X., Lu, X., Niu, P., Tang, S., Wang, L., & Guo, Y. (2018). β-Cyclodextrin-modified three-dimensional graphene oxide-wrapped melamine foam for the solid-phase extraction of flavonoids. *Journal of Separation Science*, *41*, 2207–2213.

Huang, D., Deng, C., & Zhang, X. (2014). Functionalized magnetic nanomaterials as solid-phase extraction adsorbents for organic pollutants in environmental analysis. *Analytical Methods*, *6*, 7130–7141.

Huang, H., Zhao, C., Ji, Y., Nie, R., Zhou, P., & Zhang, H. (2010). Preparation, characterization and application of *p*-tert-butyl-calix[4]arene-SBA-15 mesoporous silica molecular sieves. *Journal of Hazardous Materials*, *178*, 680–685.

Huang, Y. (2013). *Novel applications of surface-modified sporopollenin exine capsules* (Doctoral thesis, University of Hull). Retrieved on 12th February 2019 from https://hydra.hull.ac.uk/resources/hull:8432

Ibarra, I. S., Rodriguez, J. A., Galán-Vidal, C. A., Cepeda, A., & Miranda, J. M. (2015). Magnetic solid phase extraction applied to food analysis. *Journal of Chemistry*, *2015*, 1–13.

Indira, T. K., & Lakshmi, P. K. (2010). Magnetic Nanoparticles – A Review. *International Journal of Pharmaceutical Sciences and Nanotechnology*, *3*, 1035–1042.

Ionescu, M. (2005). *Chemistry and Technology of Polyols for Polyurethanes*. Shropshire, UK: Rapra Technology Limited.

Ishikawa, T. O., & Herschman, H. R. (2007). Two inducible, functional cyclooxygenase-2 genes are present in the rainbow trout genome. *Journal of Cellular Biochemistry*, *102*, 1486–1492.

Izzati, N., Nadia, N., Sabri, H., Lee, V. S., Nadiah, S., & Halim, A. (2016). 5-fluorouracil co-crystals and their potential anti-cancer activities calculated by molecular docking studies. *Journal of Chemical Crystallography*, *46*, 144–154.

Ji, Y., Yin, J., Xu, Z., Zhao, C., Huang, H., Zhang, H., & Wang, C. (2009). Preparation of magnetic molecularly imprinted polymer for rapid determination of bisphenol A in environmental water and milk samples. *Analytical and Bioanalytical Chemistry*, *395*, 1125–1133.

Jones, G., Willett, P., Glen, R. C., Leach, A. R., & Taylor, R. (1997). Development and validation of a genetic algorithm for flexible docking. *Journal of Molecular Biology*, *267*, 727–748.

Jones, O. A., Lester, J. N., & Voulvoulis, N. (2005). Pharmaceuticals: A threat to drinking water? *Trends in Biotechnology*, *23*, 163–167.

Joseph, K., Thomas, S., & Pavithran, C. (1996). Effect of chemical treatment on the tensile properties of short sisal fibre-reinforced polyethylene composites. *Polymer*, *37*, 5139–5149.

Joseph, P. V., Joseph, K., Thomas, S., Pillai, C. K. S., Prasad, V. S., Groeninckx, G., & Sarkissova, M. (2003). The thermal and crystallisation studies of short sisal fibre reinforced polypropylene composites. *Composites Part A: Applied Science and Manufacturing*, *34*, 253–266.

Kalchenko, O. I., Cherenok, S. O., Solovyov, A. V, & Kalchenko, V. I. (2009). Influence of calixarenes on chromatographic separation of benzene or uracil derivatives. *Chromatographia*, *70*, 717–721.

Kamboh, M. A., Ibrahim, W. A. W., Nodeh, H. R., Sanagi, M. M., & Sherazi, S. T. H. (2016). The removal of organophosphorus pesticides from water using a new amino-substituted calixarene-based magnetic sporopollenin. *New Journal of Chemistry*, *40*, 3130–3138.

Kamboh, M. A., & Yilmaz, M. (2013). Synthesis of N-methylglucamine functionalized calix[4]arene based magnetic sporopollenin for the removal of boron from aqueous environment. *Desalination*, *310*, 67–74.

Kane, P. (1998). *CALIXARENES: Molecular Modelling of and Potentiometrie Studies on Cation Complexes* (Doctoral thesis, Dublin City University). Retrieved on 14th February 2019 from http://doras.dcu.ie/18902/1/Paddy_Kane_20130520141016.pdf

Kang, Y., Zhou, L., Li, X., & Yuan, J. (2011). β-Cyclodextrin-modified hybrid magnetic nanoparticles for catalysis and adsorption. *Journal of Materials Chemistry*, *21*, 3704–3710.

Khairudin, K. A., Abubakar, I. J., Manan, M. M., Tiong, C. S., Chitneni, M., Abdullah, A. H., … Arshad, K. (2017). Utilization pattern of non-steroidal anti-inflammatory drugs at a primary health care in malaysia. *Indian Journal of Pharmaceutical Education and Research*, *51*, 156–161.

Khalafi-Nezhad, A., Divar, M., & Panahi, F. (2015). Magnetic nanoparticles-supported tungstic acid (MNP-TA): An efficient magnetic recyclable catalyst for the one-pot synthesis of spirooxindoles in water. *RSC Advances*, *5*, 2223–2230.

Khalijah, S., Rozi, M., Bakhshaei, S., & Abdul, S. (2016). Superhydrophobic magnetic nanoparticle-free fatty acid regenerated from waste cooking oil for the enrichment of carcinogenic polycyclic aromatic hydrocarbons in sewage sludges and landfill leachates. *RSC Advances*, *6*, 87719–87729.

Khan, A. R., Forgo, P., Stine, K. J., & D'Souza, V. T. (1998). Methods for selective modifications of cyclodextrins. *Chemical Reviews*, *98*, 1977–1996.

Khoeini-Sharifabadi, M., Saber-Tehrani, M., Waqif Husain, S., Mehdinia, A., & Aberoomand-Azar, P. (2014). Determination of residual nonsteroidal anti-inflammatory drugs in aqueous sample using magnetic nanoparticles modified with cetyltrimethylammonium bromide by high performance liquid chromatography. *Scientific World Journal*, *2014*, 1–8.

Khoobi, M., Ramazani, A., Hojjati, Z., Shakeri, R., Khoshneviszadeh, M., Ardestani, S. K., … Joo, S. W. (2014). Synthesis of novel 4 H-chromenes containing a pyrimidine-2-thione function in the presence of Fe_3O_4 magnetic nanoparticles and study of their antioxidant activity. *Phosphorus, Sulfur and Silicon and the Related Elements*, *189*, 1586–1595.

Khoobi, M., Delshad, T. M., Vosooghi, M., Alipour, M., Hamadi, H., Alipour, E., Hamedani, M. P., … Shafie, A. (2015). Polyethyleneimine-modified superparamagnetic Fe_3O_4 nanoparticles: An efficient, reusable and water tolerance nanocatalyst. *Journal of Magnetism and Magnetic Materials*, *375*, 217–226.

Kiasat, A. R., & Nazari, S. (2013). β-cyclodextrin conjugated magnetic nanoparticles as a novel magnetic microvessel and phase transfer catalyst: Synthesis and applications in nucleophilic substitution reaction of benzyl halides. *Journal of Inclusion Phenomena and Macrocyclic Chemistry*, *76*, 363–368.

Köhler, J. E. H., & Grczelschak-Mick, N. (2013). The β-cyclodextrin/benzene complex and its hydrogen bonds - a theoretical study using molecular dynamics, quantum mechanics and COSMO-RS. *Beilstein Journal of Organic Chemistry*, *9*, 118–134.

Kollman, P. A. (1996). Advances and continuing challenges in achieving realistic and predictive simulations of the properties of organic and biological molecules. *Accounts of Chemical Research*, *29*, 461–469.

Kosjek, T., Heath, E., & Kompare, B. (2007). Removal of pharmaceutical residues in a pilot wastewater treatment plant. *Analytical and Bioanalytical Chemistry*, *387*, 1379–1387.

Kosjek, T., Heath, E., & Krbavčič, A. (2005). Determination of non-steroidal anti-inflammatory drug (NSAIDs) residues in water samples. *Environment International*, *31*, 679–685.

Koutsouba, V., Heberer, T., Fuhrmann, B., Schmidt-Baumler, K., Tsipi, D., & Hiskia, A. (2003). Determination of polar pharmaceuticals in sewage water of Greece by gas chromatography-mass spectrometry. *Chemosphere*, *51*, 69–75.

Kovala-Demertzi, D. (2006). Recent advances on non-steroidal anti-inflammatory drugs, NSAIDs: Organotin complexes of NSAIDs. *Journal of Organometallic Chemistry*, *691*, 1767–1774.

Kramer, B., Rarey, M., & Lengauer, T. (1999). Evaluation of the FLEXX Incremental Construction Algorithm for Protein – Ligand Docking. *Proteins: Structure, Function & Genetics*, *37*, 228–241.

Kristmundóttir, T., Loftsson, T., & Holbrook, W. P. (1996). Formulation and clinical evaluation of a hydrocortisone solution for the treatment of oral disease. *International Journal of Pharmaceutics*, *139*, 63–68.

Kubendhiran, S., Sakthivel, R., Chen, S. M., Mutharani, B., & Chen, T. W. (2018). Innovative strategy based on a novel carbon-black-β-cyclodextrin nanocomposite for the simultaneous determination of the anticancer drug flutamide and the environmental pollutant 4-nitrophenol. *Analytical Chemistry*, *90*, 6283–6291.

Kümmerer, K. (2008). *Pharmaceuticals in the environment. Sources, Fate, Effects and Risks*. Berlin. Germany: Springer.

Kümmerer, K. (2009). The presence of pharmaceuticals in the environment due to human use - present knowledge and future challenges. *Journal of Environmental Management*, *90*, 2354–2366.

Kuo, Y. L., Liu, W. L., Hsieh, S. H., & Huang, H. Y. (2010). Analyses of non-steroidal anti-inflammatory drugs in environmental water samples with microemulsion electrokinetic chromatography. *Analytical Sciences*, *26*, 703–707.

Lamb, M.L., & Jorgensen, W.L. (1997). Computational approaches to molecular recognition L Lamb and William. *Current Opinion in Chemical Biology*, *1*, 449–457.

Lapicque, F., Netter, P., Bannwarth, B., Trechot, P., Gillet, P., Lambert, H., & Royer, R. J. (1989). Identification and simultaneous determination of non-steroidal anti-inflammatory drugs using high-performance liquid chromatography. *Journal of Chromatography B: Biomedical Sciences and Applications*, *496*, 301–320.

Lawtrakul, L., Viernstein, H., & Wolschann, P. (2003). Molecular dynamics simulations of β-cyclodextrin in aqueous solution. *International Journal of Pharmaceutics*, *256*, 33–41.

Leung, H. W., Minh, T. B., Murphy, M. B., Lam, J. C. W., So, M. K., Martin, M., … Richardson, B. J. (2012). Distribution, fate and risk assessment of antibiotics in sewage treatment plants in Hong Kong, South China. *Environment International*, *42*, 1–9.

Li, J., Qiu, C., Fan, H., Bai, Y., Jin, Z., & Wang, J. (2018). A novel cyclodextrin-functionalized hybrid silicon wastewater nano-adsorbent material and its adsorption properties. *Molecules*, *23*, 1–16.

Li, J., Yu, T., Xu, G., Du, Y., Liu, Z., Feng, Z., … Liu, J. (2018). Synthesis and application of ionic liquid functionalized β-cyclodextrin, mono-6-deoxy-6-(4-amino-1,2,4-triazolium)-β-cyclodextrin chloride, as chiral selector in capillary electrophoresis. *Journal of Chromatography A*, *1559*, 178–185.

Li, L., Fan, L., Sun, M., Qiu, H., Li, X., Duan, H., & Luo, C. (2013). Adsorbent for chromium removal based on graphene oxide functionalized with magnetic cyclodextrin-chitosan. *Colloids and Surfaces B: Biointerfaces*, *107*, 76–83.

Li, L., Lv, P., Xian, C., & Zheng, L. (2006). Synthesis of novel calix[4]arenes containing one and two substituents on the "upper rim." *Indian Journal of Chemistry - Section B Organic and Medicinal Chemistry*, *45*, 2118–2122.

Li, N., Chen, J., & Shi, Y. P. (2019). Magnetic polyethyleneimine functionalized reduced graphene oxide as a novel magnetic sorbent for the separation of polar non-steroidal anti-inflammatory drugs in waters. *Talanta*, *191*, 526–534.

Li, S., & Purdy, W. C. (1992). Cyclodextrins and their applications in analytical chemistry. *Chemical Reviews*, *92*, 1457–1470.

Li, X. S., Liu, L., Mu, T. W., & Guo, Q. X. (2000). A systematic quantum chemistry study on cyclodextrins. *Monatshefte Fur Chemie*, *131*, 849–855.

Li, Y., Zhu, N., Chen, T., Ma, Y., & Li, Q. (2018). A green cyclodextrin metal-organic framework as solid-phase extraction medium for enrichment of sulfonamides before their HPLC determination. *Microchemical Journal*, *138*, 401–407.

Liang, X., Ma, R., Hao, L., Wang, C., Wu, Q., & Wang, Z. (2018). β-Cyclodextrin polymer@Fe_3O_4 based magnetic solid-phase extraction coupled with HPLC for the determination of benzoylurea insecticides from honey, tomato, and environmental water samples. *Journal of Separation Science*, *41*, 1539–1547.

Ling, I., Alias, Y., & Raston, C. L. (2010). Structural diversity of multi-component self-assembled systems incorporating p-sulfonatocalix[4]arene. *New Journal of Chemistry*, *34*, 1802–1811.

Lipkowitz, K. B. (1995). Theoretical studies of type II-V chiral stationary phases. *Journal of Chromatography A*, *694*, 15–37.

Lipkowitz, K. B. (1998). Applications of computational chemistry to the study of cyclodextrins. *Chemical Reviews*, *98*, 1829–1873.

Liu, F., Yang, X., Wu, X., Xi, X., Gao, H., Zhang, S., … Lu, R. (2018). A dispersive magnetic solid phase microextraction based on ionic liquid-coated and cyclodextrin-functionalized magnetic core dendrimer nanocomposites for the determination of pyrethroids in juice samples. *Food Chemistry*, *268*, 485–491.

Liu, J. F., Zhao, Z. S., & Jiang, G. B. (2008). Coating Fe_3O_4 magnetic nanoparticles with humic acid for high efficient removal of heavy metals in water. *Environmental Science and Technology*, *42*, 6949–6954.

Liu, J. L., & Wong, M. H. (2013). Pharmaceuticals and personal care products (PPCPs): A review on environmental contamination in China. *Environment International*, *59*, 208–224.

Liu, J., Zou, S., Li, S., Liao, X., Hong, Y., Xiao, L., & Fan, J. (2013). A general synthesis of mesoporous metal oxides with well-dispersed metal nanoparticles via a versatile sol-gel process. *Journal of Materials Chemistry A*, *1*, 4038–4047.

Liu, T. Y., Hu, S. H., Liu, T. Y., Liu, D. M., & Chen, S. Y. (2006). Magnetic-sensitive behavior of intelligent ferrogels for controlled release of drug. *Langmuir*, *22*, 5974–5978.

Ludwig, R. (2000). Calixarenes in analytical and separation chemistry. *Fresenius' Journal of Analytical Chemistry*, *367*, 103–128.

Luo, Y. B., Zheng, H. B., Wang, J. X., Gao, Q., Yu, Q. W., & Feng, Y. Q. (2011). An anionic exchange stir rod sorptive extraction based on monolithic material for the extraction of non-steroidal anti-inflammatory drugs in environmental aqueous samples. *Talanta*, *86*, 103–108.

Luo, Y., Guo, W., Ngo, H. H., Nghiem, L. D., Hai, F. I., Zhang, J., … Wang, X. C. (2014). A review on the occurrence of micropollutants in the aquatic environmet and their fate and removal during wastewater treatment. *Science of the Total Environment*, *474*, 619–641.

Luo, Z. Y., Li, Z. Y., Liu, H. Y., Tang, M. Q., & Shi, Z. G. (2015). Click chemistry-based synthesis of water-dispersible hydrophobic magnetic nanoparticles for use in solid phase extraction of non-steroidal anti-inflammatory drugs. *Microchimica Acta*, *182*, 2585–2591.

Macias, A. T., Norton, J. E., & Evanseck, J. D. (2003). Impact of multiple cation-π interactions upon calix[4]arene substrate binding and specificity. *Journal of the American Chemical Society*, *125*, 2351–2360.

Mackenzie, G., Boa, A. N., Diego-Taboada, A., Atkin, S. L., & Sathyapalan, T. (2015). Sporopollenin, the least known yet toughest natural biopolymer. *Frontiers in Materials*, *2*, 1–5.

Mainero-Rocca, L., Gentili, A., Caretti, F., Curini, R., & Pérez-Fernández, V. (2015). Occurrence of non-steroidal anti-inflammatory drugs in surface waters of Central Italy by liquid chromatography–tandem mass spectrometry. *International Journal of Environmental Analytical Chemistry*, *95*, 685–697.

Malik, M. A., Wani, M. Y., & Hashim, M. A. (2012). Microemulsion method: A novel route to synthesize organic and inorganic nanomaterials. 1st Nano Update. *Arabian Journal of Chemistry*, *5*, 397–417.

Mandolini, L., & Ungaro, R. (2000). *Calixarenes in action*. London, UK: Imperial Collage Press.

Mar-Sojo, M., Nuñez-Delicado, E., García-Carmona, F., & Sánchez-Ferrer, A. (1999). Cyclodextrins as activator and inhibitor of latent banana pulp polyphenol oxidase. *Journal of Agricultural and Food Chemistry*, *47*, 518–523.

Mashhadizadeh, M. H., Amoli-Diva, M., & Pourghazi, K. (2013). Magnetic nanoparticles solid phase extraction for determination of ochratoxin A in cereals using high-performance liquid chromatography with fluorescence detection. *Journal of Chromatography A*, *1320*, 17–26.

Metcalfe, C. D., Koenig, B. G., Bennie, D. T., Servos, M., Ternes, T. A., & Hirsch, R. (2003). Occurrence of Neutral and Acidic Drugs in the Effluents of Canadian Sewage Treatment Plants. *Environmental Toxicology and Chemistry*, *22*, 2872.

Meucci, V., Minunni, M., Vanni, M., Sgorbini, M., Corazza, M., & Intorre, L. (2014). Selective and simultaneous determination of NSAIDs in equine plasma by HPLC with molecularly imprinted solid-phase extraction. *Bioanalysis*, *6*, 2147–2158.

Mhlana, K. (2017). *Microencapsulation of Anti Tuberculosis Drugs Using Sporopollenin* (Doctoral thesis, Nelson Mandela University). Retrieved on 13th May 2018 from http://www.netd.ac.za/

Mirzajani, R., & Ahmadi, S. (2015). Melamine supported magnetic iron oxide nanoparticles (Fe_3O_4@Mel) for spectrophotometric determination of malachite green in water samples and fish tissues. *Journal of Industrial and Engineering Chemistry*, *23*, 171–178.

Modi, C. M., Mody, S. K., Patel, H. B., Dudhatra, G. B., Kumar, A., & Avale, M. (2012). Toxicopathological overview of analgesic and anti-inflammatory drugs in animals. *Journal of Applied Pharmaceutical Science*, *2*, 149–157.

Mohammad, A. S., Mohamad, S., & Maah, M. J. (2010). Preparation and Characterization of Silica Modified with Calix[4]arene Derivatives. *Journal of Chemistry and Chemical Engineering*, *4*, 44–49.

Mokhtari, B., Pourabdollah, K., & Dalali, N. (2011). Analytical applications of calixarenes from 2005 up-to-date. *Journal of Inclusion Phenomena and Macrocyclic Chemistry*, *69*, 1–55.

Momany, F. A., & Rone, R. (1992). Validation of the general purpose QUANTA 3.2/CHARMm force field. *Journal of Computational Chemistry*, *13*, 888–900.

Morris, G. M., Goodsell, D. S., Halliday, R. S., Huey, R., Hart, W. E., Belew, R. K., & Olson, A. J. (1998). Automated docking using a Lamarckian genetic algorithm and an empirical binding free energy function. *Journal of Computational Chemistry*, *19*, 1639–1662.

Muhammad, E. F., & Adnan, R. (2015). Computational Investigation of the Monomer Insulin-β-CD Complex for the New Insulin Formulation. *Australian Journal of Basic and Applied Sciences*, *9*, 7–13.

Nachtigall, S. M. B., Cerveira, G. S., & Rosa, S. M. L. (2007). New polymeric-coupling agent for polypropylene/wood-flour composites. *Polymer Testing*, *26*, 619–628.

Nadendla, R. R. (2004). Molecular modeling: A powerful tool for drug design and molecular docking. *Resonance*, *9*, 51–60.

Nair, K. C. M., & Thomas, S. (2003). Effect of interface modification on the mechanical properties of polystyrene-sisal fiber composites. *Polymer Composites*, *24*, 332–343.

Najafi, E., Aboufazeli, F., Zhad, H. R. L. Z., Sadeghi, O., & Karimi, M. (2013). A novel magnetic ion imprinted nano-polymer for selective separation and determination of low levels of mercury(II) ions in fish samples. *Food Chemistry*, *141*, 4040–4045.

Neouze, M. A., & Schubert, U. (2008). Surface modification and functionalization of metal and metal oxide nanoparticles by organic ligands. *Monatshefte Fur Chemie*, *139*, 183–195.

Neri, P., Sessler, J. L., & Wang, M. X. (2016). *Calixarenes and beyond*. *Calixarenes and Beyond*. Switzerland: Springer International Publishing Switzerland.

Nodeh, H. R., Wan Ibrahim, W. A., Sanagi, M. M., & Aboul-Enein, H. Y. (2016). Magnetic graphene-based cyanopropyltriethoxysilane as adsorbent for simultaneous determination of polar and non-polar organophosphorus pesticides in cow's milk samples. *RSC Advances*, *6*, 24853–24864.

Noorashikin, M. S., Raoov, M., Mohamad, S., & Abas, M. R. (2013). Cloud point extraction of parabens using non-ionic surfactant with cylodextrin functionalized ionic liquid as a modifier. *International Journal of Molecular Sciences*, *14*, 24531–24548.

Noorashikin, M. S., Raoov, M., Mohamad, S., & Abas, M. R. (2014). Extraction of parabens from water samples using cloud point extraction with a non-ionic surfactant with β-cyclodextrin as modifier. *Journal of Surfactants and Detergents*, *17*, 747–758.

Ollers, S., Singer, H. P., Fassler, P., & Muller, S. R. (2001). Simultaneous quantification of neutral and acidic pharmaceuticals and pesticides at the low-ng/l level in surface and waste water. *Journal of Chromatography A*, *911*, 225–234.

Ozmen, E. Y., Sezgin, M., Yilmaz, A., & Yilmaz, M. (2008). Synthesis of β-cyclodextrin and starch based polymers for sorption of azo dyes from aqueous solutions. *Bioresource Technology*, *99*, 526–531.

Pandya, A., Sutariya, P. G., Lodha, A., & Menon, S. K. (2013). A novel calix[4]arene thiol functionalized silver nanoprobe for selective recognition of ferric ion with nanomolar sensitivity via DLS selectivity in human biological fluid. *Nanoscale*, *5*, 2364–2371.

Park, K., & Cho, A. E. (2017). Using reverse docking to identify potential targets for ginsenosides. *Journal of Ginseng Research*, *41*, 534–539.

Park, S., Lim, S., & Choi, H. (2006). Chemical vapor deposition of iron and iron oxide thin films from Fe(II) dihydride complexes. *Chemistry of Materials*, *18*, 5150–5152.

Parker, J. (2001). Spores. *Encyclopedia of Genetics*, *1*, 1882–1883.

Pascoe, D., Karntanut, W., & Müller, C. T. (2003). Do pharmaceuticals affect freshwater invertebrates? A study with the cnidarian Hydra vulgaris. *Chemosphere*, *51*, 521–528.

Patnaik, P. (2017). *Handbook of environmental analysis: Chemical pollutants in air, water, soil, and solid wastes, third edition*. *Handbook of Environmental Analysis: Chemical Pollutants in Air, Water, Soil, and Solid Wastes, Third Edition*. Boca Raton, FL: CRC Press.

Paul, A., Joseph, K., & Thomas, S. (1997). Effect of surface treatments on the electrical properties of low-density polyethylene composites reinforced with short sisal fibers. *Composites Science and Technology*, *57*, 67–79.

Paunov, V. N., Mackenzie, G., & Stoyanov, S. D. (2007). Sporopollenin micro-reactors for in-situ preparation, encapsulation and targeted delivery of active components. *Journal of Materials Chemistry*, *17*, 609–612.

Pehlivan, E., & Yildiz, S. (1988). Modified sporopollenin as a novel anion, cation and ligand exchange medium. *Analytical Letters*, *21*, 297–309.

Peng, X., Yu, Y., Tang, C., Tan, J., Huang, Q., & Wang, Z. (2008). Occurrence of steroid estrogens, endocrine-disrupting phenols, and acid pharmaceutical residues in urban riverine water of the Pearl River Delta, South China. *Science of the Total Environment*, *397*, 158–166.

Peng, Y., Gautam, L., & Hall, S. W. (2019). The detection of drugs of abuse and pharmaceuticals in drinking water using solid-phase extraction and liquid chromatography-mass spectrometry. *Chemosphere*, 223, 438–447.

Phonsiri, V., Choi, S., Nguyen, C., Tsai, Y.-L., Coss, R., & Kurwadkar, S. (2019). Monitoring occurrence and removal of selected pharmaceuticals in two different wastewater treatment plants. *SN Applied Sciences*, *1,* 798–808.

Pirouz, M. J., Beyki, M. H., & Shemirani, F. (2015). Anhydride functionalised calcium ferrite nanoparticles: A new selective magnetic material for enrichment of lead ions from water and food samples. *Food Chemistry*, *170*, 131–137.

Popr, M. M. (2016). *Synthesis of cyclodextrin derivatives for practical application* (Doctoral thesis, Charles University in Prague). Retrieved on 13th February 2019 from https://is.cuni.cz/webapps/zzp/download/140055457

Quinn, B., Gagné, F., & Blaise, C. (2009). Evaluation of the acute, chronic and teratogenic effects of a mixture of eleven pharmaceuticals on the cnidarian, Hydra attenuata. *Science of the Total Environment*, *407*, 1072–1079.

Raffaini, G., & Ganazzoli, F. (2010). A molecular dynamics study of the inclusion complexes of C60 with some cyclodextrins. *Journal of Physical Chemistry B*, *114*, 7133–7139.

Rahim, N. Y., Tay, K. S., & Mohamad, S. (2016). β-Cyclodextrin functionalized ionic liquid as chiral stationary phase of high performance liquid chromatography for enantioseparation of β-blockers. *Journal of Inclusion Phenomena and Macrocyclic Chemistry*, *85*, 303–315.

Rahim, N. Y., Tay, K. S., & Mohamad, S. (2018). Chromatographic and spectroscopic studies on β-cyclodextrin functionalized ionic liquid as chiral stationary phase: Enantioseparation of NSAIDs. *Adsorption Science and Technology*, *36*, 130–148.

Raoov, M., Mohamad, S., & Abas, M. R. (2013). Synthesis and characterization of β-cyclodextrin functionalized ionic liquid polymer as a macroporous material for the removal of phenols and As(V). *International Journal of Molecular Sciences*, *15*, 100–119.

Rashidi Nodeh, H., Wan Ibrahim, W. A., Kamboh, M. A., & Sanagi, M. M. (2017). New magnetic graphene-based inorganic-organic sol-gel hybrid nanocomposite for simultaneous analysis of polar and non-polar organophosphorus pesticides from water samples using solid-phase extraction. *Chemosphere*, *166*, 21–30.

Reddersen, K., Heberer, T., & Duunnbier, U. (2002). Identification and significance of phenazone drugs and their metabolites in ground- and drinking water. *Chemosphere*, *49*, 539–544.

Repo, E. (2011). *EDTA-and DTPA-Functionalized silica gel and chitosan adsorbents for the removal of heavy* (Doctoral thesis, Lappeenranta University of Technology). Retrieved on 18th February 2019 from https://www.tib.eu/en/search/id/TIBKAT%3A667169903/EDTA-and-DTPA-functionalized-silica-gel-and-chitosan/

Rescifina, A., Surdo, E., Cardile, V., Avola, R., Eleonora Graziano, A. C., Stancanelli, R., … Ventura, C. A. (2019). Gemcitabine anticancer activity enhancement by water soluble celecoxib/sulfobutyl ether-β-cyclodextrin inclusion complex. *Carbohydrate Polymers*, *206*, 792–800.

Rodil, R., Quintana, J. B., López-Mahía, P., Muniategui-Lorenzo, S., & Prada-Rodríguez, D. (2009). Multi-residue analytical method for the determination of emerging pollutants in water by solid-phase extraction and liquid chromatography-tandem mass spectrometry. *Journal of Chromatography A*, *1216*, 2958–2969.

Rodrıguez, I., Quintana, J. B., Carpinteiro, J., Carro, A. M., Lorenzo, R. A., & Cela, R. (2003). Determination of acidic drugs in sewage water by gas chromatography–mass spectrometry as tert-butyldimethylsilyl derivatives. *Journal of Chromatography A*, *985*, 265–274.

Rozi, S. K. M. (2018). *Synthesis, characterizations, applications of magnetic nanoparticles based on functionalized free fatty acid as new adsorbents* (Doctoral thesis, Universiti Malaya). Retrieved on 15th April 2019 from http://studentsrepo.um.edu.my

Roux, S., Garcia, B., Bridot, J., Salome, M., Marquette, C., Lemelle, L., … Tillement, O. (2005). Synthesis , characterization of dihydrolipoic acid capped gold nanoparticles, and functionalization by the electroluminescent luminol. *Langmuir*, *21*, 2526–2536.

Rozi, S. K. M., Nodeh, H. R., Kamboh, M. A., Manan, N. S. A., & Mohamad, S. (2017). Novel palm fatty acid functionalized magnetite nanoparticles for magnetic solid-phase extraction of trace polycyclic aromatic hydrocarbons from environmental samples. *Journal of Oleo Science*, *66*, 771–784.

Ruckenstein, E., & Li, Z. F. (2005). Surface modification and functionalization through the self-assembled monolayer and graft polymerization. *Advances in Colloid and Interface Science*, *113*, 43–63.

Sacher, F., Lange, F. T., Brauch, H.-J., & Blankenhorn, I. (2001). Pharmaceuticals in groundwaters analytical methods and results of a monitoring program in Baden-Wurttemberg, Germany. *Journal of Chromatography A*, *938*, 199–210.

Sadri, F., Ramazani, A., Massoudi, A., Khoobi, M., Tarasi, R., Shafiee, A., … Joo, S. W. (2014). Green oxidation of alcohols by using hydrogen peroxide in water in the presence of magnetic Fe_3O_4 nanoparticles as recoverable catalyst. *Green Chemistry Letters and Reviews*, *7*, 257–264.

Šafaříková, M., & Šafařík, I. (1999). Magnetic solid-phase extraction. *Journal of Magnetism and Magnetic Materials*, *194*, 108–112.

Sahihi, M., & Ghayeb, Y. (2014). An investigation of molecular dynamics simulation and molecular docking: Interaction of citrus flavonoids and bovine β-lactoglobulin in focus. *Computers in Biology and Medicine*, *51*, 44–50.

Santos, J. L., Aparicio, I., Alonso, E., & Callejón, M. (2005). Simultaneous determination of pharmaceutically active compounds in wastewater samples by solid phase extraction and high-performance liquid chromatography with diode array and fluorescence detectors. *Analytica Chimica Acta*, *550*, 116–122.

Saraji, M., & Ghani, M. (2014). Dissolvable layered double hydroxide coated magnetic nanoparticles for extraction followed by high performance liquid chromatography for the determination of phenolic acids in fruit juices. *Journal of Chromatography A*, *1366*, 24–30.

Sayigan, S. C. (2013). *Determination of characteristics of adsorbent for adsorption heat pumps* (Master's thesis, Izmir Institute of Technology). Retrieved on 18th February 2019 from http://library.iyte.edu.tr/tezler/master/enerjimuh/T001216.pdf

Sayin, S., Gubbuk, I. H., & Yilmaz, M. (2013). Preparation of calix[4]arene-based sporopollenin and examination of its dichromate sorption ability. *Journal of Inclusion Phenomena and Macrocyclic Chemistry*, *75*, 111–118.

Sayin, S., Ozcan, F., & Yilmaz, M. (2013). Two novel calixarene functionalized iron oxide magnetite nanoparticles as a platform for magnetic separation in the liquid-liquid/solid-liquid extraction of oxyanions. *Materials Science and Engineering C*, *33*, 2433–2439.

Scalia, S., Villani, S., & Casolari, A. (1999). Inclusion complexation of the sunscreen agent 2-ethylhexyl-*p*-dimethylaminobenzoate with hydroxypropyl-beta-cyclodextrin: effect on photostability. *The Journal of Pharmacy and Pharmacology*, *51*, 1367–1374.

Scheytt, T. J., Mersmann, P., & Heberer, T. (2006). Mobility of pharmaceuticals carbamazepine, diclofenac, ibuprofen, and propyphenazone in miscible-displacement experiments. *Journal of Contaminant Hydrology*, *83*, 53–69.

Schuette, J. M., Ndou, T. T., & Warner, I. M. (1992). Cyclodextrin-induced asymmetry of achiral nitrogen heterocycles. *Journal of Physical Chemistry*, *96*, 5309–5314.

Schulz-Dobrick, M., Sarathy, K. V., & Jansen, M. (2005). Surfactant-free synthesis and functionalization of gold nanoparticles. *Journal of American Chemical Society*, *127*, 12816–12817.

Segneanu, A. E., Damian, D., Hulka, I., Grozescu, I., & Salifoglou, A. (2016). A simple and rapid method for calixarene-based selective extraction of bioactive molecules from natural products. *Amino Acids*, *48*, 849–858.

Shamsipur, M., Beigi, A. A. M., Teymouri, M., Rasoolipour, S., & Asfari, Z. (2009). Highly sensitive and selective poly(vinyl chloride)-membrane potentiometric sensors based on a calix[4]arene derivative for 2-furaldehyde. *Analytical Chemistry*, *81*, 6789–6796.

Sharmin, E., & Zafar, F. (2012). Polyurethane : An Introduction. *Polyurethane*, *1*, 3–16.

Shaw, G., Sykes, M., Humble, R. W., Mackenzie, G., Marsden, D., & Pehlivan, E. (1988). The use of modified sporopollenin from lycopodium clavatum as a novel ion-or ligand-exchange medium. *Reactive Polymers, Ion Exchangers, Sorbents*, *9*, 211–217.

Shen, X., Chen, Q., Zhang, J., & Fu, P. (2011). Supramolecular structures in the presence of ionic liquids. *Supramolecular Structures in the Presence of Ionic Liquids: Theory, Properties, New Approaches*, *1*, 427–482.

Shinkai, S. (1993). Calixarene-The third generation of supramolecules. *Tetrahedron*, *49*, 8933–8968.

Shukri, D. S. M., Sanagi, M. M., Ibrahim, W. A. W., Abidin, N. N. Z., & Aboul-Enein, H. Y. (2015). Liquid chromatographic determination of nsaids in urine after dispersive liquid–liquid microextraction based on solidification of floating organic droplets. *Chromatographia*, *78*, 987–994.

Sonnenschein, M. F. (2015). *Polyurethanes: Science, Technology, Markets, and Trends*. Hoboken, New Jersey: John Wiley & Sons, Inc.

Soutoudehnia Korrani, Z., Wan Ibrahim, W. A., Rashidi Nodeh, H., Aboul-Enein, H. Y., & Sanagi, M. M. (2016). Simultaneous preconcentration of polar and non-polar organophosphorus pesticides from water samples by using a new sorbent based on mesoporous silica. *Journal of Separation Science*, *39*, 1144–1151.

Sreejit Rajiv Menon. (2016). *Design and development of 2-functionalized calix[4]arenes and their investigation in the separation of lanthanides* (Doctoral thesis, University of Toledo). Retrieved on 14th February 2019 from http://rave.ohiolink.edu/etdc/view?acc_num=toledo1461715995

Sreekala, M. S., & Thomas, S. (2003). Effect of fibre surface modification on water-sorption characteristics of oil palm fibres. *Composites Science and Technology*, *63*, 861–869.

Starowicz, M., Starowicz, P., Zukrowski, J., Przewoźnik, J., Lemański, A., Kapusta, C., & Banaś, J. (2011). Electrochemical synthesis of magnetic iron oxide nanoparticles with controlled size. *Journal of Nanoparticle Research*, *13*, 7167–7176.

Steed, J. W., & Atwood, J. L. (2009). *Supramolecular Chemistry*. West Sussex, UK: John Wiley & Sons, Ltd.

Steed, J. W., Turner, D. R., & Wallace, K. J. (2007). *Core Concepts in Supramolecular Chemistry and Nanochemistry*. West Sussex, UK: John Wiley & Sons, Ltd.

Stewart, D. R., & Gutsche, C. D. (1999). Isolation, characterization, and conformational characteristics of *p*-tert-butylcalix[9-20]arenes. *Journal of the American Chemical Society*, *121*, 4136–4146.

Studio, D. (2015). Dassault Systemes BIOVIA, Discovery Studio Modelling Environment, Release 4.5.

Suwandecha, T., Rungnim, C., Namuangruk, S., Ruktanonchai, U., Sawatdee, S., Dechraksa, J., & Srichana, T. (2017). Host-guest interactions between sildenafil and cyclodextrins: Spectrofluorometric study and molecular dynamic modeling. *Journal of Molecular Graphics and Modelling*, *77*, 115–120.

Szejtli, J. (2004). Past , present , and future of cyclodextrin research. *Pure and Applied Chemistry*, *76*, 1825–1845.

Taeghwan Hyeon. (2003). Chemical synthesis of magnetic nanoparticles. *Chemical Communications*, *1*, 927–934.

Takami, S., Sato, T., Mousavand, T., Ohara, S., Umetsu, M., & Adschiri, T. (2007). Hydrothermal synthesis of surface-modified iron oxide nanoparticles. *Materials Letters*, *61*, 4769–4772.

Tang, X., Li, X., Sun, Y., Xiao, Y., & Wang, Y. (2018). Thiol-ene click derived structurally well-defined per(3,5-dimethyl)phenylcarbamoylated cationic cyclodextrin separation material for achiral and chiral chromatography. *Journal of Separation Science*, *41*, 2710–2718.

Tarasi, R., Khoobi, M., Niknejad, H., Ramazani, A., Ma, L., Bahadorikhalili, S., & Sha, A. (2016). β-cyclodextrin functionalized poly (5-amidoisophthalicacid) grafted Fe_3O_4 magnetic nanoparticles: A novel biocompatible nanocomposite for targeted docetaxel delivery. *Journal of Magnetism and Magnetic Materials*, *417*, 451–459.

Tartaj, P., del Puerto Morales, M., Veintemillas-Verdaguer, S., Gonzalez-Carreno, T., & Serna, C. J. (2003). The preparation of magnetic nanoparticles for applications in biomedicine. *Journal of Physics D: Applied Physics*, *36*, 182–197.

Taylor, P., Heberer, T., & Stan, H. (1997). Determination of clofibric acid and n-(phenylsulfonyl)-sarcosine in sewage, river and drinking water. *International Journal of Environmental Analytical Chemistry*, *67*, 113–124.

Telli, A. H. (2014). *Synthesis and characterization of toluene diisocyanate* (Master thesis, Middle East Technical University). Retrieved on 18th February 2019 from http://etd.lib.metu.edu.tr/upload/12618307/index.pdf

Teranishi, K. (2000). Practicable regiospecific bifunctionalization on the secondary face of α- and β-cyclodextrins. *Chemical Communications*, (14), 1255–1256.

Terekhova, I. V., & Kumeev, R. S. (2010). Thermodynamics of inclusion complexes between cyclodextrins and isoniazid. *Russian Journal of Physical Chemistry A*, *84*, 1–6.

Thomas A. Ternes, Meisenheimer, M., McDowell, D., Sacher, F., Brauch, H.-J., Haist-Gulde, B., … Zulei-Seibert, N. (2002). Removal of pharmaceuticals during drinking water treatment. *Environmental Science and Technology*, *36*, 3855–3863.

Thomasson, M. J., Baldwin, D. J., Diego-Taboada, A., Atkin, S. L., MacKenzie, G., & Wadhawan, J. D. (2010). Electrochemistry and charge transport in sporopollenin particle arrays. *Electrochemistry Communications*, *12*, 1428–1431.

Toledo-Neira, C., & Álvarez-Lueje, A. (2015). Ionic liquids for improving the extraction of NSAIDs in water samples using dispersive liquid-liquid microextraction by high performance liquid chromatography-diode array-fluorescence detection. *Talanta*, *134*, 619–626.

Tudisco, C., Oliveri, V., Cantarella, M., Vecchio, G., & Condorelli, G. G. (2012). Cyclodextrin anchoring on magnetic Fe_3O_4 nanoparticles modified with phosphonic linkers. *European Journal of Inorganic Chemistry*, *32*, 5323–5331.

Tungala, K., Adhikary, P., & Krishnamoorthi, S. (2013). Trimerization of β-cyclodextrin through the click reaction. *Carbohydrate Polymers*, *95*, 295–298.

Tutar, H., Yilmaz, E., Pehlivan, E., & Yilmaz, M. (2009). Immobilization of candida rugosa lipase on sporopollenin from lycopodium clavatum. *International Journal of Biological Macromolecules*, *45*, 315–320.

van der Boogard, M. (2003). *Cyclodextrin-containing supramolecular structures* (Doctoral thesis, University of Groningen). Retrieved on 13th February 2019 from https://www.rug.nl/research/portal/files/10067863/thesis.pdf

Vane, J. R. (1971). Inhibition of prostaglandin synthesis as a mechanism of action for aspirin-like drugs. *Nature New Biology*, *231*, 232–235.

Varady, J., Wu, X., & Wang, S. (2002). Competitive and reversible binding of a guest molecule to its host in aqueous solution through molecular dynamics simulation: Benzyl alcohol/β-cyclodextrin system. *Journal of Physical Chemistry B*, *106*, 4863–4872.

Vashist, S. K. (2013). Magnetic nanoparticles-based biomedical and bioanalytical applications. *Journal of Nanomedicine & Nanotechnology*, *4*, 1–2.

Vicens, J., & Böhmer, V. (1991). *Calixarenes: A versatile class of macrocyclic compounds*. Dordrecht, The Netherlands: Kluwer Academic Publishers.

Wan Ibrahim, W. A., Nodeh, H. R., Aboul-Enein, H. Y., & Sanagi, M. M. (2015). Magnetic solid-phase extraction based on modified ferum oxides for enrichment, preconcentration, and isolation of pesticides and selected pollutants. *Critical Reviews in Analytical Chemistry*, *45*, 270–287.

Wang, J., He, B., Yan, D., & Hu, X. (2017). Implementing ecopharmacovigilance (EPV) from a pharmacy perspective: A focus on non-steroidal anti-inflammatory drugs. *Science of the Total Environment*, *603–604*, 772–784.

Wang, N., Zhou, L., Guo, J., Ye, Q., Lin, J. M., & Yuan, J. (2014). Adsorption of environmental pollutants using magnetic hybrid nanoparticles modified with β-cyclodextrin. *Applied Surface Science*, *305*, 267–273.

Wang, R., Li, W., & Chen, Z. (2018). Solid phase microextraction with poly(deep eutectic solvent) monolithic column online coupled to HPLC for determination of non-steroidal anti-inflammatory drugs. *Analytica Chimica Acta*, *1018*, 111–118.

Wang, W., Ma, R., Wu, Q., Wang, C., & Wang, Z. (2013). Magnetic microsphere-confined graphene for the extraction of polycyclic aromatic hydrocarbons from environmental water samples coupled with high performance liquid chromatography-fluorescence analysis. *Journal of Chromatography A*, *1293*, 20–27.

Wang, Y., Sun, Y., Gao, Y., Xu, B., Wu, Q., Zhang, H., & Song, D. (2014). Determination of five pyrethroids in tea drinks by dispersive solid phase extraction with polyaniline-coated magnetic particles. *Talanta*, *119*, 268–275.

Wang, Z., Ling, B., Zhang, R., & Liu, Y. (2008). Docking and molecular dynamics study on the inhibitory activity of coumarins on aldose reductase. *Journal of Physical Chemistry B*, *112*, 10033–10040.

Weissermel, K., & Arpe, H.-J. (2003). *Industrial Organic Chemistry*. Weinheim, Germany: Wiley-VCH.

Wen, X., Tu, C., & Lee, H. K. (2004). Two-step liquid-liquid-liquid microextraction of nonsteroidal antiinflammatory drugs in wastewater. *Analytical Chemistry*, *76*, 228–232.

Wierucka, M., & Biziuk, M. (2014). Application of magnetic nanoparticles for magnetic solid-phase extraction in preparing biological, environmental and food samples. *Trends in Analytical Chemistry*, *59*, 50–58.

Woehrle, G. H., & Hutchison, J. E. (2005). Thiol-functionalized undecagold clusters by ligand exchange: Synthesis, mechanism, and properties. *Inorganic Chemistry*, *44*, 6149–6158.

Wu, Z., Pittman, C. U., & Gardner, S. D. (1996). Grafting isocyanate-terminated elastomers onto the surfaces of carbon fibers: Reaction of isocyanate with acidic surface functions. *Carbon*, *34*, 59–67.

Xie, L., Jiang, R., Zhu, F., Liu, H., & Ouyang, G. (2014). Application of functionalized magnetic nanoparticles in sample preparation. *Analytical and Bioanalytical Chemistry*, *406*, 377–399.

Xu, P., Zeng, G. M., Huang, D. L., Feng, C. L., Hu, S., Zhao, M. H., … Liu, Z. F. (2012). Use of iron oxide nanomaterials in wastewater treatment: A review. *Science of the Total Environment*, *424*, 1–10.

Yaacob, S. F. F. S., Razak, N. S. A., Aun, T. T., Rozi, S. K. M., Jamil, A. K. M., & Mohamad, S. (2018). Synthesis and characterizations of magnetic bio-material sporopollenin for the removal of oil from aqueous environment. *Industrial Crops and Products*, *124*, 442–448.

Yaftian, M. R., Burgard, M., Wieser, C., Dieleman, C. B., & Matt, D. (1998). Extractive properties towards rare-earth metal ions of calix[4]arenes substituted at the narrow rim by phosphoryl and amide groups. *Solvent Extraction and Ion Exchange*, *16*, 1131–1149.

Yaftian, M. R., Taheri, R., & Matt, D. (2003). Lower-rim polyphosphorylated calix[4]arenes. Their use as extracting agents for thorium (IV) and europium (III) ions. *Phosphorus, Sulfur and Silicon and the Related Elements*, *178*, 1225–1230.

Yang, E. C., Zhao, X. J., Hua, F., & Hao, J. K. (2004). Semi-empirical PM3 study upon the complexation of β-cyclodextrin with 4,4′-benzidine and *o*-tolidine. *Journal of Molecular Structure: THEOCHEM*, *712*, 75–79.

Yang, H. (2008). *UC781: Beta-cyclodextrin complexation and formulation as an anti-hiv microbicide* (Doctoral thesis, University of Pittsburgh). Retrieved on 13th February 2019 from http://d-scholarship.pitt.edu/6278/

Yang, W., & M., de V. M. (2005). Effect of 4-sulphonato-calix[n]arenes and cyclodextrins on the solubilization of niclosamide, a poorly water soluble anthelmintic. *The AAPS Journal*, *7*, 241–248.

Yang, Y., Ok, Y. S., Kim, K. H., Kwon, E. E., & Tsang, Y. F. (2017). Occurrences and removal of pharmaceuticals and personal care products (PPCPs) in drinking water and water/sewage treatment plants: A review. *Science of the Total Environment*, *596–597*, 303–320.

Yao, C., Li, T., Twu, P., Pitner, W. R., & Anderson, J. L. (2011). Selective extraction of emerging contaminants from water samples by dispersive liquid-liquid microextraction using functionalized ionic liquids. *Journal of Chromatography A*, *1218*, 1556–1566.

Yilmaz, A., Yilmaz, E., Yilmaz, M., & Bartsch, R. A. (2006). Removal of azo dyes from aqueous solutions using calix[4]arene and β-cyclodextrin. *Dyes and Pigments*, *74*, 54–59.

Yilmaz, E., Memon, S., & Yilmaz, M. (2010). Removal of direct azo dyes and aromatic amines from aqueous solutions using two β-cyclodextrin-based polymers. *Journal of Hazardous Materials*, *174*, 592–597.

Yu, J. T., Bouwer, E. J., & Coelhan, M. (2006). Occurrence and biodegradability studies of selected pharmaceuticals and personal care products in sewage effluent. *Agricultural Water Management*, *86*, 72–80.

Yusuf, K., Aqel, A., Dyab, A. K. F., ALOthman, Z. A., & Badjah-Hadj-Ahmed, A. Y. (2016). Effect of sporopollenin microparticle incorporation into the hexyl methacrylate-based monolithic columns for capillary liquid chromatography. *Journal of Liquid Chromatography and Related Technologies*, *39*, 752–761.

Zain, N. N. M., Raoov, M., Abu Bakar, N. K., & Mohamad, S. (2016). Cyclodextrin modified ionic liquid material as a modifier for cloud point extraction of phenolic compounds using spectrophotometry. *Journal of Inclusion Phenomena and Macrocyclic Chemistry*, *84*, 137–152.

Zayats, M., Katz, E., Baron, R., & Willner, I. (2005). Reconstitution of apo-glucose dehydrogenase on pyrroloquinoline quinone-functionalized Au nanoparticles yields an electrically contacted biocatalyst. *Journal of the American Chemical Society*, *127*, 12400–12406.

Zhang, H., Zhang, G., Bi, X., & Chen, X. (2013). Facile assembly of a hierarchical core@shell Fe_3O_4@CuMgAl-LDH (layered double hydroxide) magnetic nanocatalyst for the hydroxylation of phenol. *Journal of Materials Chemistry A*, *1*, 5934–5942.

Zhao, Y. G., Cai, M. Q., Chen, X. H., Pan, S. D., Yao, S. S., & Jin, M. C. (2013). Analysis of nine food additives in wine by dispersive solid-phase extraction and reversed-phase high performance liquid chromatography. *Food Research International*, *52*, 350–358.

Ziylan, A., & Ince, N. H. (2011). The occurrence and fate of anti-inflammatory and analgesic pharmaceuticals in sewage and fresh water: Treatability by conventional and non-conventional processes. *Journal of Hazardous Materials*, *187*, 24–36.

Zoete, V., Meuwly, M., & Karplus, M. (2004). Investigation of glucose binding sites on insulin. *Proteins: Structure, Function & Bioinformatics, 55*, 568–581.

LIST OF PUBLICATIONS AND PAPERS PRESENTED

Publications:

Yaacob, S. F. F. S., Kamboh, M. A., Ibrahim, W. A. W., & Mohamad, S. (2018). New sporopollenin-based β-cyclodextrin functionalized magnetic hybrid adsorbent for magnetic solid-phase extraction of nonsteroidal anti-inflammatory drugs from water samples. *Royal Society Open Science*, *5*, 171311–171324.

Syed Yaacob, S. F. F., Mohd Jamil, A. K., Kamboh, M. A., Wan Ibrahim, W. A., & Mohamad, S. (2018). Fabrication of calixarene-grafted bio-polymeric magnetic composites for magnetic solid phase extraction of non-steroidal anti-inflammatory drugs in water samples. *PeerJ*, *6*, 5108–5132.

Paper presented:

Syed Fariq Fathullah Syed Yaacob, & Sharifah Mohamad. Extraction of NSAIDs by using magnetic solid phase extraction of sporopollenin based beta cyclodextrin, SKAM30 International Conference of Analytical Sciences (2017), Malaysia.